CYLINDER WALL TEMPERATURE MEASUREMENT IN AN AIR-COOLED TWO-STROKE CYCLE S.I. ENGINE

ABSTRACT

The cylinder wall surface temperature of an engine has effects on lubrication, on pollution, on heat transfer and on engine operating problems. An experimental study of the cylinder wall surface temperatures on an air-cooled two-stroke cycle S.I. engine was conducted to determine the effects of speed, load and fuel-oil ratio on the cylinder wall surface temperature.

A suitable engine was coupled to a dynamometer and instrumented to provide data on interior and exterior cylinder wall temperatures, engine speed and load, and fuel and air flow rates. Three co-axial surface thermocouples, having a thermal junction 6 microns below the combustion chamber surface were used to measure the time averaged cylinder wall surface temperature at various operating conditions. From the results of this experiment, it was found that cylinder wall surface temperature increases with speed and load, though in the latter case it decreases when load is increased above half the maximum brake mean effective pressure. It was also found that as bsfc increases the cylinder wall surface temperature decreases.

ACKNOWLEDGEMENT

The author wishes to express his deepest sense of gratitude to the following individuals and organization for their aid and assistance throughout the course of this study:

Dr. Thomas LeFeuvre for his invaluable guidance, counsel and instructions.

Kohler Canada Ltd. for their interest and supply of the two-stroke cycle S.I. engine.

Dr. R. Henry for providing the multichannel recorder for experimental measurement.

Dr. Y.C. Lee for providing the equipment for air flow calibration and a switch selector.

Mr. G. Toth and his technical staff for their generous assistance.

Mr. K.T. Heng, Mr. P. Bharati, Mr. V. Algarwal and Mr. R. Rajagopalan for their very kind assistance and opinions.

TABLE OF CONTENTS

LIST OF FIGURES

LIST OF TABLES

ABBREVIATIONS

A/F	air-fuel ratio
BDC	bottom dead centre
bmep, Bmep	brake mean effective pressure
bsfc, Bsfc	brake specific fuel consumption
BTDC	before top dead centre
^oC	degree centigrade
CST	cylinder wall surface temperature
emf	electromotive force
f	natural frequency
f_n	natural frequency
^oF	degree fahrenheit
F/O	fuel-oil ratio
h_c	coefficient of heat convection Kcal/m^2-hr-^oC
K	constant varies with viscosity invluence No.
p	cylinder chamber gas pressure
mv	millivolt
N	viscosity influence No.
n	revolution per minute
$\dot{q}$	heat transfer rate
TC	thermocouple
TDC	top dead centre
T_g	cylinder chamber gas temperature
T_w	cylinder wall surface temperature
t	time
X	distance from cylinder wall liner
η_{th}	thermal efficiency
μ	viscosity of fluid

CHAPTER 1

INTRODUCTION

The development and application of air-cooled two-stroke cycle S.I. engines have been carried out for the last few decades. Although in former years, no substantial problems regarding piston wear, ring gumming, scuffing and piston seizure etc. resulted from the operation of the engine, to-day the modern high speed air-cooled two-stroke cycle engines are experiencing these problems at an increasing rate. This could lead to serious operational disturbances, if not to the total deterioration and destruction of engines.

It is to be pointed out here that a multitude of factors affect these problem areas such as breakdown of lubricant film, inadequacy of fuel oil mixing, shortage of additives and high cooling air temperature. These problems could be understood better if more investigations were to be carried out. Apart from the material structure of the engine, the engine design criteria and lubricant properties, temperature measurement of the cylinder wall surface is considered one of the essential factors contributing to these engine problems.

The purpose of the present investigation is to develop a method to measure the cylinder wall surface temperature (abbreviated as CST henceforth) of an air-cooled two-stroke cycle engine. This method could hopefully be ultilized in industry where engineers are currently using subsurface thermocouples embedded as close to the cylinder wall surface as possible. It is also expected that the development of this method will facilitate further studies in the areas of: CST effects on lubricant film, CST effects on cylinder and piston wear, CST as a means to calculate heat flux, and the CST influences on exhaust hydrocarbon concentration of this type of engine.

During the course of this investigation, a Kohler air-cooled two-stroke cycle S.I. engine was employed. The engine was mounted on a specially built test bed with its power output absorbed by a Heenan & Froude hydraulic dynamometer. CST measuring methods were reviewed. Bendersky type (1)* co-axial thermocouples were chosen to be installed on the cylinder wall to render direct temperature measurements. Details of this type of thermocouple are given in chapter 2.

A brief description of the CST effects based on a literature survey is discussed in the following paragraphs.

<u>Effect of CST on lubricant film</u>

In the case of engine lubrication, ordinary hydrodynamic lubrication theory is not directly applicable. CST measurement shows that the lubricant film experiences a peak temperature exceeding its recommended temperature range which is $250^{o}F$ to $400^{o}F$ (2).

* Numbers in parenthesis designate references on p. 107.

The questions arising here are how to maintain a steady lubricant film on the cylinder wall liner and how this lubricant film behaves in the actual running condition? What temperature range is the lubricant film facing in the air-cooled two-stroke cycle S.I. engines? Will the lubricant film have enough time to degrade or decompose and consequently lose its lubricating properties? These questions are not clearly understood and should be the subject of future studies.

Generally speaking, through the maintenance of the lubricant film on the cylinder wall liner, many operating problems such as piston seizure, piston ring wear, cylinder liner wear, and scuffing are avoided. This is discussed in detail in appendix A where base oils, additives, fuel-oil ratio and their influences on engine operating problems are outlined.

Lubricant film thickness has been measured in many past experiments. Various methods were discussed by Poppinga (3). Contradicting results were published by using the electrical and optical approaches (4) and (5). Shaw and Nussdorfer (4) concluded in their work that the lubricant film is continuous, but Courtney, Pratt and Tudor (5) said that the lubricant film never exists continuously throughout the entire cycle of operation. Nevertheless, the dependence of the lubricant film on CST is obvious. Poppinga (3) in his book noted that the temperature influences the thermal conductivity of the lubricant film existing in the cylinder chamber considerably. He also mentioned that thermal destruction of the lubricant film exists at both extremely low and high cylinder wall liner temperatures.

Tabor (6) concluded that the temperature at which boundary lubrication occurs could be a measure of the strength with which the lubricant film adheres to the surface, the higher the temperature, the more strongly is the film adsorbed on the surface. Here, of course, the rate of oxidation and thermal deterioration of the lubricant film should be carefully observed and studied to prevent failure of the lubricant film at extremely high temperatures as was pointed out by Courtney Pratt and Tudor (5). They revealed that a great amount of deterioration in the lubricant film resulted as the temperature of the component parts of the engine increased.

Effect of CST on cylinder and piston ring wear

The problem of wear is approached, in many cases, through discussion of those conditions most closely associated with wear; the temperature of the moving parts, their material and design, and the characteristics of the lubricant used on these surfaces.

Nutt, Landen and Edgar (7) discussed the effects of surface temperature on wear of diesel engine cylinders and piston rings in detail. Although their work is not expected to apply to all other conditions and engines, a similar correlation may prove to be adequate to derive the condition of cylinder wear. It is shown in their work that the wear rate of the piston is high at low cooling jacket temperature (which is a linear function of the liner temperature in their case), it decreases as the cooling jacket temperature increases and again rises while cooling jacket temperature rises still higher than 175°F. A coincidence in Poppinga's book (3) pointed out that wear at low CST (70°F, say) is very high, it soon drops down as CST increases. But this wear rate again increases when the CST reaches 436°F. He also mentioned that there is an increase in wear in the upper part of the cylinder as well as in the case of the uppermost piston rings when subjected to high CST.

It is of no doubt that wear is a most undesirable aspect of engine operation. It is realized that CST is not the sole factor that governs this problem, yet, more research in this area should be promoted to clarify the situation.

CST as a means to find heat flux

Heat flux at the surface of cylinder wall could be computed with the aid of CST measurement. The basic equation for this computation (neglecting heat radiation) is :-

$$\dot{q}(t) = h_c(t)\ (T_g(t) - T_w(t)) \tag{1.1}$$

Such work has been carried out by numerous researchers on various types of engines (see reference 8, 9, 10 and 11). Evaluation of the average heat flux could be achieved with the help of equation (1.1). Also, the instantaneous heat flux could be evaluated by measuring the instantaneous CST with a high speed recording system as done by LeFeuvre, Myers, Uyehara and Shipinski (12).

The heat flux thus obtained could possibly be verified from heat transfer across the cylinder wall by assuming one-dimensional heat flow through the cylinder wall. This is given below as:

$$\partial T/\partial t = \partial^2 T/\partial X^2 \qquad (1.2)$$

The heat flux solved from equation (1.2) at X = 0, i.e. at the gas side surface should equal the heat flux computed by equation (1.1) using empirical data suggested by Annand (8), Nusselt (8), Eichelberg (9), Overbye (10) and LeFeuvre (11).

CST influences the heat transfer coefficient

Jaklitsch in the discussion section of Vincent and Henein's paper (13) stated clearly the dependency of heat transfer coefficient of convection between gas and cylinder wall. The equation given is as follows:

$$h_c = 23500\ p/(RT_w) + 4.9\ T_o/T_w \qquad (1.3)$$

From the above equation, it can be observed that the heat transfer coefficient of convection is inversely proportional to the CST and hence the influence of CST should not be overlooked in determining the heat transfer coefficient of convection.

Effects of CST on exhaust hydrocarbon concentration

Two-stroke cycle engines are contributing significant hydrocarbon pollutants. Early investigations about engine variable effects on exhaust hydrocarbon concentration (14), (15) found that an increased coolant temperature reduced the exhaust hydrocarbon concentration. Also Wentworth (16) revealed that increasing the combustion chamber surface temperature lowers the exhaust hydrocarbon concentration and he finally concluded that the exhaust hydrocarbon concentration is a function of the average surface liner temperature.

Analyses of the cylinder and the exhaust gas composition could possibly be carried out in a small two-stroke cycle S.I. engine as was suggested by Ohigashi and Hamamoto (17). The relationship between the hydrocarbon concentration and the CST could therefore be established for two-stroke cycle S.I. engines with the help of this investigation.

CHAPTER 2

EQUIPMENT AND INSTRUMENTATION

The equipment and instrumentation which were used in the present investigation are described in this chapter. Details of the test bed, engine, dynamometer, their arrangement, and the measuring instrumentation are described in the following sections.

2.1 Test bed

Engine vibration was found a major problem in running two-stroke cycle engine tests by N.R.C., Nortran and Kohler of Canada. This vibration problem was also noted by Hazzard (18). In order to eliminate this problem, a heavy test block should be used so as to provide a low natural frequency of oscillation of the base. Since the vibration transmission is depended on the ratio of natural frequency to applied frequency (19), i.e.,

$$\text{Transmissibility} = 1/((f/f_n)^2 - 1) \qquad (2.1)$$

the transmissibility could be reduced by using a heavy block for the same applied frequency and therefore restricts the running dynamic amplitude of the unit.

The test bed installed is of the concrete block type. A schematic diagram of the test bed installation is shown in Fig. 2.1. I-beams were embedded in the concrete block to accommodate future changes of set up. This was done with great care especially in leveling the surfaces of the

I-beams. Adjustable stands were made to supported the I-beams before pouring the concrete. Leveling was checked before and after the completion of the test bed. It was so arranged that two sets of I-beams were separated to allow independent mounting of the engine and the dynamometer. This has the advantage that the dynamometer is not subjected to engine vibrations which may be deleterious to the torque measuring mechanism and affect its accuracy.

2.2 Engine

The engine chosen for the present investigation is a Kohler K440-2AX model air-cooled two-stroke S.I. engine. Specification of this engine is given in Table 2.1. Other engines such as a chain saw engine and a lawn mover engine have also been considered. As a result of the growing market of snowmobile engines (19), it was decided that investigation on this particular engine seemed appropriate.

2.2.1 Modification of engine ignition system

An electric starter was added to the manual start Kohler engine in this investigation. The detailled wiring diagram per Kohler service manual is shown in Fig. 2.2. A rpm meter was connected to the ignition coil as well. The engine was timed by a dial indicator to the manufacturer's specification. Ignition at 20^{o} BTDC was set (without automatic spark advancing mechanism). Braker-point gaps and spark plug gaps were set to 0.016 in. and 0.020 in. respectively.

2.2.2 Muffler system

An ACS 1804-31A muffler was used for this engine according to the manufacturer's recommendation. The muffler was connected to the engine through a Y manifold and was supported by a stiffener to avoid vibration caused by the unsteady exhaust flow.

2.2.3 Engine power data

Power data supplied by Kohler of Canada was checked to assure engine performance. Results shown are satisfactory after the engine was timed to the appropriate point of ignition. This is shown in Fig. 2.3. Values at speeds higher than 5,500 rpm were difficult to obtain due to the back pressure built up in the exhaust system existing in the test cell.

2.3 Dynamometer

A Heenan & Froude hydraulic dynamometer model D.P. X.O. was selected for the present investigation. The advantages of using this dynamometer are: its comparatively low cost, minimum maintenance required, and it covers all ranges of operating speeds and power output for this engine.

Specification of the dynamometer is given in Fig. 2.4. Water inlet pressure was measured by a pressure gage made by Webster Air Equipment Ltd.. The water outlet temperature was read through a thermometer installed in the outlet water passageway. Both of these measurements were used as indications for the standard operating condition of the dynamometer.

2.4 Arrangement of engine, carden shaft, coupling and the dynamometer

The dynamometer is connected to the engine by a carden shaft and a flexible coupling. A photograph of this arrangement is shown in Fig. 2.5. In addition, a schematic diagram is given in Fig. 2.6. The design of this arrangement was based on the recommendation suggested by the dynamometer manufacturer to give the least misalignment and whirling.

2.5 Instrumentation used for measurement

2.5.1 Speed measurement

A Hewlett Packard 5310A electric digital counter was used to read the engine speed. Signals were directed from the dynamometer shaft by a magnetic sensing element. A supplementary rpm meter was also used for speed indication, this rpm meter was connected to the primary ignition coil of the engine ignition system.

2.5.2 Fuel flow measurement

The fuel flow is measured by using a "Manostat" (variable area flow meter) made by Fisher Scientific Co. The fuel-oil mixture flows from the gasoline supply line through the Manostat into the carburetor and consequently shows a reading on the Manostat. The reading will then be converted into flow rate by using an appropriate conversion curve (see Fig. 2.7) which was obtained with help of fuel-oil density and viscosity measurements.

Steps to obtain these conversion curves are :-

(a) to measure the viscosity of the fuel-oil mixture; a "Temp-Trol" bath and a 50/D489 viscometer from Precision Scientific Co. were used to find the viscosities of the fuel-oil mixture as is shown in Fig. 2.8. This instrument allows the calculation of a viscosity influence number which relates to the fuel-oil flow rate.

(b) to measure the density of the fuel-oil mixture; the density of the fuel-oil mixture was determined by weighing a known volume of the mixture on an electric balance made by E. Mettler Zurich Co.

(c) to compute the flow rates versus "Manostat" readings according to supplier's catalog. Details of the computation are given in appendix B.

Direct measurements were taken in order to check the accuracy of the conversion curves. A comparison between the direct measurements versus "Manostat" readings and the computed curve shows an average deviation of approximately 1% for fuel-oil ratio at 20:1. This is shown in Fig. 2.9.

2.5.3 Air flow measurement

Intake air to the carburetor was measured by an orifice-type air container. Details are given in appendix C.

2.5.4 Temperature measurement

The null method was adopted for the temperature measurement in the present investigation. T type (copper--constantan), J type (iron-constantan), K type (chromel--alumel) and spark plug gasket thermocouples (T type) were used for temperature measurement at the exterior cylinder wall surface, the cylinder wall inner surface (CST), exhaust manifold and spark plug gasket respectively. Their location and installation are given separately in the following paragraphs.

(a) T type thermocouples (copper-constantan): The T type thermocouples were made to acquire information on the external cylinder surface. A Dynatech 416 TC welder made by Precision Scientific was used to weld these thermocouples. Sixteen thermocouple junctions were held on the external cylinder surface by plastic aluminum. Outputs of these thermocouples were connected to a selector switch, to permit readout with a potentiometer.

(b) J type thermocouples (iron-constantan): Special Bendersky type (1) thermocouples were chosen to measure the CST. These thermocouples allow the direct measurement of the cylinder wall surface temperature. A sketch of this type of co-axial thermocouples from Midtherm Co. is shown in Fig. 2.10.

This Bendersky type thermocouple was selected for its similarity in material (iron sleeve) with the cylinder sleeve. This limits the change of heat transfer phenomena through the cylinder wall as much as possible.

The co-axial surface thermocouples were mounted flush to the cylinder surface. However, there existed a slight difference between the co-axial thermocouple surface and the cylinder wall surface. This is due to the curvature of the cylinder wall surface. Calculation showed the difference is approximately 0.0007 in. and is therefore negligible.

During installation, it was intended not to change the feature of the original design, hence, the disturbance to the fins was minimal as shown in the installation detail in Fig. 2.11. Special bushings were made to ensure locking of the co-axial thermocouples which were threaded into the cylinder block. Graphite powder was employed for easy replacement.

The graphite powder was also used to seal the clearance between the threads to avoid any leakage of pressure caused by the installation of the thermocouples. The leakage was shown to be negligible both analytically (appendix D) and experimentally (Fig. 2.3).

(c) Location of the J type and the T type thermocouples: The regions of highest suspected temperature on the cylinder surface were selected to locate the J type co-axial thermocouples. They are on the first cylinder which is the one closest to the air shroud exit since this cylinder generally runs hotter. Three spots selected are : A - 24^{o} from TDC, B - 128^{o} from TDC (close to BDC) and C - 86^{o} from TDC (near the exhaust port) as shown in Fig. 2.12. External surface thermocouples of T type were located at various places on both cylinders. Efforts were made to locate some of the T type thermocouples (No. 1, 2, 4 and 7) in the vicinity of the co-axial J type thermocouples. Detail locations are shown in Fig. 2.12 and Fig. 2.13.

(d) Megopak K type thermocouples: Two Megopak K type thermocouples from Honeywell Co. were used to measure the exhaust temperature of both cylinders. To allow installation, additional plates were welded onto the exhaust pipes. Both thermocouples were threaded into the insulated exhaust pipes and their sensing junctions were set at the centres of the exhaust pipes.

(e) Spark plug gasket thermocouples: Two spark plug gasket thermocouples were installed to check the spark plug temperatures which should not exceed 500°F during engine operation. Readings are shown directly on temperature indicators.

The outputs from the J type and K type thermocouples were connected to a multichannel recorder, model MC 611, made by Watanabe Instruments Corp. The outputs from the T type thermocouples were connected to a potentiometer made by Leeds & Northrup Co. These two recording devices gave the same mv reading when subjected to the same input.

The J type, K type and T type thermocouples were checked before installation. The calibration check was mainly to determine the emf developed by these thermocouples as a function of the temperature difference between their measuring junctions and a cold junction at the ice point, i.e. 32°F.

A comparison technique (20) was adopted as the standard calibration method. Measurements were taken from a low temperature to the boiling point of water. They were compared with standard thermometer readings. A constant temperature water bath was used for this calibration. Results were found satisfactory and they are shown in Table 2.2.

CHAPTER 3

EXPERIMENTAL DATA AND RESULTS

Preliminary test runs were performed after the set up was completed. The engine was run continuously for break--in at the rated power of 6 Bhp at 3,000 rpm for one hour and followed by another hour at 8 Bhp at 4,000 rpm according to the 'Safety Standards for Small Craft" (21).

Engine performance was assured after the break-in as was noted in section 2.2.3. A total of eighty hours testing was carried out and 141 successive data points were collected in this experiment. Difficulties were experienced while tests were tried at speeds higher than 5,000 rpm. At high speeds, it was found difficult to maintain either the speed or the load for a period long enough to obtain a steady CST.

During the investigation, the author has a chance to observe the cylinder wall surface after fourty hours of test run. There was no signs of significant wear or scuffing. This observation was made during the replacement of one of the co-axial thermocouples which was accidentally broken.

The parameters selected for investigation, test run procedure and precautions, the repeatability of the experiment as well as the accuracy of experimental results, and the experimental results themselves are presented in the following sections.

3.1 Parameters

In the present investigation of CST, engine speed (from 3,000 rpm to 5,000 rpm) and bmep (from 5 psi to 60 psi) are the two major parameters. Another parameter considered is the fuel-oil ratio, which is varied from 20:1 to 60:1.

3.2 Test Runs

A fuel-oil ratio of 20:1 was first selected to perform the constant load and constant speed test. This was followed by fuel-oil ratio of 40:1 and then 60:1. For each change of fuel-oil ratio, the crankcase was drained by removing the cover at the bottom of the engine. A two-hour test run at 4,000 rpm, 5 lbs loading was performed. since there is no guideline to be followed (14, 21, 22 and 23), it is believed that a two-hour test run would wash away the residual fuel-oil mixture remaining in the crankcase, combustion gas chamber and the carburetion system.

For each test run, the engine operating condition was kept steady for a period long enough to allow constant outputs from the thermocouples. It was usually from 10 minutes to 15 minutes after a warming up period of 20 minutes. Precautions for test runs are listed in Table 3.1.

3.3 Repeatability of results

The repeatability of the present investigation was checked by repeating a standard condition at random intervals.

In Table 3.2, test runs No. 7, 16, 29, 30, 31, 52, 62, 64, 101 were performed to obtain CST versus bmep curve at 3,600 rpm and a fuel-oil ratio of 20:1, while test runs No. 102, 104, 111, 117 and 129 were performed later at the same speed and the fuel-oil ratio. The results reveal that both test run data fell on the same curve for all three co-axial J type thermocouples as shown in Figure 3.1.

3.4 Sources of error

There always exists possible errors in the experimental results. In the present experiment, however, a theoretical analysis of the overall effects of all possible errors on the experimental results of CST is not applicable. It is therefore important to know the limits of error of every individual portion that affects the results. The sources of error, in this experiment, are the water pressure, the room temperature, the engine speed, the accuracy of thermocouples, the multichannel recorder deviation and the visual mistakes.

(a) Water pressure - There is some flutuation on the water supply pressure. Even though the fluctuation is not severe and sometimes hardly noticeable, still, it has some effect during a steady run. In order to eliminate this problem, inlet water pressure to the dynamometer was always kept at maximum allowable pressure of 40 ± 2 psi.

(b) Room temperature - The test cell room temperature is controllable by means of air dampers located in the ceiling of the cell to the extent of maintaining the day-to-day room temperature. It was found impossible to change the room temperature as desired.

(c) Engine speed - Fluctuation of engine speed was observed during the test runs. Maximum fluctuation was ± 20 rpm.

(d) Accuracy of thermocouples - The limits of error of the thermocouples are shown in Table 3.3 (24).

(e) Multirecorder error - The linearity of the multirecorder is ± 0.3% at full scale according to the manufacturer's manual.

(f) Visual mistakes - Visual mistakes in reading all instruments are inevitable. These were minimized by double checking the readings.

3.5 Experimental results

Experimental results are tabulated in Table 3.4, Table 3.5 and Table 3.6 where operating conditions for test runs, test data of CST and exhaust gas temperature and the external cylinder surface temperature test data are listed in detail.

CHAPTER 4

DISCUSSION AND CONCLUSIONS

The present investigation demonstrates a method of measuring cylinder wall surface temperature on an air-cooled two-stroke cycle S.I. engine. This is the first time that this method of CST measurement has been used to determine the lubricated wall temperature of a two-stroke cycle engine.

The CSTs obtained at the three locations mentioned in section 2.5.4 show some differences. It was found that the highest temperature occurs near the TDC at the air shroud exit side as compared with the other two locations near BDC and the exhaust port. The highest CST experienced was approximately 510^{o}F.

In this chapter, the CST dependency on bmep, on speed and on fuel-oil ratio are discussed. The nature and the trend of curves showing CST versus various parameters are plotted and studied. The external cylinder surface temperature and exhaust gas temperature are also discussed. Several conclusions are drawn from experimental results at the end of this chapter.

All curves shown in this chapter (except those specified) are for the co-axial thermocouple A which is located 24^{o} from the TDC. Other curves showing similar results (co-axial thermocouples B and C) are given in Fig. 4.10 to Fig. 4. 24.

4.1 CST and its bmep dependency

Figures 4.1, 4.2 and 4.3 show the CST versus bmep at various constant speeds for fuel-oil ratio at 20:1, 40:1, and 60:1 respectively.

It is interesting to note that CST increases as the bmep increases initially, but this increase is followed by a decrease at high bmep values. This could be observed from all the three figures presented. Similar results were found by Underwood and Catlin (25) in their measurements on piston crown temperature of a six cylinder two-cycle diesel engine. Despite the difference in measuring positions in the engine, this trend of decreasing cylinder chamber surface temperature at high loadings is a very interesting phenomena to be studied. More about this phenomena is discussed in section 4.4.

4.2 CST and its speed dependency

Plots of CST versus speed are shown in Figures 4.4 where various constant bmeps were considered at a fuel-oil ratio of 20:1. From Fig. 4.4, it is observed that as the speed increases from 3,000 rpm to 4,000 rpm, CST rises fairly slowly but starts to accelerate when the speed increases from 4,000 rpm to 5,000 rpm. The reason for this change is not clearly understood although it could possibly be caused by the reduction of oil film thickness due to higher piston speed as was pointed out by Poppinga (3).

However, the increase of CST is explainable. Since as the speed of an engine increases, the cylinder surface is subjected to more frequent sliding contacts which in turn produces more heat and consequently increases the wall liner temperature. Moreover, more energy would be released from the combustion in order to achieve higher speeds. Works presented by Poppinga (3), Underwood and Catlin (25) and Wentworth (16) on other types of engines showed a common agreement on this speed dependency.

4.3 CST and its fuel-oil ratio dependency

Data obtained from this experiment showed a general increase in CST as the fuel-oil ratio increases. Obviously this does not include extremely lean fuel-oil mixtures such as a fuel-oil ratio of 100:1. This is because too lean a fuel-oil ratio mixtures will cause unsteady engine performance and result in severe operating problems such as wear, scuffing and breakdown of oil films.

Figures 4.5 and 4.6 show the CST versus bmep at various fuel-oil ratios of 20:1, 40:1 and 60:1 at 3,600 rpm and 4,000 rpm respectively. These two figures reveal that CST does increase as the fuel-oil ratio increases but the magnitude of such increase is only in the order of few degrees F. This is quite peculiar considering the basic heat conduction through the oil film, for the same operating conditions but different fuel-oil ratios. The oil film thickness apparently remains almost the same while the amount of oil supplied differs appreciably. It is suspected that the gasoline particles in the mixture impinging on the cylinder wall liner may also possibly act as a lubricant.

4.4 Bsfc and its effect on CST

Bsfc values were computed from fuel flow measurements and the corresponding operating conditions. It was discovered that the bsfc for this engine increased tremendously at high bmep values. This is shown in Fig. 4.7 and Fig. 4.8 where CST curves are also drawn. It can be seen from these two figures that as the bsfc increases sharply, the CST drops simutaneously in all cases. Since a higher bsfc designates more fuel per stroke consumed for the same horsepower output, the author believes that higher bsfc will reduce the combustion gas temperature and consequently affect the CST. As a matter of fact, from the results of the measurement of the exhaust gas temperature (which could be an indication to the combustion gas temperature) higher bsfc values usually lowered the exhaust gas temperature. This is also shown in Fig. 4.7 and Fig. 4.8. Nevertheless, the exhaust gas temperature itself should not be used to predict the CST history simply because there does not exist any linear relationship between them.

In conclusion, the variation of bsfc in the operation of this engine is found to be one of the reasons that might contribute to the complex phenomena of CST discussed in section 4.1. This is to say that if the bsfc can possibly be controlled at constant value, there might be no CST drop at high bmep values. This would, of course, be undesirable in the sense of increasing the possibility of the thermal degradation of lubricants. However, it seems inpractical to control the bsfc without affecting the actual operating conditions of this engine.

4.5 External cylinder surface temperature and the CST

The external cylinder surface temperature was previously used to predict the cylinder wall surface temperature. Linearity was then established between them and used to predict the CST by applying one-dimensional heat conduction equations, references (7) and (13). In references (7) and (13), the heat flux from the external wall surface to the coolant was determined and then used to predict the cylinder wall surface temperature. However, the present investigation showed that unless a steady coolant temperature was maintained, this linearity is not necessarily true.

In this experiment, a cooling air shroud was provided to ensure forced-convection. Air became much hotter as it approached the cooling shroud exit. The external cylinder surface temperature will be different everywhere in accord with the local coolant temperature. It is obvious that the external surface temperature thus measured should no longer be used to predict the CST of this engine despite the fact that it might affect the CST to a certain extent. In addition, the cooling air flow rate, governed by the fan speed which is a function of engine speed, further restricts the use of external cylinder surface temperature to predict the CST.

Fig. 4.9 shows the external cylinder surface temperature at five different locations. No. 9 and No. 11 are on the cylinder closest to the cooling fan and No. 1, 6 and No. 7 on the other cylinder. The significant difference of the external surface temperature between the two cylinders can be seen. The temperature on the cylinder closest to the cooling fan is much lower because of the lower coolant temperature. CST curves for co-axial thermocouples A, B and C are also drawn in Fig. 4.9 to be compared with external surface temperatures at Nos. 6, 1 and 7 respectively. It can be seen that high CST at A did not generate high external surface temperature at No. 6 as compared with the other two locations.

4.6 Conclusions

The following conclusions were drawn from this investigation.

(a) This experiment suggests a better method to determine the CST for air-cooled two-stroke cycle S.I. engines.

(b) The direct measurement of CST enables further studies on the influences of CST on engine operating problems, on the lubricant film itself, on unburned hydrocarbon concentration in the exhaust, on cylinder wear, and in determining the heat transfer through the cylinder wall for this type of engine.

(c) CST increases with bmep up to approximately 50% of maximum bmep value and then decreases as the bmep keeps increasing in this experiment. This decrease is believed to be due to the influence of the bsfc on the CST. As was observed, CST varies inversely with the bsfc.

(d) CST increases with engine speed in this experiment.

(e) Exhaust gas temperature should not be used as an indication of CST.

(f) External surface temperature should not be used to predict the CST.

(g) CST differs from place to place on the cylinder wall liner, the highest CST in this experiment was experienced near the top portion of the cylinder farthest from the cooling fan.

(h) Fuel-oil ratio has little influence on the CST, its effect on CST can be neglected.

CHAPTER 5

PROPOSALS AND SUGGESTIONS FOR FURTHER STUDIES

The present experimental set up was designed to accommodate future modifications to cover as many other parameter studies as possible. Parameters to be studied, suggestions of test cell controls and other instrumentation are proposed in this chapter.

5.1 Other parameters to be studied

(a) Cooling air flow rate - the cooling air effect could possibly be controlled by additional cooling controll devices such as fans, blowers, and air temperature regulating devices. This parameter is considered important in CST studies.

(b) Lubricants and additives - the effect of various lubricants and additives as well as their mixing rate might be another significant factor in CST studies. This factor is discussed in appendix A.

(c) Spark timing - CST might be analysed further through the change of spark timing. It is generally expected that advancing the spark timing (earlier ignition) will decrease the CST due to the change of combustion gas temperature, although this is not clearly known and should be the subject for future studies.

(d) Free-convection - it might be meaningful to measure the CST without the cooling fan and the cooling air shroud from the view point of practical application of this type of engine. The application of this type of engine in the snowmobile industry sometimes does not include the use of cooling fans.

5.2 Test cell controls

(a) Test cell temperature - the test cell temperature should be controllable. This might require modifications to the existing test cell temperature control system. It could also be achieved by the installation of an air-conditioner in the test cell. Neither of these methods, of course, could be used to reduced the cell temperature to simulate winter conditions. A simple way to simulate the winter conditions is to induct cooling air from outside the building. With this control available, it would be possible to study the ambient temperature effect on the CST.

(b) Exhaust system - the existing exhaust system is not sucking gas from engine exhaust. Unless a fan is installed in the exhaust system, other approaches should be considered.

5.3 Instrumentation for further studies

(a) Engine analyzer - an engine analyzer and its accessories such as a rotational function generator, a pressure transducer, a charge amplifier etc. should be provided for better performance analysis.

(b) Viscometer and oil bath - it will be most convenient to have this kind of equipment for the study of two-stroke cycle engine lubrication problems and fuel flow measurements.

(c) Air-flow measuring device - intake air measurement was a problem in the present investigation. This is discussed in detail in appendix C. It is therefore suggested that a carefully selected air-flow measuring device be added to give accurate air-flow measurements at all operating conditions. The device thus selected should include a big pressure damping chamber and a large outlet to avoid an inadequate intake-air supply and/or interference with the engine performance.

APPENDIX A

SOME FINDINGS ON ENGINE OPERATING PROBLEMS AND THEIR RELATIONSHIP WITH LUBRICANT AND CST IN TWO-CYCLE S.I. ENGINES

In past years, oil companies and engine manufacturers have been looking for the ideal lubricant to be used in two-cycle S.I. engines. This lubricant must reduce sliding friction of the working parts to a minimum. It must have good load-carrying properties at high temperatures. It must have "wetting" properties and it must form an adsorbed film to seal the piston rings and prevent blow by. It must burn cleanly, leaving minimum deposits which should be soft. For these purposes, different base stocks were tested and various additives were added to investigate their effects on two-cycle S.I. engine problems. In the following paragraphs, a list of engine operating problems, their relations with lubricants and additives, and the temperature effects are given.

A.1 Piston seizure

As the temperature of cylinder wall increases, the temperature of the lubricant film increases as well and its viscosity and load carrying ability drop. This trend leads to the point of surface contact. The increased friction causes the engine speed to decrease and generates additional heat in rubbing surfaces which in turn accelerates the overall process. This condition is threshold to seizure and is referred to as piston seizure.

A.1.1 Lubricant and piston seizure - The viscosity of the lubricant at 400°F or above obviously affects piston seizure. In order to maintain sufficient viscosity at these high temperatures, V.I. improvers or other additives should be added to prevent piston seizure.

A.1.2. Tightening temperature and piston seizure - Higher tightening temperature prevents piston seizure to a great extent. It was found that oils with higher viscosity are more desirable. The behavior of oils showed that in general a higher oil viscosity results in a higher tightening temperature (26).

A.2. Piston varnish

The oxidation of a lubricating oil often leads to the formation of oil-insoluble products. These products are sometimes found as particles which settle from the oil in the form of sludge, or as lacquer, or varnish like, coatings on the piston surface. Moreover, the composition of the fuel also plays a major portion in the formation of oil-insolubles.

A.2.1 Lubricant composition and piston varnish - Lubricants high in aromatics and sulfur form more insoluble oxidation products. This is particularly true of highly polar aromatics having a condensed ring structure (27). Various additives also affect the formation of insolubles.

A.2.2 Temperature as a role in piston varnish - The effect of temperature upon the formation of oil-insolubles from the oil can be explained by the well known exponential relation between temperature and the rate of oxidation. From this standpoint, low operating temperatures are desirable.

A.3 Piston wear

The undesirable separation of materials caused by sliding friction is called wear. This type of friction usually proceeds in accord with Coulomb's law of dry friction, which is wholly independent of surface pressure and sliding velocity and only dependent on the condition of the sliding surface.

A.3.1 Lubricant film and piston wear - The lubricating oil which impinges on the cylinder walls being swept by the piston must retain its film strength sufficiently to lubricate satisfactorily the piston skirt proper and, also, to lubricate the piston rings in their facial contact with cylinder wall in order to avoid wear caused by dry friction.

A.3.2 CST and piston wear - The CST is often at a high level, which will definitely cause degradation or decomposition of the lubricating oil that impinges on the wall and this will cause wear. To overcome this problem, oils with good thickening properties and strong chain construction of molecules were recommended by Hass (22) and McReynolds and Holman (23).

A.4 Ring gumming (or ring sticking)

The ring being held and prevented from fully performing its function as a gas seal leads to excessive blow-by and loss of power. Experiments conducted by Pugh (28) revealed that ring gumming was accelerated at high piston temperature.

A.5 Spark plug misfire (or spark plug fouling)

Colyer and Sieker (29) mentioned that high power output leads to high CST. This might consequently increase the tendency for spark plug misfire.

In general, leaner fuel-oil ratios lessen spark plug misfire (30). Additives or unleaded gasoline could also be used to eliminate misfire.

The spark plug gasket temperature could be a very good indication for the spark plug misfire.

A.6 Exhaust port plugging (or exhaust port clogging)

Sytz and Izumi (31) believed that the engine deposits sould be related to port plugging. Deposits arise mainly from oil and fuel degradation which are due to the high CST. Additives could be used to eliminate the cause of deposition.

A.7 Preignition

High combustion chamber temperature often causes preignition. Haas (22) mentioned that deposits remaining on the piston crown tend to produce preignition. He suggested the use of ashless additives in base stocks in the SAE 30 to SAE 50 range to eliminate the preignition problem.

The spark plug gasket temperature, pressure transducer and cylinder combustion chamber gas temperatures might be used to indicate preignition.

APPENDIX B

CONVERSION CURVES FOR FUEL-OIL FLOW MEASUREMENT

The equations for the calculation of the conversion curves for fuel-oil flow measurement from "Manostat" catalog are:

Net weight of immersed float:

$$F = W(\rho_f - \rho)/\rho_f \tag{B.1}$$

Viscosity influence number:

$$N = \mu/(F\rho)^{\frac{1}{2}} \tag{B.2}$$

Constant C:

$$C = 453.6\ D_f(F\rho)^{\frac{1}{2}}/\rho_o \tag{B.3}$$

Standard ml/min for each value of K, the rate of flow:

$$V_o = CK \tag{B.4}$$

where ρ is the density of fluid in gms/ml at condition of flow.

ρ_f is the density of float in gms/ml from Manostat catalog.

ρ_o is the density of fluid in gms/ml at standard condition (70°F).

W is the weight of float in gms from Manostat catalog.

D_f is the diameter of float in inches from Manostat catalog.

By knowing N from Eq. (B.2), K values against the tube readings could be determined from a predictability chart supplied by the manufacturer. Again, from Eq. (B.4), the flow rates corresponding to the tube readings were computed and plotted. The detail computation for various fuel-oil ratios is summarized in Table B.1 and Table B.2.

APPENDIX C

AIR FLOW MEASUREMENT

An attempt is made to measure the intake air for the Kohler K440-2AX engine during the present investigation. The equipment being used is an orifice type air-container. Air flows through the orifice opening to the container and finally goes to the carburetor for mixing. The pressure difference across the orifice plate could then be read by a manometer and thereafter converted to flow rate (see Fig. C.1).

The conversion of the manometer reading to CFM was then calibrated by the traversing pitot tube method. Direct measurements of the velocity profiles in a fully developed region were obtained. A plot of one of these velocity profiles is shown in Fig. C.2. Two sets of readings from two identical pitot tubes were obtained and showed only slight deviations. This calibration was done on an instrument set up by Dr. S. D. Park of our department as shown in Fig. C.3 (32).

It was subsequently found during the running of the engine tests that the air container used is insufficient in volume to provide adequate pressure damping for the engine at outputs higher than 10 Bhp. However, the intake air flow rates were recorded at low speed and low bmep. They were used to find the air fuel ratios at various loadings and speeds. The results are shown in Fig. C.4.

Modification on the existing air container is not practical. Owing to the limitation of time, it was not feasible idea to buy another instrument such as the Go-power measuring device, orifice type meters etc. Other methods have also been taken into consideration. A wet test meter and a vane type mean velocity instrument both appeared unfeasible when applied to a discontinuous flow measurement.

APPENDIX D

POSSIBILITY OF PRESSURE LEAKAGE THROUGH THE CYLINDER WALL DUE TO INSTALLATION OF CO-AXIAL THERMOCOUPLES.

The cylinder wall was tapped for the installation of the co-axial surface thermocouples. Hence, there exists a possibility of pressure leakage through the tolerance between the internal and external threads. In order to eliminate this possibility, graphite powder was used to seal the tolerance. A calculation based on an energy balance was done and the result shows negligible leakage. This was confirmed when the author was measuring the engine performance as mentioned in section 2.2.4.

The model used for this calculation is a stretched passageway with its length equal to the length of the helical passageway between the cylinder block and the co-axial surface thermocouple threads. The energy balance equation used is (known as Bernoulli's equation) as follows:

$$p^o/\rho^o + V^{o2}/2g = p'/\rho' + V'^2/2g + h_f g/g_c \qquad (D.1)$$

where
- o designates the conditions at the inside wall surface.
- ' designates the conditions at the outside wall surface.
- p is the pressure.
- ρ is the density of the lubricant being pushed through the tolerance
- h_f is the friction head which is given in the equation below.

$$h_f = 64LV'^2 g_c/(R_e D2g) \qquad (D.2)$$

Where L is the equivalent length of the helical passageway.

D is the equivalent diameter of the area between the internal and external threads.

This calculation is based on extreme conditions such as maximum pressure, maximum area, straight passageway and so on. Result shows velocity at exit is about 1,500 in/sec, i.e.

$$V' = (-32\mu L/(\rho D^2) + ((-32\mu L/(\rho D^2))^2 + 2\Delta p/(\rho g))^{\frac{1}{2}}) \times g$$

$$\doteq 1,468 \quad \text{in/sec}$$

Data for the above calculation is listed below.

ρ = 0.0298 lb/in^3

L = 3.91 in.

μ = 3231.25 lb-sec/in^2

D = 0.7569×10^{-2} in.

Δp = 485.3 lb/in^2

g = 386.4 in/sec^2

Multiplying the velocity obtained by the cross-sectional area of the passageway, the volume flow rate is obtained.

Volume flow rate = V' x A = 0.066 in^3/sec.

For engine running at 1,000 rpm or 1,000/60 cycle/sec, the leakage flow per cycle is 0.0039 in^3/cycle. This is approximately 0.03% of the volume of the cylinder, therefore the pressure leakage can be neglected.

Table 2.1 Engine Specification (Kohler K440-2AX)

MODEL:	Kohler K440-2AX air-cooled, two-stroke, loop scavenged.
MAX. Bhp at rpm:	36/6500
DISPLACEMENT:	26.6 cu. in., 436 ccm
BORE:	2.677 in., 68 mm
C.R.:	7.8 : 1
CYLINDERS:	Die cast aluminum with cast iron sleeves, two cylinders.
IGNITION:	Low tension flywheel magneto with external high tension coils.
CARBURECTOR:	Walbro model WR
DIRECTION of Rotation :	CCW view from P.T.O.
FUEL USED:	Fina regular plus Fina Poly-B snowmobile oil.
FLYWHEEL RING GEAR :	Yes.
ELECTRIC STARTER:	12 Volt Bendix starter and rectifier.
MUFFLER:	ACS 1804-31A with Y manifold.

Table 2.2 Calibration of Thermocouples

TC TYPE	TC No.	READ mv	CONVT °F	READ mv	CONVT °F	READ mv	CONVT °F	READ mv	CONVT °F	READ mv	CONVT °F
J	A	0	32	3.01	136.4	3.65	158	4.25	178.2	5.21	210.2
	B	0	32	2.99	135.6	3.65	158	4.26	178.4	5.21	210.2
	C	0	32	3.00	136	3.64	157.6	4.26	178.4	5.23	210.7
K	1	0	32	2.34	136	2.85	158	3.32	178.5	4.05	209.8
	2	0	32	2.34	136	2.84	157.6	3.30	177.8	4.04	209.6
T	1	0.01	32.3	2.37	135.9	2.91	158.2	3.41	178.2	4.23	210.2
	2	0	32	2.36	135.4	2.92	158.5	3.40	177.7	4.22	209.7
	3	0.02	32.5	2.39	136.8	2.92	158.5	3.43	178.8	4.22	209.7
	4	0	32	2.35	135.2	2.90	157.7	3.40	177.7	4.22	209.7
	5	0.02	32.5	2.36	135.4	2.92	158.5	3.39	177.3	4.23	210.2
	6	0	32	2.37	135.9	2.92	158.5	3.41	178.2	4.22	209.7
	7	0.01	32.3	2.37	135.9	2.92	158.5	3.41	178.2	4.22	209.7
	8	0.01	32.3	2.37	135.9	2.90	157.7	3.40	177.7	4.24	210.6
	9	0	32	2.39	136.8	2.90	157.7	3.40	177.7	4.22	209.7
	10	0.02	32.5	2.34	134.7	2.92	158.5	3.40	177.7	4.21	209.4
	11	0.02	32.5	2.36	135.4	2.90	157.7	3.41	178.2	4.22	209.7
	12	0.01	32.3	2.36	135.4	2.92	158.5	3.40	177.7	4.23	210.2
	13	0.01	32.3	2.37	135.9	2.92	158.5	3.42	178.5	4.23	210.2
	14	0	32	2.36	135.4	2.89	157.3	3.40	177.7	4.23	210.2
	15	0	32	2.36	135.4	2.92	158.5	3.41	178.2	4.22	209.7
	16	0	32	2.36	135.4	2.92	158.5	3.41	178.2	4.23	210.2
STANDARD TEMPERATURE			32		136		158		178		210

Note: Standard temperature is measured by thermometer made by Fisher Scientific. Deviation of the thermometer reading is .5 of the sub-division (33). In this experiment, .5°F.

Table 3.1 Precautions for Engine Tests

Before starting the engine

(a) water supply to keep at 40 $\pm$ 2 psi.

(b) set dynamometer at no load.

(c) water outlet to be at almost closed position.

(d) set the potentiometer.

During engine test run

(a) keep spark plug temperature below 500°F.

(b) keep dynamometer outlet water below 135°F.

After engine shut-off

(a) unload dynamometer.

(b) open drain cock on dynamometer.

(c) turn water supply valve off.

Table 3.2 An Example of Repeatability of CST Data

TEST No.	CO-AXIAL TC (^{o}F) A	B	C
7	419	363	380
16	346	323	325
29	302	276	282
30	326	301	311
31	388	352	362
52	410	362	373
62	394	366	365
64	403	346	356
101	419	364	386
102	415	380	381
104	399	378	384
111	306	278	290
117	375	342	344
129	384	348	356

Note: These test data were obtained at engine speed of 3,600 rpm and F/O = 20.

Table 3.3 Limits of Error for Thermocouples

TC TYPE	TEMPERATURE RANGE (^{o}F)	STANDARD LIMIT OF ERROR
T	+200 --- +700	± 3/4 %
J	0 --- +600	--
K	530 --- 2300	± 3/4 %

Table 3.4 Operating Conditions for Test Runs

TEST No.	F/O	SPEED rpm	LOAD lb	BHP hp	FUEL FLOW ml/min	BSFC lb/hp-hr	η_{th} %	BMEP psi
49	20	3000	2.1	1.58	12	0.73	18	7.84
41	20	3000	2.76	2.07	13.4	0.64	21	10.27
12	20	3000	4.3	3.23	18	0.56	24	16.01
61	20	3000	6.2	4.65	23	0.49	27	23.07
131	20	3000	6.5	4.88	30	0.6	22	24.19
42	20	3000	6.7	5.03	31	0.61	22	25
132	20	3000	8.1	6.08	40	0.65	21	30.15
133	20	3000	9.35	7.01	55	0.78	17	34.8
56	20	3000	10.6	7.95	64	0.8	17	39.65
134	20	3000	10.9	8.18	84	1.02	13	40.38
45	20	3000	12.8	9.6	93	0.96	14	47.64
34	20	3400	2.4	2.04	15	0.72	19	8.75
35	20	3400	5	4.25	28	0.65	21	18.61
118	20	3400	5.8	4.93	29.3	0.59	23	21.4
130	20	3400	6.1	5.19	34	0.65	21	22.7
57	20	3400	6.6	5.61	26.5	0.47	29	24.56
103	20	3400	7	5.95	44	0.73	18	26.05
60	20	3400	8.3	7.06	42.7	0.6	22	30.71
50	20	3400	8.7	7.4	60	0.81	17	32.4
58	20	3400	10	8.5	72	0.84	16	37.22
38	20	3400	11.4	9.7	81	0.83	16	42.43
40	20	3400	14	11.9	108	0.9	15	51.93
29	20	3600	2	1.8	8	0.45	30	7.36
111	20	3600	2.1	1.89	10	0.54	25	7.82
30	20	3600	3	2.7	14	0.52	26	11.33
16	20	3600	4.1	3.69	23	0.63	21	15.38
117	20	3600	5.37	4.77	29	0.6	22	19.73
129	20	3600	5.7	5.13	33	0.64	21	21.21
31	20	3600	6	5.4	37	0.68	20	22.33
52	20	3600	6.6	5.94	38.3	0.64	21	24.56
7	20	3600	7	6.3	39.4	0.62	22	26.05

cont.

Table. 3.4 Operating Conditions for Test Runs (cont.)

TEST No.	F/O	SPEED rpm	LOAD lb	BHP hp	FUEL FLOW ml/min	BSFC lb/hp-hr	η_{th} %	BMEP psi
101	20	3600	7.1	6.39	41	0.63	21	26.54
102	20	3600	7.6	6.84	50	0.73	18	28.29
104	20	3600	9.4	8.46	101	1.18	11	34.98
62	20	3600	10.5	9.45	108	1.13	12	38.91
64	20	3600	13	11.7	120	1.01	13	48.38
113	20	4000	2.2	2.2	16	0.7	19	8.23
116	20	4000	4.4	4.4	27	0.61	22	16.5
128	20	4000	5.3	5.3	29	0.55	24	19.61
125	20	4000	6.3	6.3	37	0.58	23	23.5
46	20	4000	6.5	6.5	38	0.58	23	24.19
21	20	4000	6.7	6.7	39	0.57	24	25
119	20	4000	7.7	7.7	43	0.55	24	28.66
47	20	4000	8.2	8.2	59	0.71	19	30.63
54	20	4000	8.9	8.9	97	1.08	12	33.31
121	20	4000	9.5	9.5	92	0.96	14	35.36
112	20	4000	10	10	93	0.92	15	37.22
105	20	4000	10.9	10.9	133	1.21	11	40.57
18	20	4000	13	13	155	1.18	11	48.38
115	20	4200	4.5	4.73	29	0.61	22	16.75
79	20	4200	5.9	6.2	34	0.55	24	21.59
109	20	4200	6	6.3	35	0.55	24	22.15
126	20	4200	6.3	6.62	38	0.57	24	23.45
20	20	4200	7.5	7.88	43	0.54	25	27.93
85	20	4200	8.2	8.61	61	0.7	19	30.52
67	20	4200	9.2	9.66	81	0.83	16	34.06
86	20	4200	10	10.5	116	1.1	12	37.22
106	20	4200	11	11.55	139	1.19	11	40.94
87	20	4200	13	13.65	134	0.97	14	48.38
89	20	4200	14.3	15.02	133	0.88	15	53.28
114	20	4500	3.8	4.28	28	0.65	21	14.14

Table 3.4 Operating Conditions for Test Runs (cont.)

TEST No.	F/O	SPEED rpm	LOAD lb	BHP hp	FUEL FLOW ml/min	BSFC lb/hp-hr	η_{th} %	BMEP psi
110	20	4500	4.3	4.84	31	0.63	21	16.08
108	20	4500	6.3	7.09	39	0.55	24	23.45
22	20	4500	6.9	7.76	40	0.51	26	25.8
73	20	4500	7.3	8.21	41	0.5	27	27.16
74	20	4500	8.5	9.56	55	0.57	24	31.63
99	20	4500	9	10.13	60	0.59	23	33.5
91	20	4500	10.9	12.26	87	0.85	16	40.5
90	20	4500	13	14.63	152	1.03	13	48.41
81	20	4500	14	15.75	160	1.01	13	52.11
98	20	4600	4.1	4.72	28	0.58	23	15.2
96	20	4600	5.4	6.21	39	0.63	21	20
77	20	4600	6.8	7.82	52	0.66	20	25.31
65	20	4600	8.2	9.43	65	0.68	20	30.4
24	20	4600	8.9	10.24	63	0.61	22	33
76	20	4600	9.5	10.93	66	0.6	22	35.3
9	20	4600	11.3	13	135	1.03	13	42.2
97	20	4600	13	14.95	163	1.08	12	48.38
55	20	4600	14.5	16.68	177	1.05	13	54.1
100	20	5000	3.2	4	33	0.81	17	11.91
84	20	5000	4.8	6	45	0.75	18	17.87
95	20	5000	8	10	65	0.64	21	29.89
88	20	5000	9.4	11.75	81	0.68	20	35
94	20	5000	10	12.5	103	0.82	16	37.22
75	20	5000	15	18.75	181	0.96	14	55.83
83	20	5000	15.4	19.25	182	0.94	14	57.32
92	20	5000	16	20	202	1.0	13	59.55
93	20	5000	17	22.1	223	1.0	13	63.27
216	40	3400	6	5.1	23	0.45	30	22.15
202	40	3400	7.7	6.55	37	0.56	24	28.7
220	40	3400	10.8	9.18	85	0.92	15	40.27
203	40	3600	5.7	5.13	28	0.55	24	21.33
223	40	3600	7.25	6.53	32	0.49	27	27

Table 3.4 Operating Conditions for Test Runs (cont.)

TEST No.	F/O	SPEED rpm	LOAD lb	BHP hp	FUEL FLOW ml/min	BSFC lb/hp-hr	η_{th} %	BMEP psi
208	40	3600	7.8	7.02	37	0.52	26	29.03
219	40	3600	10.8	9.72	86	0.88	15	40.2
213	40	4000	4.8	4.8	27	0.56	24	17.87
204	40	4000	5.3	5.3	28	0.52	26	19.73
207	40	4000	6.6	6.6	42	0.63	21	24.75
210	40	4000	7.4	7.4	43	0.57	24	27.73
209	40	4000	7.6	7.6	44	0.58	23	28.21
211	40	4000	9.1	9.1	74	0.81	17	33.87
218	40	4000	10.5	10.5	99	0.94	14	39.15
214	40	4200	4.9	5.15	28	0.54	25	18.2
205	40	4200	5.2	5.46	32	0.59	23	19.54
206	40	4200	6.5	6.83	34	0.5	27	24.27
221	40	4200	7.4	7.77	45	0.57	24	27.73
212	40	4200	8.9	9.35	82	0.87	15	33.12
217	40	4200	10.2	10.71	106	0.98	14	37.78
313	60	3000	3.2	2.4	19	0.8	17	11.91
309	60	3000	5.6	4.2	26	0.61	22	20.84
317	60	3000	6.8	5.1	29	0.57	24	25.35
326	60	3000	7.3	5.48	36	0.65	21	27.24
323	60	3400	1	0.85	8.7	1.02	13	3.72
324	60	3400	2.5	2.13	17	0.81	17	9.31
325	60	3400	5.1	4.34	24	0.55	24	18.98
327	60	3400	7.4	6.29	40	0.63	21	27.54
328	60	3400	8.3	7.06	45.5	0.64	21	30.89
312	60	3600	3	2.7	18.8	0.69	19	11.17
308	60	3600	5.3	4.77	31.3	0.65	21	19.73
316	60	3600	6.5	5.85	33	0.56	24	24.21
303	60	3600	7.1	6.39	48	0.75	18	26.43
329	60	3600	7.7	6.93	41	0.59	23	28.66
311	60	4000	1.7	1.7	14	0.82	16	6.33
306	60	4000	4.5	4.5	31	0.68	20	16.75

Table 3.4 Operating Conditions for Test Runs (cont.)

TEST No.	F/O	SPEED rpm	LOAD lb	BHP hp	FUEL FLOW ml/min	BSFC lb/hp-hr	η_{th} %	BMEP psi
305	60	4000	5.6	5.6	33	0.59	23	20.84
315	60	4000	6.2	6.2	35	0.56	24	23.11
301	60	4000	7	7	40	0.57	24	26.05
334	60	4000	8.1	8.1	57	0.7	19	30
304	60	4000	8.5	8.5	61	0.71	19	31.64
336	60	4000	9.1	9.1	85	0.93	15	34
331	60	4000	10.3	10.3	98	0.94	14	38.5
321	60	4000	12	12	113	0.93	14	44.66
307	60	4200	4.8	5.04	22	0.65	21	17.87
314	60	4200	6	6.3	40	0.63	21	22.33
302	60	4200	6.7	7.03	47	0.66	20	24.94
337	60	4200	7.8	8.2	59	0.71	19	29
310	60	4200	8.9	9.33	75	0.8	17	33.13
330	60	4200	9.4	9.87	91	0.91	15	35
318	60	4200	10.2	10.71	105	0.97	14	37.96
320	60	4200	12	12.6	130	1.02	13	44.66
322	60	4600	4.5	5.18	35	0.67	20	16.75

Table 3.5 Test Data of CST and Exhaust Gas Temperature

TEST	CO-AXIAL SURFACE TC (^{o}F)			EXHAUST GAS TC (^{o}F)	
No	A	B	C	1st CYL.	2nd CYL.
49	287	276	270	811	778
41	302	290	288	842	879
12	338	320	315	926	920
61	381	342	343	995	968
131	386	345	347	1010	990
42	389	347	352	985	997
132	403	362	358	1020	989
133	408	367	360	992	946
56	393	358	355	901	885
134	388	354	354	895	866
45	392	378	373	925	925
34	296	282	280	858	879
35	368	333	334	1018	1031
118	382	342	345	1010	1000
130	386	344	347	1074	1033
57	400	351	359	1043	1036
103	403	357	360	1094	1110
60	418	374	376	1099	1099
50	417	377	380	1100	1100
58	404	386	386	1133	1133
38	394	375	376	977	963
40	404	372	355	845	854
29	302	276	282	863	820
111	306	278	290	883	840
30	326	301	311	926	973
16	346	323	325	1011	1011
117	375	342	344	1031	1031
129	384	348	356	1074	1074
31	388	352	362	1052	1112
52	410	362	373	1094	1094
77	419	363	380	1112	1112

Table 3.5 Test Data of CST and Exhaust Gas Temperature (continuation)

TEST No.	CO-AXIAL SURFACE TC (°F) A	B	C	EXHAUST GAS TC (°F) 1st CYL.	2nd CYL.
101	419	364	386	1137	1115
102	415	380	381	1122	1094
104	399	378	384	1031	1010
62	394	366	365	951	942
64	403	346	356	924	903
113	312	290	293	883	883
116	360	330	337	1025	1025
128	382	346	350	1112	1098
125	408	363	369	1158	1158
46	415	372	376	1112	1145
21	420	379	379	1128	1196
119	453	385	396	1179	1163
47	446	388	394	1121	1128
54	424	382	385	1098	1086
121	405	378	380	1074	1074
112	395	371	373	1060	1080
105	405	364	364	1010	1010
18	399	360	357	1052	1052
115	366	338	342	1031	1031
79	398	352	362	1086	1086
109	402	358	367	1179	1137
126	416	370	374	1158	1158
20	438	390	397	1124	1158
85	462	396	399	1205	1191
67	430	385	386	1187	1184
86	402	367	369	1031	1002
106	402	358	362	1012	1010
87	422	375	381	960	935
89	444	378	365	995	971
114	363	326	334	968	989

Table 3.5 Test Data of CST and Exhaust Gas Temperature (continuation)

TEST No.	CO-AXIAL SURFACE TC (^oF) A	B	C	EXHAUST GAS TC (^oF) 1st CYL.	2nd CYL.
110	375	338	347	1037	1031
108	420	378	390	1079	1185
22	443	394	399	1133	1193
73	457	399	403	1158	1178
74	470	413	416	1158	1193
99	475	419	420	1203	1210
91	455	391	400	1150	1150
90	430	378	386	1120	1120
81	423	382	385	952	952
98	398	338	342	956	956
96	432	375	383	1158	1150
77	466	406	401	1196	1167
65	474	420	426	1205	1148
24	480	427	428	1225	1225
76	476	425	424	1205	1158
9	442	390	385	1133	1133
97	425	394	383	1124	1120
55	432	387	390	1021	990
100	426	380	381	990	985
84	454	405	410	1124	1149
95	501	432	430	1222	1232
88	508	434	435	1261	1261
94	504	432	435	1232	1258
75	433	389	399	1011	1011
83	431	384	390	995	995
92	454	370	381	980	1023
93	466	380	373	993	993
216	384	340	350	1074	1052
202	414	362	369	1120	1052
220	376	327	337	980	910
203	386	350	354	1094	1074

Table 3.5 Test Data of CST and Exhaust Gas Temperature (continuation)

TEST No	CO-AXIAL SURFACE TC (°F) A	B	C	EXHAUST GAS TC (°F) 1st CYL.	2nd CYL.
223	422	375	383	1124	1120
208	420	382	384	1137	1108
219	380	352	356	989	960
213	376	343	347	1100	1100
204	383	350	356	1115	1115
207	422	382	384	1158	1137
210	450	389	396	1208	1201
209	460	392	400	1201	1190
211	434	379	380	1150	1137
218	393	356	359	1066	1035
214	384	346	354	1120	1115
205	396	352	360	1118	1121
206	439	380	386	1179	1185
221	462	392	399	1208	1208
212	442	385	390	1145	1141
217	396	366	370	1076	1052
313	310	283	295	930	950
309	362	328	340	1052	1052
317	397	342	350	1094	1052
326	405	360	363	1137	1074
323	259	239	244	528	536
324	297	276	278	824	820
325	367	332	334	994	968
327	414	365	365	1074	1028
328	440	380	383	1052	989
312	323	308	314	925	950
308	381	352	356	1061	1080
316	410	370	380	1098	1094
303	425	377	386	1115	1104
329	433	384	385	1158	1074
311	290	280	285	883	905

Table 3.5 Test Data of CST and Exhaust Gas Temperature (continuation)

TEST No	CO-AXIAL SURFACE TC (^{o}F) A	B	C	EXHAUST GAS TC (^{o}F) 1st CYL.	2nd CYL.
306	370	340	346	1094	1115
305	396	362	370	1120	1140
315	420	376	386	1130	1162
301	443	400	407	1185	1185
334	457	398	404	1203	1209
304	451	394	396	1158	1162
336	428	386	386	1099	1093
331	390	359	364	1104	1104
321	393	336	340	1010	1010
307	386	346	354	1094	1108
314	430	380	387	1137	1158
302	446	385	402	1222	1203
337	461	406	417	1209	1209
310	445	400	409	1150	1179
330	422	390	392	1092	1092
318	396	370	370	1080	1080
320	399	358	367	1031	1000
322	425	375	378	1110	1115

Table 3.6 External Cylinder Surface Temperature Test Data

TEST No	EXTERNAL CYLINDER SURFACE THERMOCOUPLES (°F) 1	2	3	4	5	6	7	9	10	11	12	13	14	15	16
49	254	258	252	261	192	241	262	229	258	211	240	261	253	241	241
41	274	274	283	283	191	272	276	226	276	201	254	312	271	256	260
12	297	299	306	304	214	297	302	254	295	243	283	306	294	277	294
61	306	318	324	320	222	302	317	272	328	257	285	316	311	284	297
131	315	323	324	324	234	303	322	281	330	264	290	324	322	306	310
42	323	323	336	333	226	330	327	267	337	260	294	326	325	302	314
132	322	331	332	331	228	313	328	267	336	262	301	333	330	310	319
133	324	332	332	331	230	316	329	273	340	266	301	330	328	311	323
56	324	333	339	331	235	321	331	285	342	272	296	327	323	298	317
134	310	317	318	313	203	302	311	265	344	261	294	333	328	295	310
45	345	345	358	347	234	369	354	274	371	280	302	337	340	317	353
34	268	267	277	277	191	266	271	231	275	218	250	275	265	249	253
35	308	304	318	317	214	306	311	257	320	249	284	318	304	286	289
118	306	316	322	325	221	330	323	268	327	255	295	326	310	301	297
130	316	324	330	328	235	304	326	272	337	271	300	330	324	310	308
57	328	335	344	346	240	326	342	284	348	274	306	338	343	312	320
103	326	338	346	346	244	321	342	283	355	280	306	340	338	316	320
60	326	338	348	348	240	329	339	286	360	277	312	337	338	310	323
50	344	350	337	356	250	337	355	297	364	288	318	350	347	322	336
58	335	345	353	348	246	337	347	296	363	284	310	341	343	315	337
38	342	340	354	346	232	355	340	283	368	265	306	339	338	312	335
40	343	341	356	341	232	357	335	286	385	280	307	340	338	311	341
29	258	255	266	263	190	256	266	222	273	212	238	265	261	243	243
111	265	266	275	283	196	252	278	235	281	220	248	286	280	258	260
30	284	283	296	297	206	287	294	248	297	228	267	296	291	265	268
16	298	297	308	305	209	295	301	250	302	238	276	306	293	275	286
117	303	311	314	324	215	295	320	262	301	248	281	314	306	289	296
129	319	323	322	334	217	304	329	262	326	251	287	325	317	308	303
31	320	320	334	337	225	324	329	271	340	256	299	333	327	302	312
52	325	328	329	336	226	331	332	283	343	272	298	332	338	308	324
7	338	340	351	351	237	348	348	291	361	284	317	351	343	311	338
101	338	340	348	357	236	340	357	301	361	286	322	344	350	321	338

Table 3.6 External Cylinder Surface Temperature Test Data (continuation)

TEST No	EXTERNAL CYLINDER SURFACE THERMOCOUPLES (°F) 1	2	3	4	5	6	7	9	10	11	12	13	14	15	16
102	345	346	347	346	241	330	350	298	347	275	312	338	345	308	317
104	333	339	344	343	243	318	348	280	340	256	305	319	325	300	308
62	320	332	317	328	217	293	332	267	319	248	282	309	300	274	292
64	321	323	329	329	227	312	328	271	345	268	287	319	314	287	309
113	265	272	263	278	196	253	274	229	273	206	244	265	260	248	253
116	303	311	301	327	201	292	324	243	310	243	275	302	295	286	302
128	314	324	317	336	213	303	332	252	322	251	281	311	304	301	300
125	323	332	325	341	216	333	340	258	327	268	288	317	310	308	311
46	340	347	329	345	219	340	350	263	335	279	288	323	320	292	301
21	351	347	365	365	247	360	360	293	370	284	320	356	348	327	342
119	348	358	353	351	243	343	368	288	375	280	314	355	347	328	348
47	345	350	360	365	245	358	359	283	380	277	311	352	325	324	337
54	345	355	358	355	253	350	356	299	375	294	319	350	348	327	343
121	342	346	340	347	250	338	352	278	370	292	319	347	342	322	342
112	337	343	338	344	244	327	343	271	366	282	305	323	319	315	337
105	321	323	317	323	219	313	321	266	354	278	298	312	312	306	321
18	326	342	348	332	224	334	334	266	331	260	298	323	325	300	320
115	304	313	327	329	220	293	324	260	339	251	292	335	325	300	303
79	322	323	332	337	231	309	330	272	343	278	303	333	329	308	304
109	312	321	335	335	238	297	331	272	342	282	315	340	336	315	313
126	330	343	345	355	240	321	351	279	357	274	319	346	342	318	326
20	357	355	372	363	244	371	368	288	364	283	321	356	357	331	347
85	345	356	365	367	250	347	368	294	380	293	328	361	367	340	343
67	332	344	354	354	250	350	350	292	368	287	319	352	352	326	329
86	331	333	341	340	226	334	338	288	353	268	315	343	340	309	326
106	328	330	336	339	225	299	340	278	335	268	285	341	336	312	326
87	344	350	341	341	237	333	358	272	358	270	299	330	348	326	343
89	329	339	346	346	240	323	338	274	383	286	298	333	332	310	326
114	296	305	292	312	242	285	315	265	304	256	283	320	297	294	295
110	305	316	322	326	245	294	322	271	310	261	292	329	310	300	305
108	343	351	358	368	266	312	368	298	343	297	326	356	344	338	340
22	369	376	372	380	275	395	377	316	373	318	338	380	366	353	363

Table 3.6 External Cylinder Surface Temperature Test Data (continuation)

TEST	EXTERNAL CYLINDER SURFACE THERMOCOUPLES (^{o}F)														
No	1	2	3	4	5	6	7	9	10	11	12	13	14	15	16
73	357	368	360	386	248	357	380	288	380	311	334	381	368	340	349
74	366	370	364	384	248	363	380	286	383	331	344	374	366	349	352
99	375	376	366	388	251	369	389	270	386	340	350	376	370	368	372
91	365	372	360	378	252	370	374	284	362	337	342	378	360	341	357
90	344	350	362	362	257	356	360	286	358	312	321	354	340	339	340
81	338	349	345	361	239	325	360	277	328	295	316	344	333	325	330
98	309	314	318	320	203	287	318	254	311	257	283	325	314	303	308
96	348	349	350	357	252	325	350	273	357	274	319	369	353	341	348
77	343	346	350	352	265	344	358	275	357	278	339	366	353	340	344
65	384	390	389	393	280	381	389	310	381	325	362	390	382	380	388
24	392	406	404	405	306	394	397	329	390	341	356	389	394	387	395
76	389	404	401	394	299	402	400	324	382	338	357	394	382	387	389
9	357	358	371	366	253	378	369	302	365	327	329	373	352	347	362
97	357	362	364	362	266	330	358	302	358	329	333	364	350	349	361
55	346	355	361	358	252	343	358	301	338	298	319	351	353	328	345
100	348	349	342	337	263	347	349	255	350	306	311	349	333	327	340
84	351	365	375	381	274	360	382	298	386	316	328	365	369	356	358
95	378	381	368	371	299	354	371	314	375	354	349	377	378	351	351
88	378	384	381	376	310	355	375	314	380	366	350	382	380	354	348
94	350	366	368	368	288	362	372	306	372	337	343	356	351	344	347
75	356	360	356	373	248	343	363	302	373	308	324	350	349	330	349
83	346	354	354	366	244	341	362	315	375	301	323	340	340	322	348
92	335	342	357	359	240	335	358	299	369	295	320	335	336	316	330
93	354	361	369	355	258	348	358	297	399	312	324	341	345	338	341
216	307	313	320	325	200	286	328	220	338	252	271	328	328	303	305
202	337	339	337	346	238	321	340	268	351	277	297	329	331	313	321
220	301	298	307	310	225	277	312	231	327	248	270	298	310	298	300
203	321	331	338	335	238	317	332	268	348	274	294	327	333	314	316
223	324	329	332	334	240	318	332	268	348	279	295	327	335	309	309

Table 3.6 External Cylinder Surface Temperature Test Data (continuation)

TEST No	EXTERNAL CYLINDER SURFACE THERMOCOUPLES (°F) 1	2	3	4	5	6	7	9	10	11	12	13	14	15	16
208	352	360	349	366	245	320	358	283	363	282	306	340	340	316	314
219	328	332	339	339	236	305	338	271	351	279	302	344	346	320	324
213	305	313	321	328	231	300	326	258	346	255	285	329	335	300	303
204	325	334	340	330	242	318	335	273	353	276	302	333	338	317	316
207	345	354	362	368	252	346	363	283	375	292	317	348	365	339	348
210	350	356	369	379	260	348	367	293	382	292	316	358	360	342	348
209	350	356	376	381	260	332	375	288	389	294	315	380	379	345	347
211	348	348	366	358	257	347	357	278	368	298	325	362	357	340	343
218	332	338	340	338	244	315	336	262	341	274	307	341	343	326	330
214	310	318	323	329	230	301	328	259	329	271	297	350	350	307	308
205	328	335	345	341	246	319	347	280	355	304	339	340	332	317	316
206	342	351	361	365	250	340	364	285	369	285	316	351	361	336	338
221	360	368	370	374	279	335	372	301	381	300	325	381	376	350	356
212	357	366	354	374	248	336	371	279	368	294	316	357	357	349	353
217	335	343	352	352	231	313	350	263	356	297	316	343	344	333	334
313	262	267	274	278	199	254	275	219	278	224	243	268	274	263	258
309	301	310	315	318	225	296	313	248	324	258	275	305	314	297	303
317	310	319	324	324	232	310	322	250	349	272	282	313	325	305	312
326	324	328	339	339	240	324	331	266	360	283	293	326	335	315	328
323	2224	228	230	232	176	215	231	186	233	192	209	223	230	222	222
324	249	255	259	259	188	230	257	207	262	210	231	250	254	243	245
325	299	307	313	313	222	312	312	245	320	254	272	300	305	288	299
327	329	337	342	339	244	329	337	266	365	287	298	327	341	300	337
328	343	351	357	356	260	354	356	282	386	290	309	340	355	332	353
312	277	285	292	296	216	271	294	239	296	242	260	285	290	278	273
308	320	328	334	335	249	317	333	275	345	281	298	326	335	320	318
316	346	354	354	364	261	338	360	288	368	330	317	345	357	338	344
303	329	341	347	350	248	335	345	266	378	292	298	330	347	322	336
329	342	353	360	362	261	348	358	283	370	325	313	345	331	335	340
311	260	267	270	265	204	251	275	223	276	226	246	268	273	262	258

Table 3.6 External Cylinder Surface Temperature Test Data (continuation)

TEST No	EXTERNAL CYLINDER SURFACE THERMOCOUPLES (^{o}F) 1	2	3	4	5	6	7	9	10	11	12	13	14	15	16
306	317	323	327	329	239	296	326	265	336	268	293	322	329	309	307
305	337	340	354	354	255	332	352	285	359	288	311	342	354	332	334
315	338	344	353	369	260	333	366	288	366	293	313	345	353	335	332
301	379	382	388	388	283	369	386	314	391	320	343	379	368	364	368
334	385	385	390	389	300	370	382	314	388	322	339	381	370	372	372
304	356	362	364	368	255	353	365	299	362	301	317	350	350	347	351
336	338	340	344	346	250	335	347	280	350	284	298	332	334	329	330
331	315	318	323	320	246	309	312	275	318	275	281	308	308	312	315
321	305	314	320	315	221	294	323	246	337	261	274	302	313	294	305
307	323	328	337	329	249	315	325	276	348	280	305	334	340	322	318
314	344	354	357	361	258	330	358	288	267	294	315	349	354	337	333
302	344	362	360	372	265	340	372	286	380	300	326	361	362	348	344
337	386	385	390	392	287	317	385	312	386	321	355	380	362	377	380
310	378	386	380	386	294	366	384	304	391	333	358	374	381	379	375
330	350	355	358	358	261	343	352	285	355	309	334	346	357	355	352
318	335	342	347	354	247	355	353	274	359	285	300	333	330	321	327
320	328	335	344	346	243	330	347	269	358	284	295	326	333	315	326
322	319	322	333	337	230	306	319	251	351	268	291	322	337	315	316

Table B.1 Calculation Results of Fuel Flow Rates

FUEL-OIL RATIO		60:1	40:1	20:1
f	gm/ml	2.28	2.28	2.28
	gm/ml	0.7031	0.7177	0.7497
o	gm/ml	0.7031	0.7177	0.7497
W	gm	0.3055	0.3055	0.3055
D_f	in	0.25	0.25	0.25
t	sec	113.3	125.2	136.8
	poise/100	0.3306	0.3729	0.4256
F	gm	0.2113	0.2093	0.2051
F	gm^2/ml	0.1486	0.1502	0.1537
$(F\ )^{\frac{1}{2}}$		0.3854	0.3876	0.3921
N		0.8577	0.9620	1.0855
C		62.1648	61.2468	59.3056

Table B.2 Fuel Flow Rate Conversion

TUBE READING	V_o = CK ml/min 60:1	40:1	20:1
20	307.72	297.05	284.67
18	273.53	266.42	250.86
16	236.23	226.61	213.5
14	198.93	191.09	182.66
12	164.12	159.24	150.04
10	131.17	126.17	118.61
8	97.6	93.71	88.37
7	82.06	78.4	72.95
6	66.52	61.86	56.34
5	50.35	47.47	43.89
4	35.43	33.07	30.54
3	21.45	19.6	17.2
2	10.26	9	7.89
1	2.11	1.84	1.6

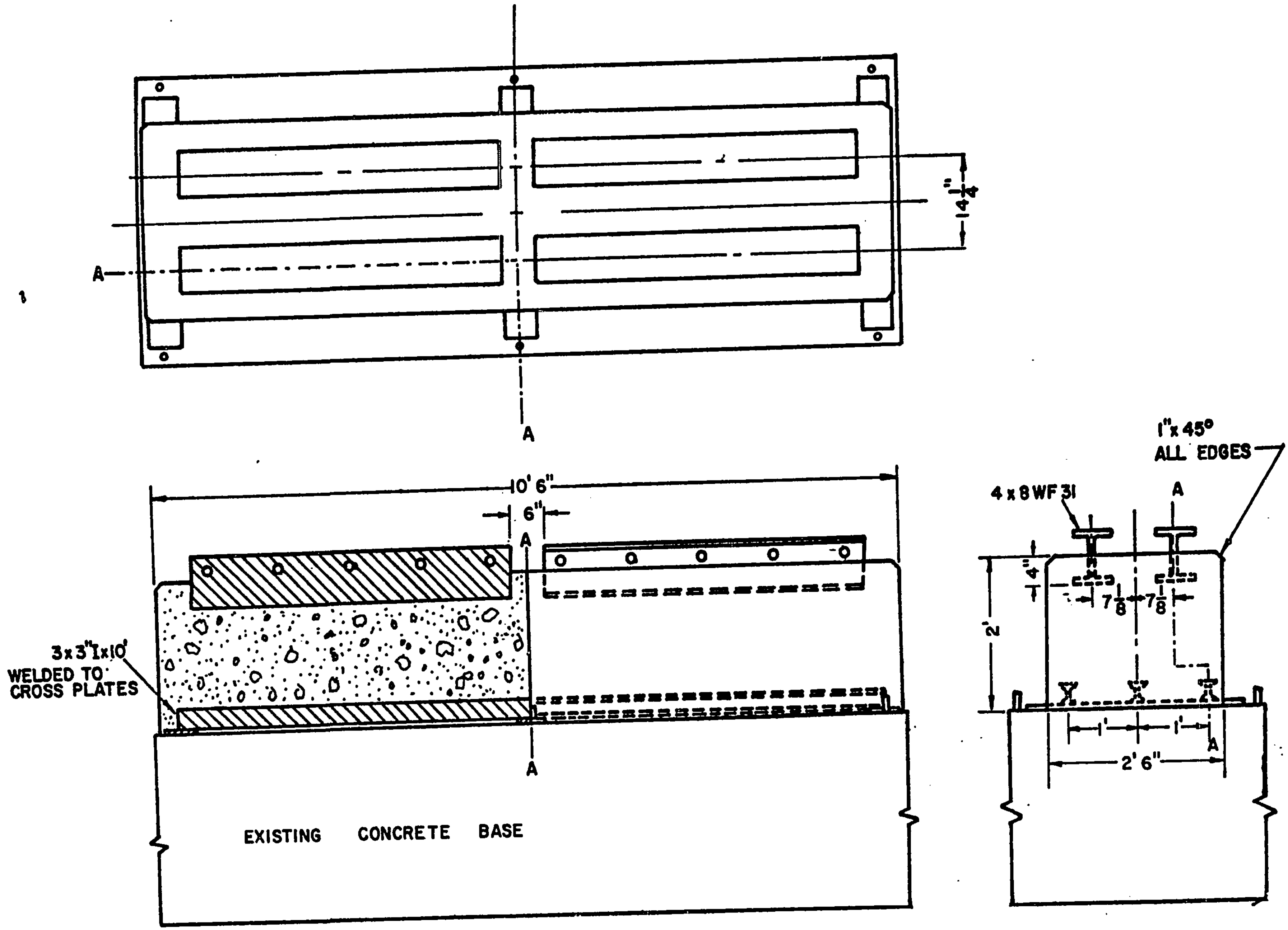

FIG. 2.1 ENGINE TEST BED DETAIL

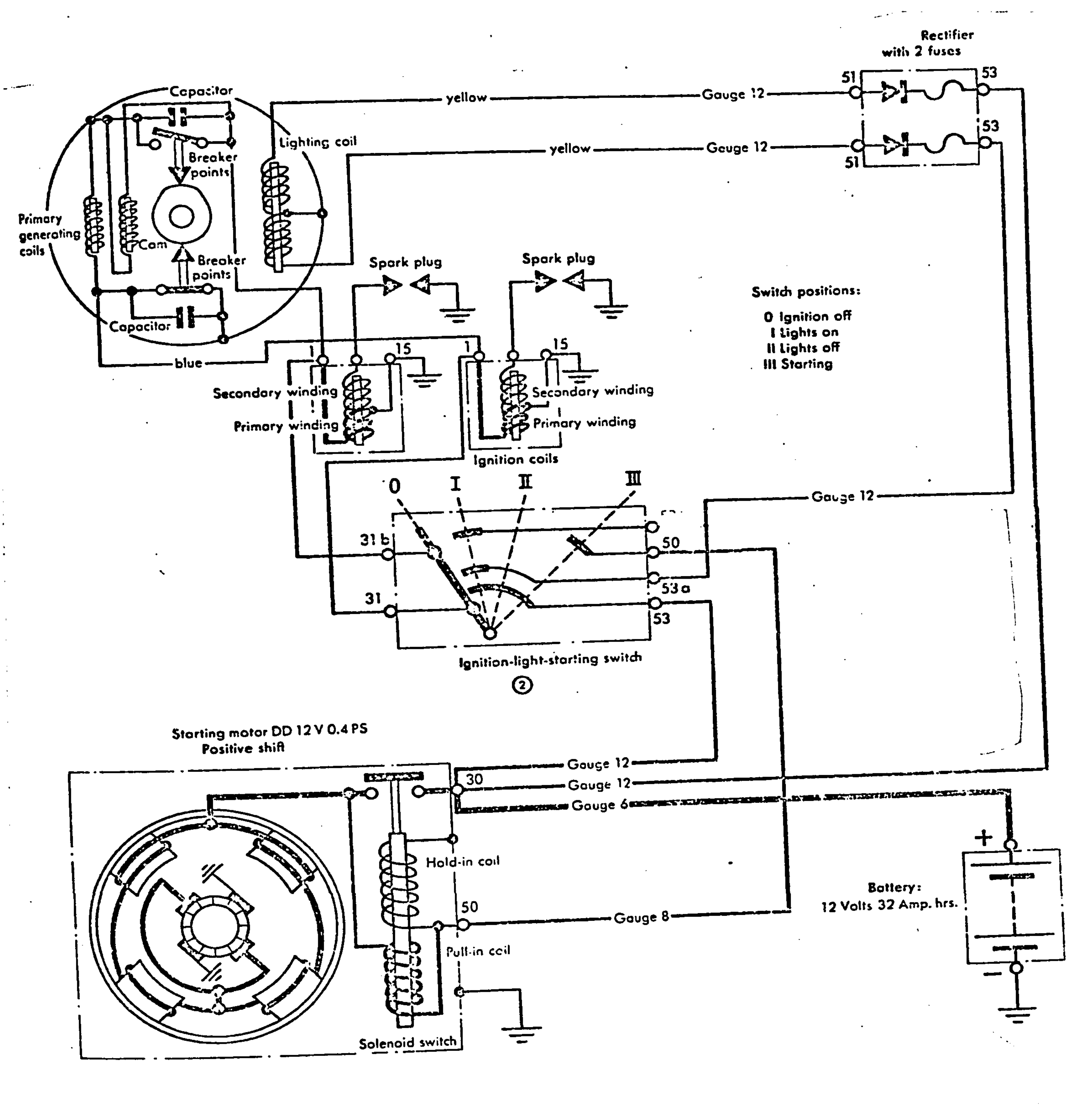

Fig. 2.2 Wiring Diagram for Electric Starting System of K440-2AX Engine

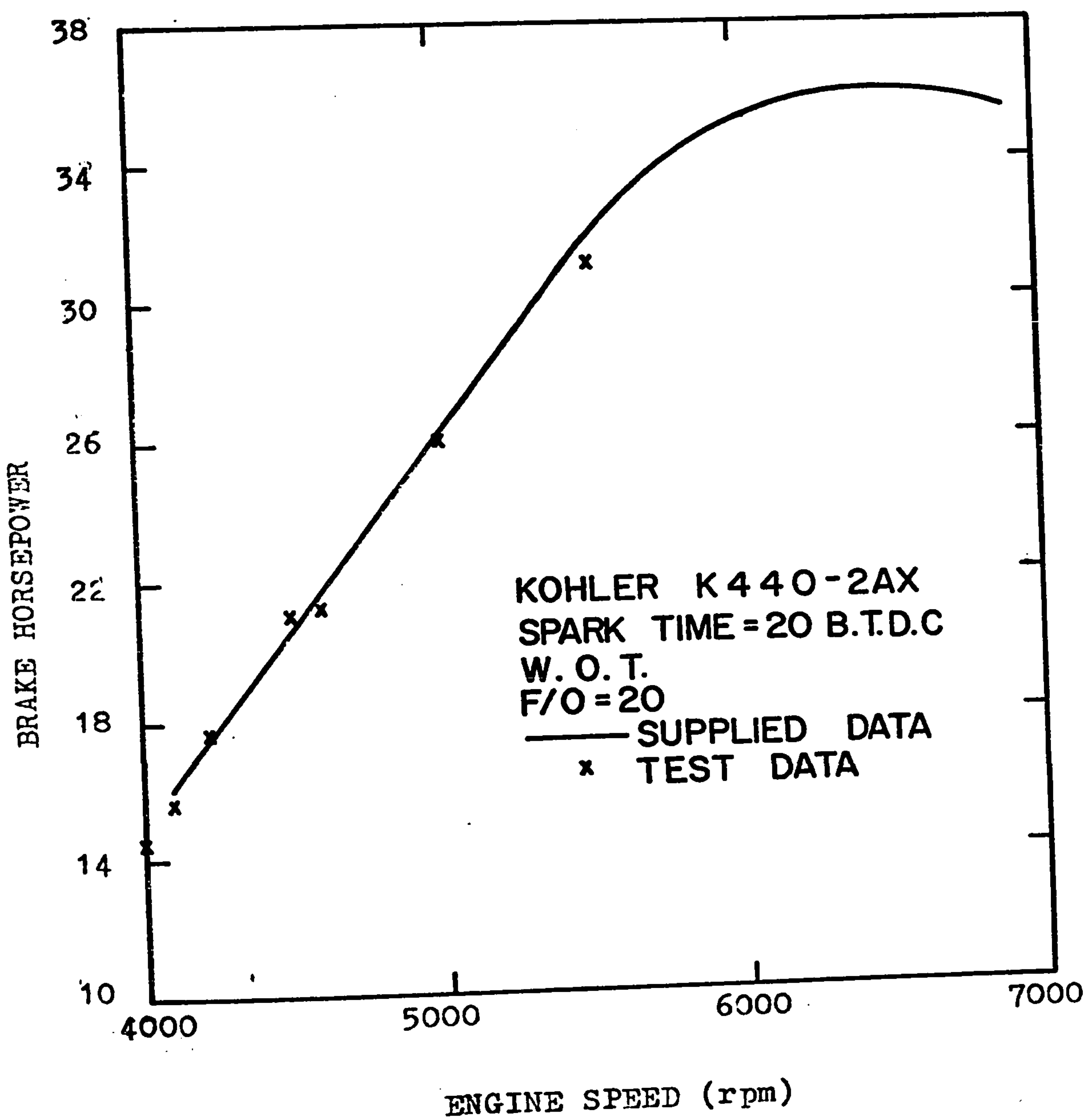

Fig. 2.3 Engine Power Data Curve

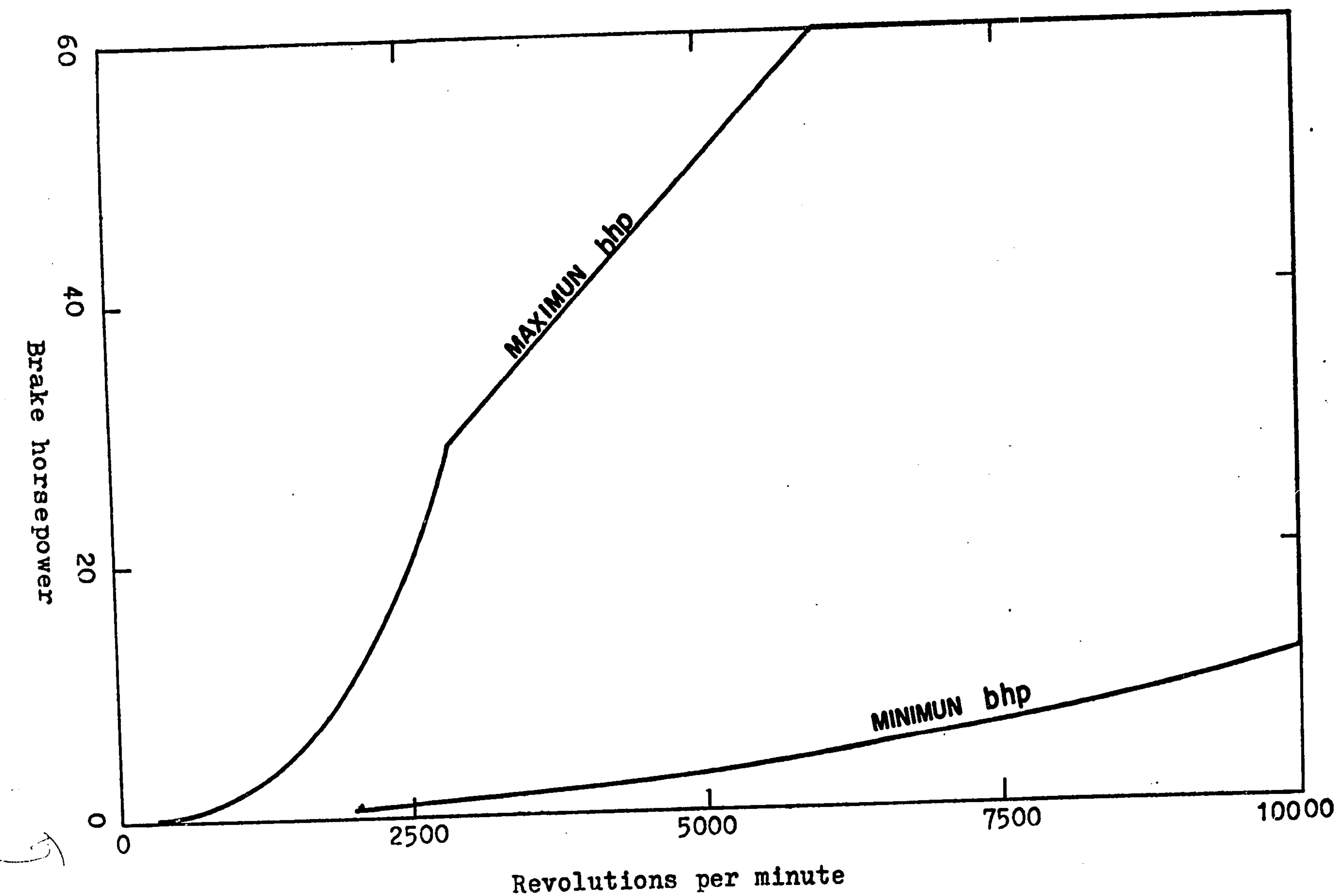

Fig. 2.4 Specification of Heenan & Froude Hydraulic Dynamometer

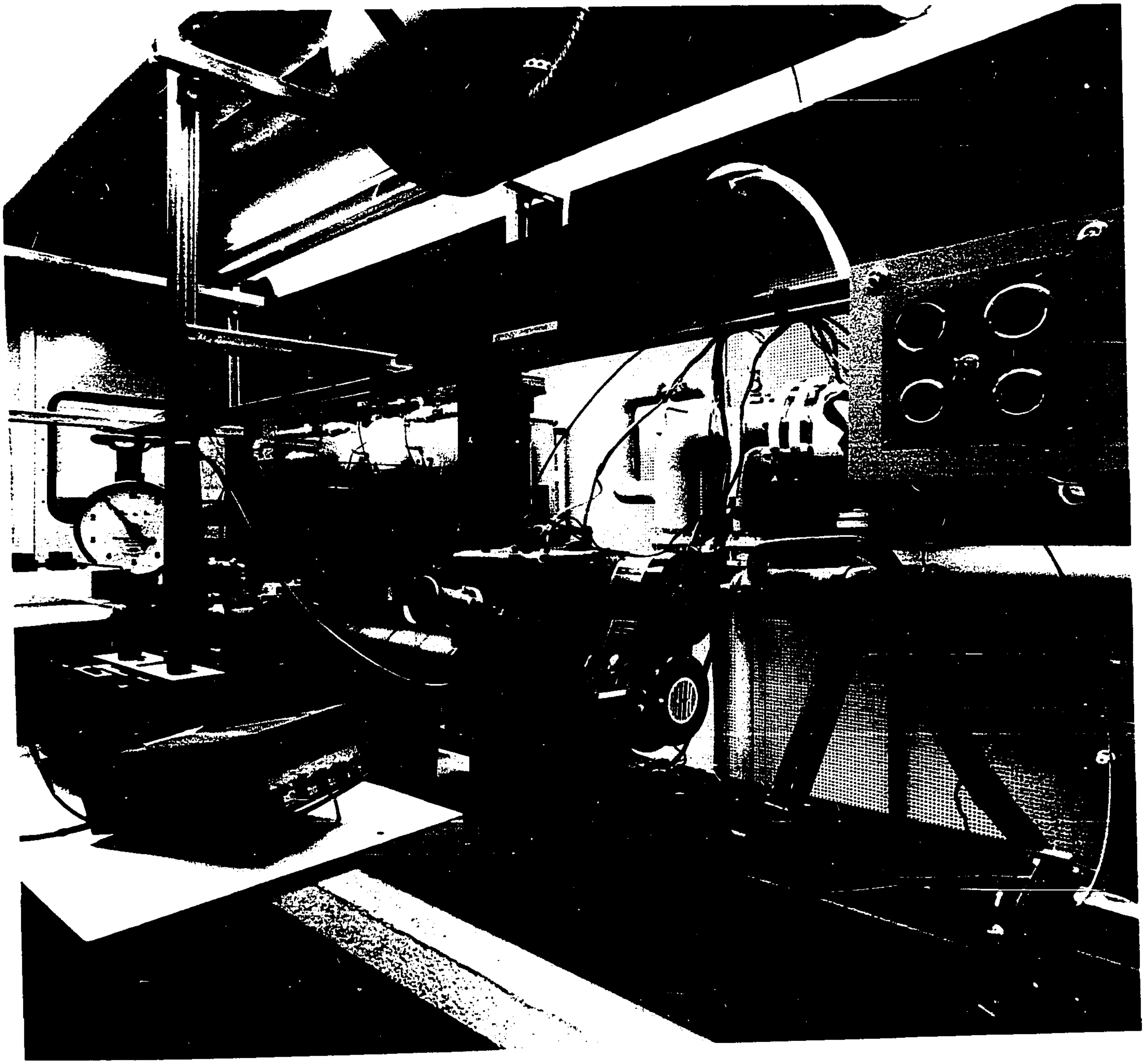

Fig. 2.5 Arrangement of Engine Test Set-up

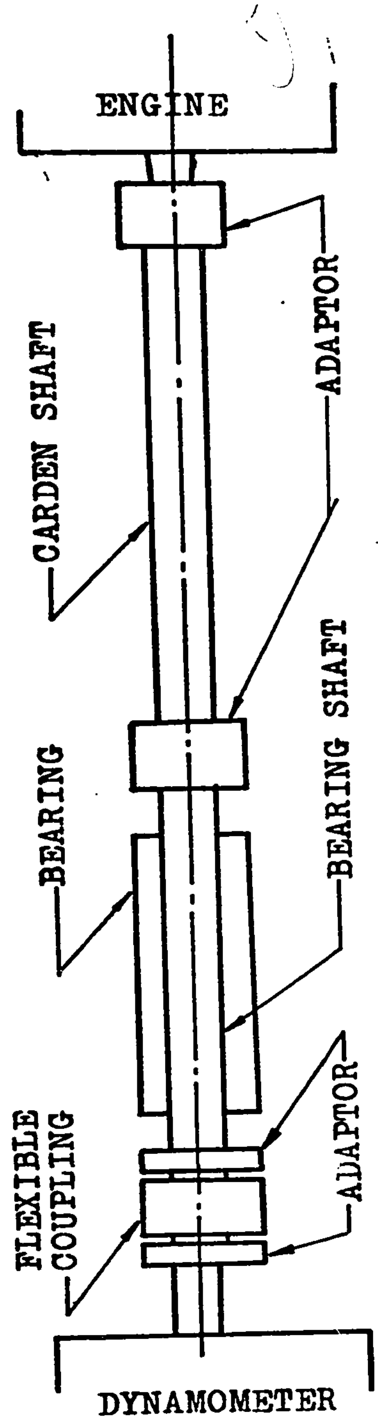

Fig. 2.6 Schematic diagram of engine set up

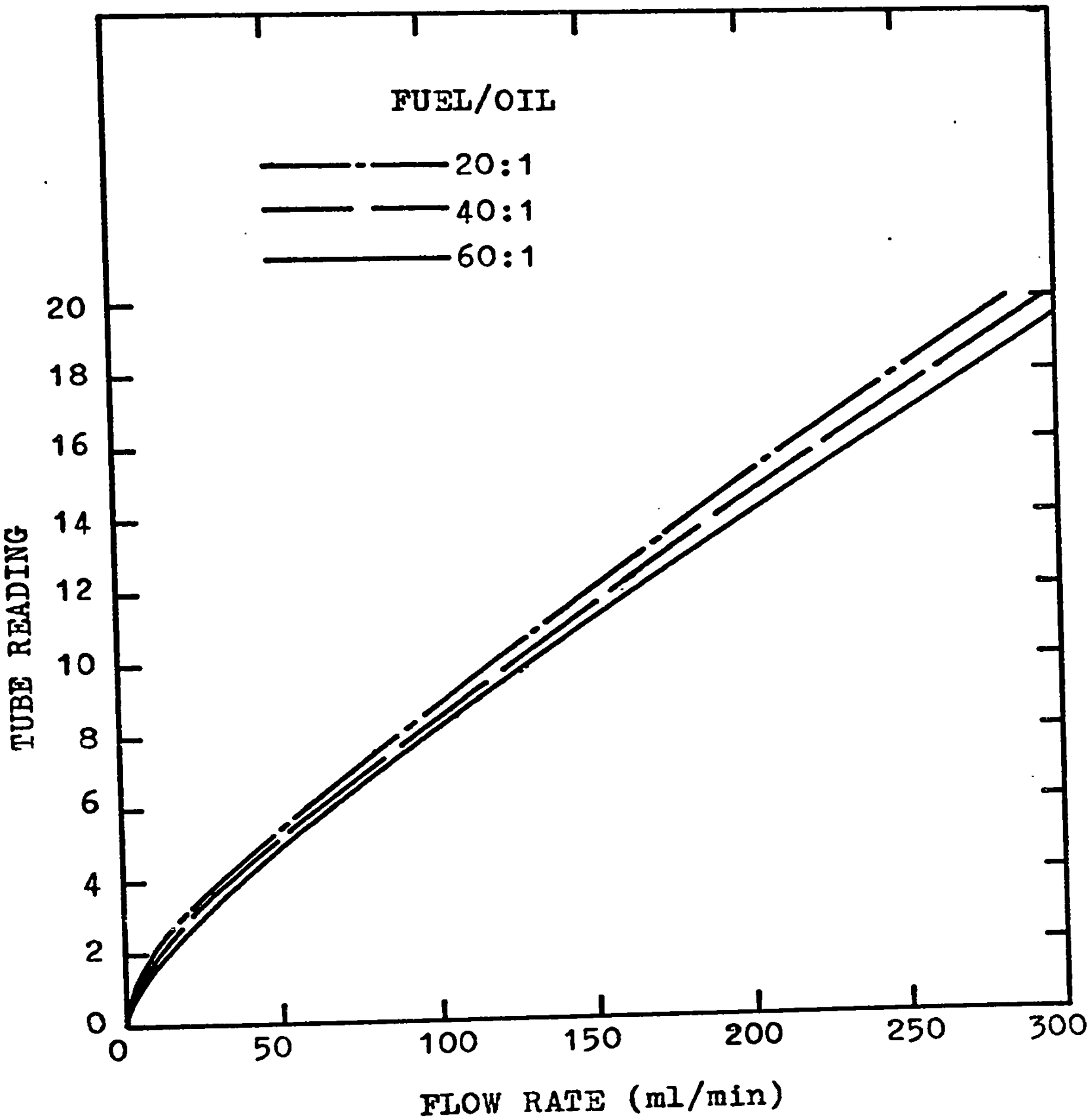

Fig. 2.7 Fuel-Oil Flow Rate Conversion Curves

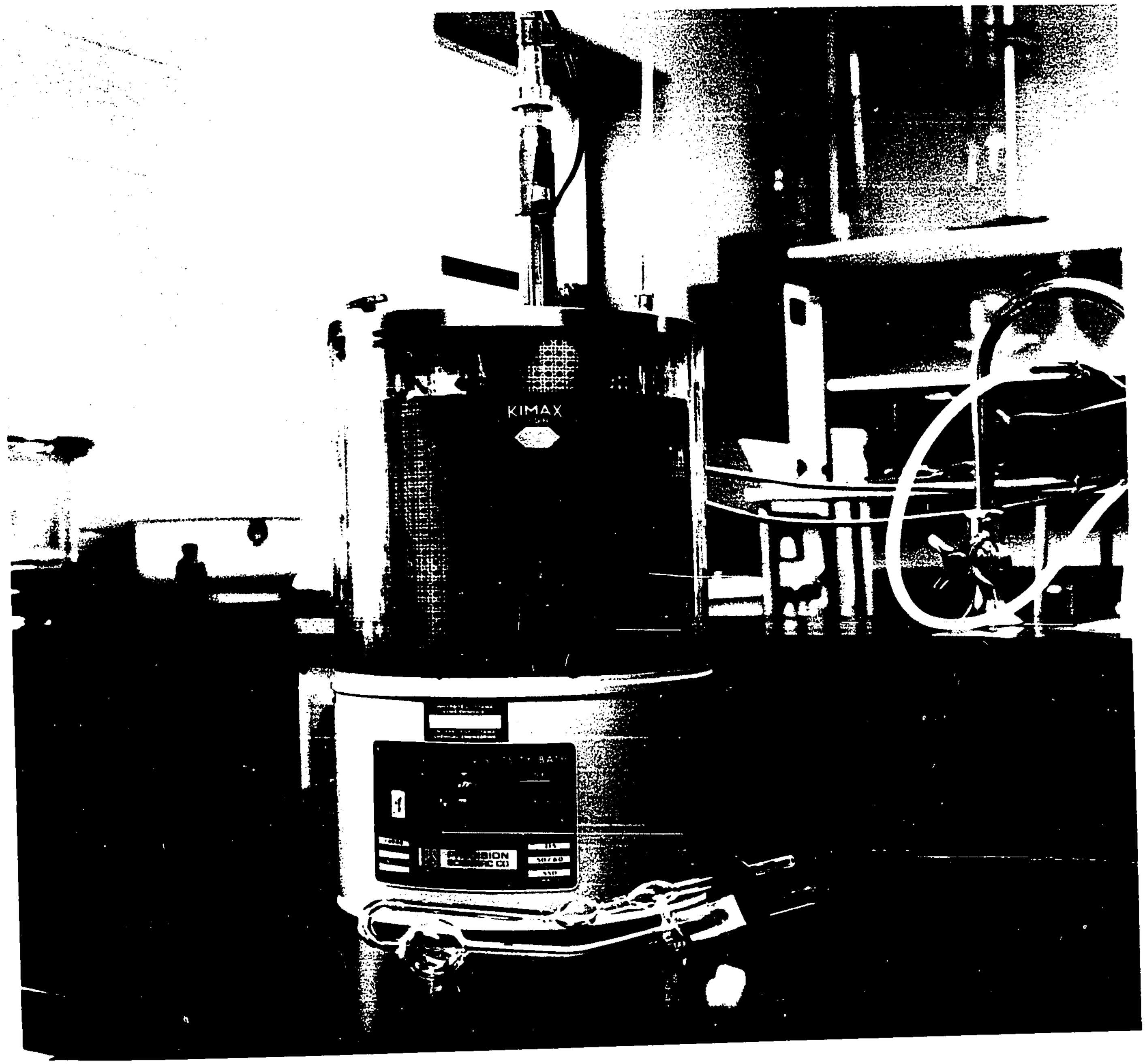

Fig. 2.8 Viscosity Measurement Device ("Temp-Trol" Bath and 50/D489 Viscometer)

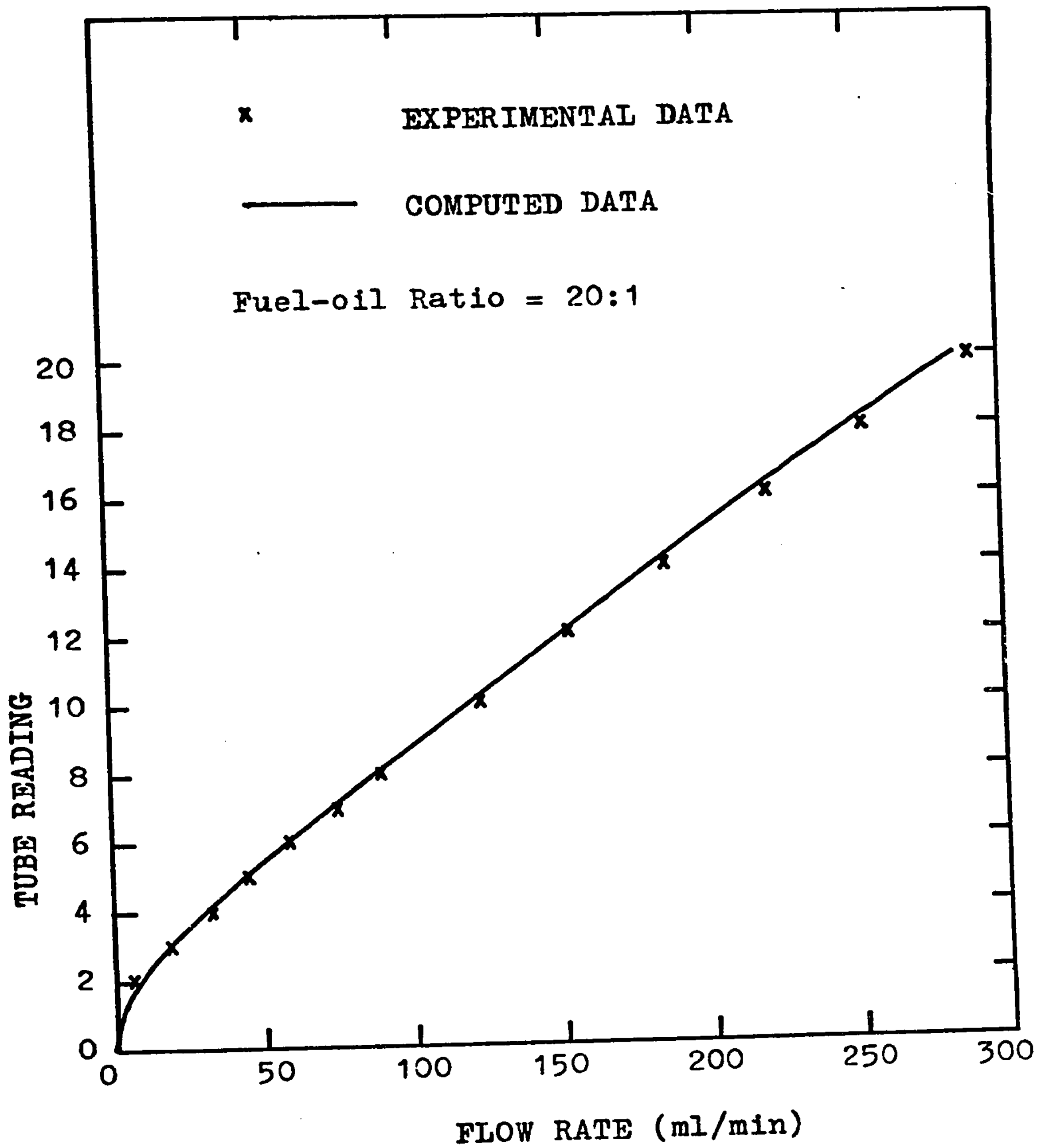

Fig. 2.9 Comparison Between Computed Flow Rate and Direct Measurement

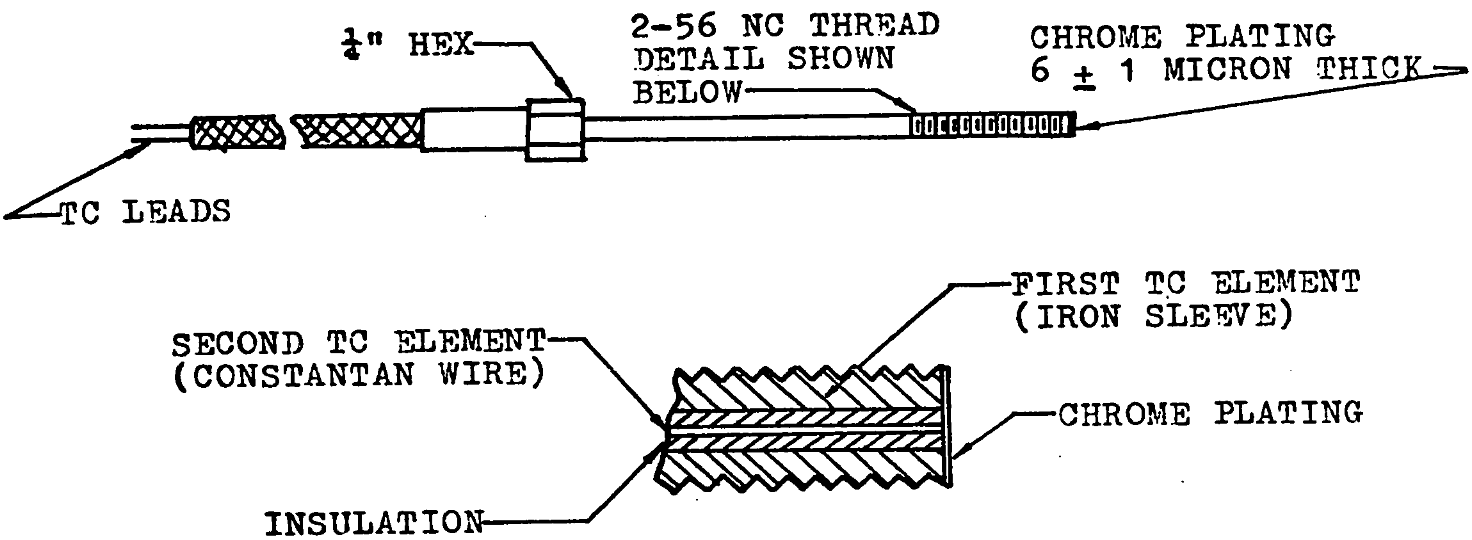

Fig. 2.10 Co-axial Surface Thermocouple
(TCS-101, Midtherm Co.)

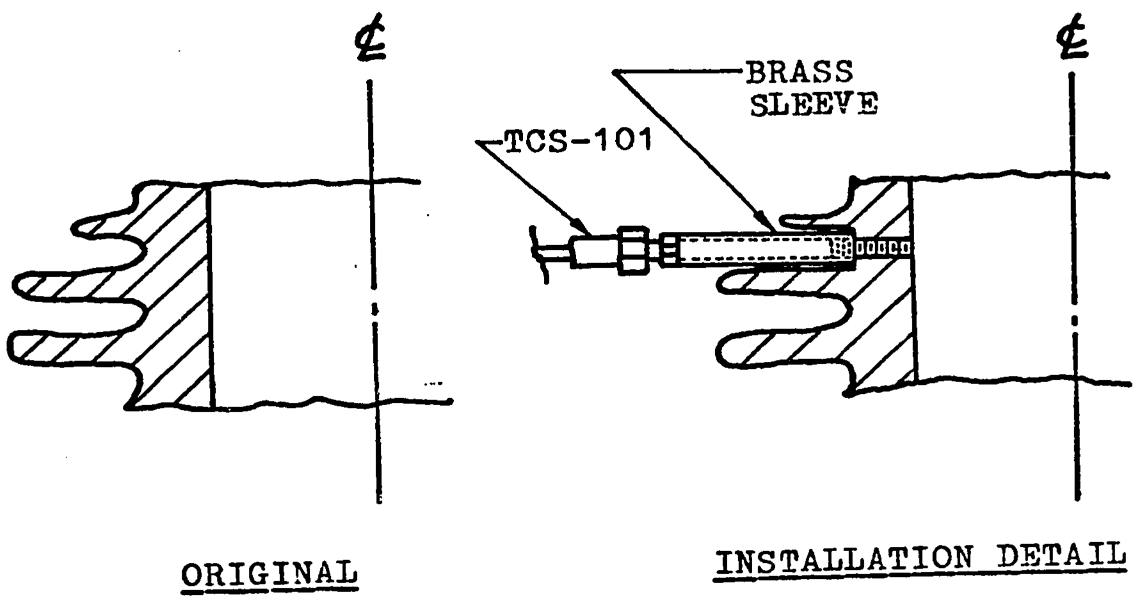

Fig. 2.11 Installation of Co-axial TC on Cylinder
Block (not to scale)

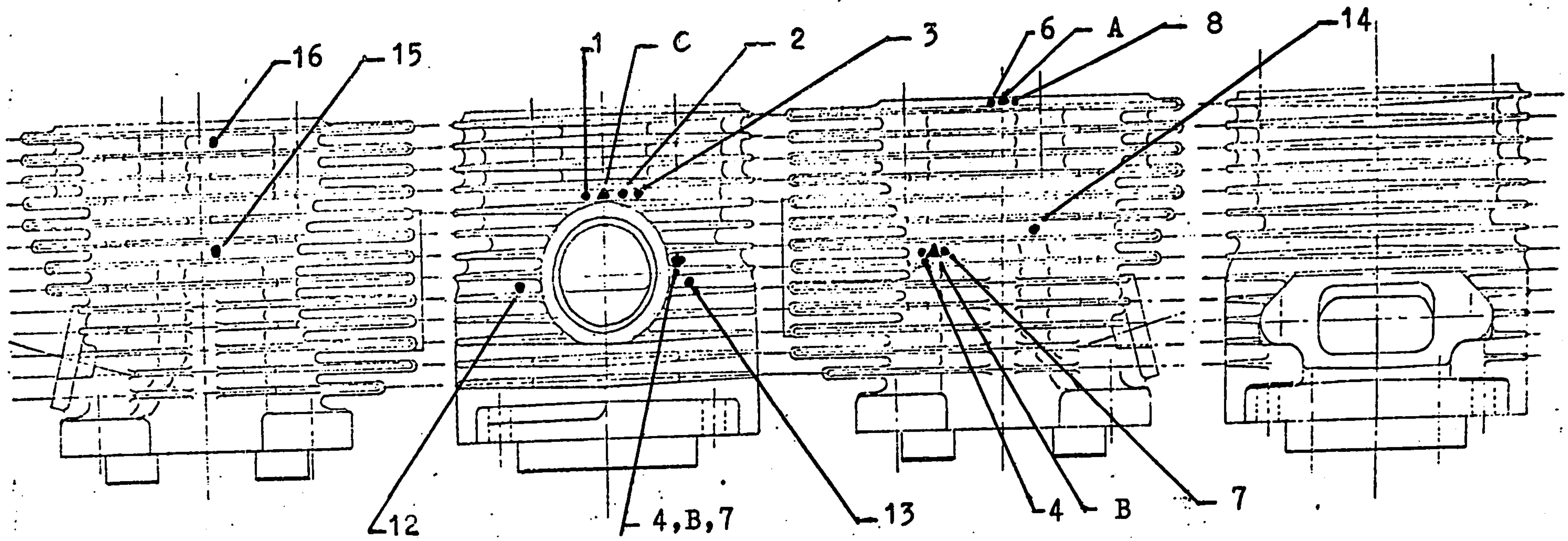

A, B, AND C ARE CO-AXIAL SURFACE THERMOCOUPLES

1, 2, 3, 4, 6, 7, 8, 12, 13, 14, 15, 16 ARE T TYPE THERMOCOUPLES

Fig. 2.12a Location of T Type and J Type Thermocouples on Fist Cylinder

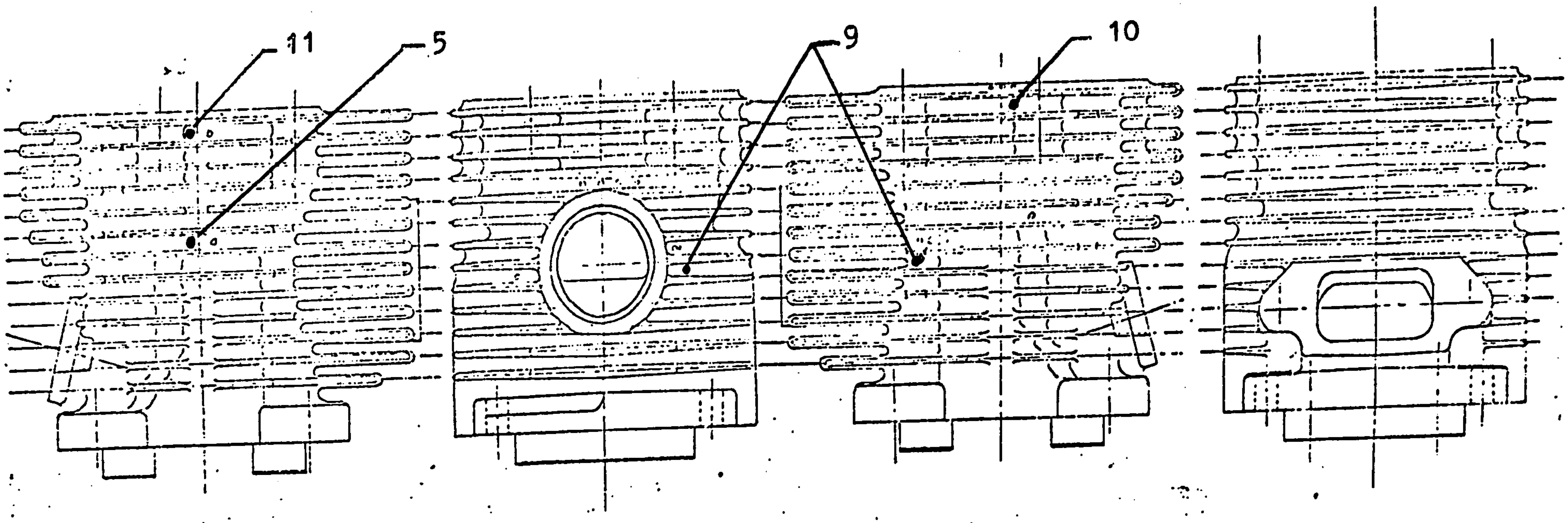

Fig. 2.12b Location of T Type Thermocouples on
Second Cylinder

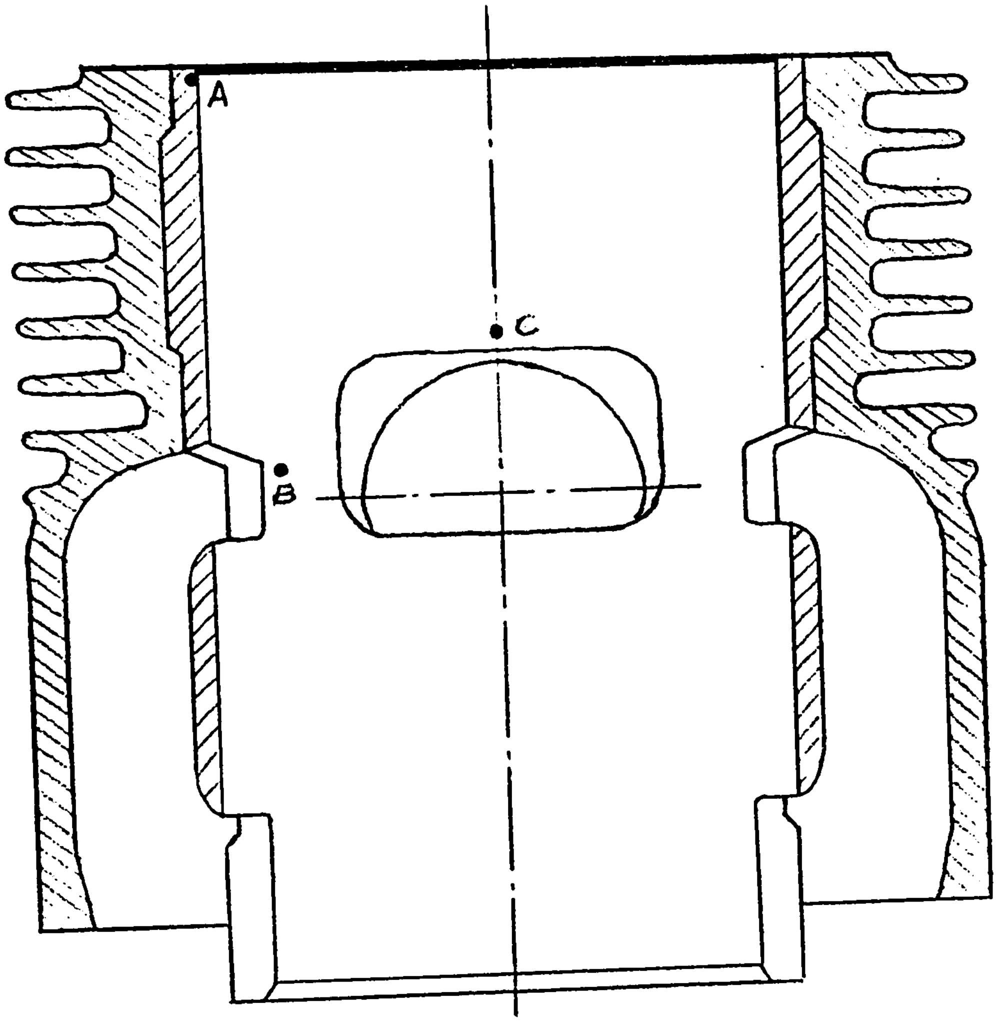

Cross-sectional view of the 1st cylinder of K440-2AX engine

Fig. 2.13 Detail Location of J-Type Co-axial Thermocouples

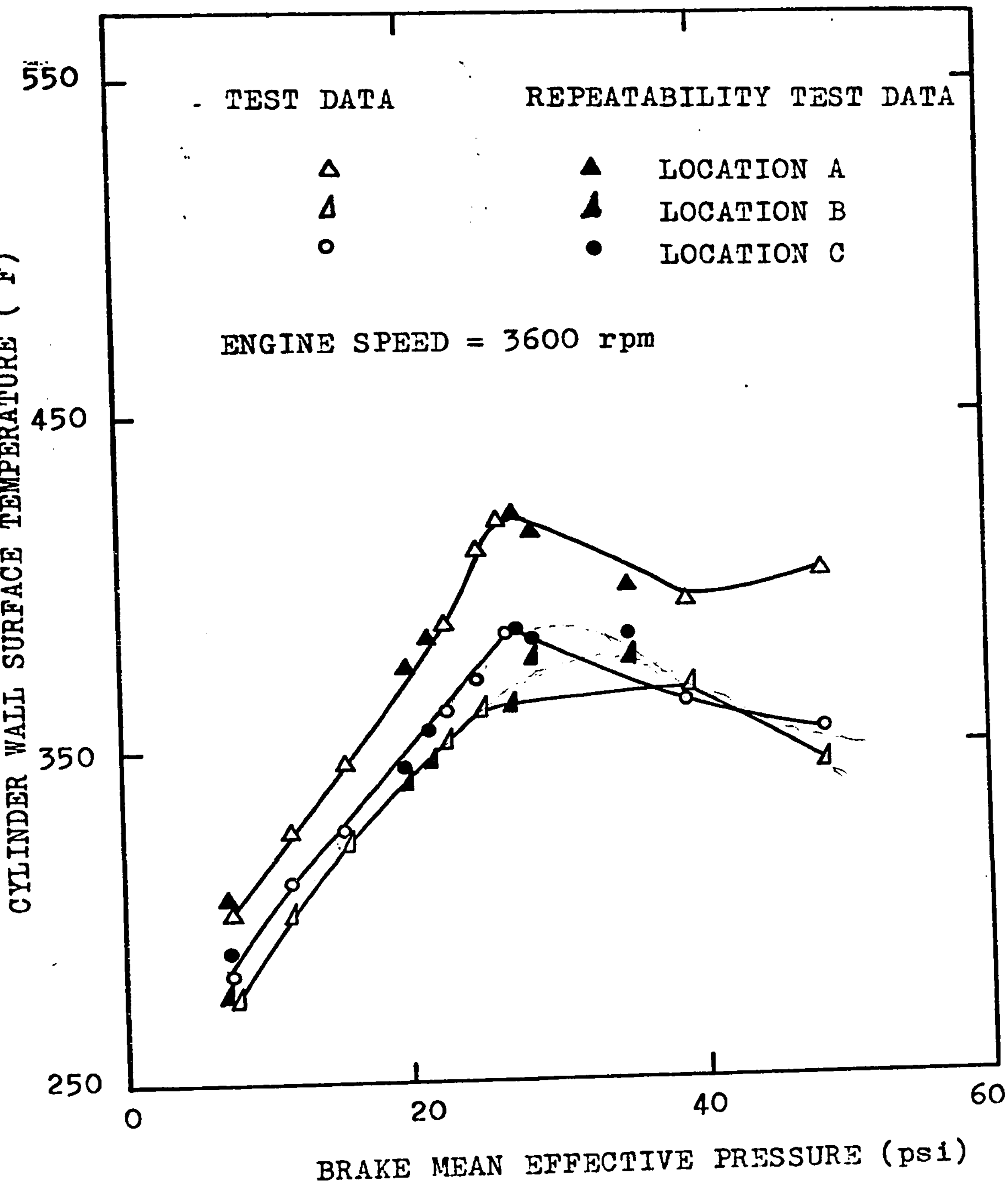

Fig. 3.1 Repeatability of CST Measurement

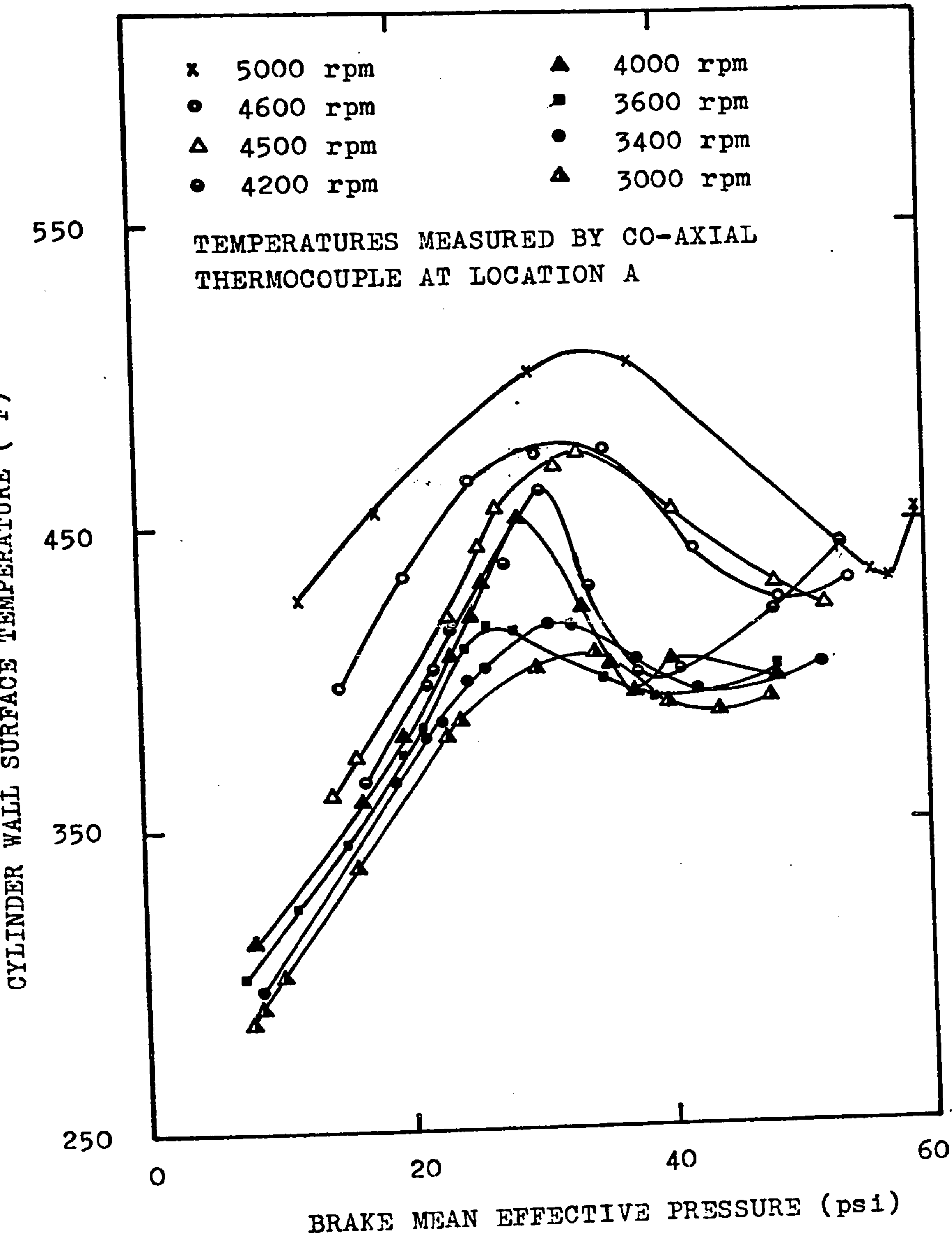

Fig. 4.1 CST as a Function of Bmep (F/O = 20)

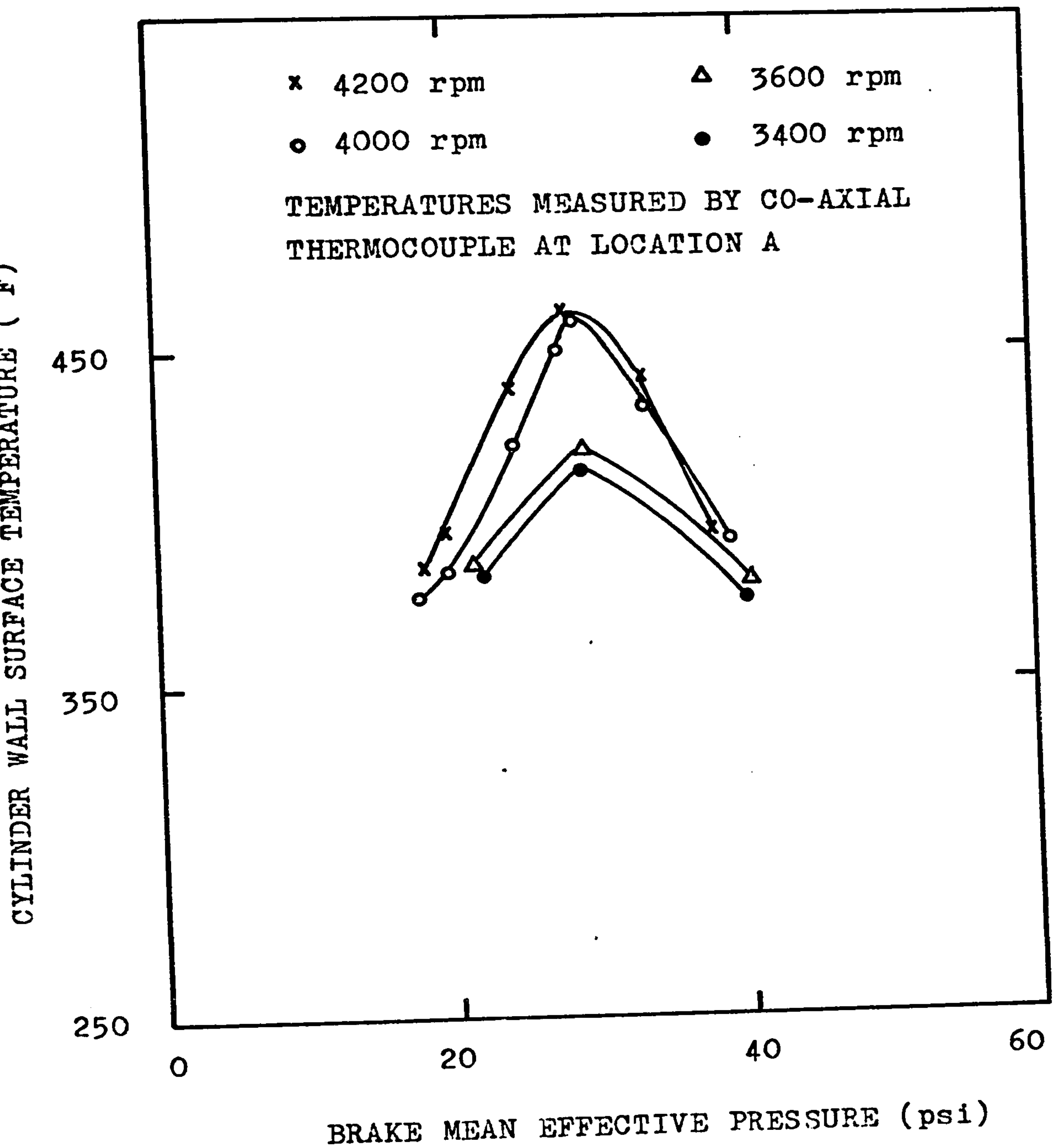

Fig. 4.2 CST as a Function of Bmep (F/O = 40)

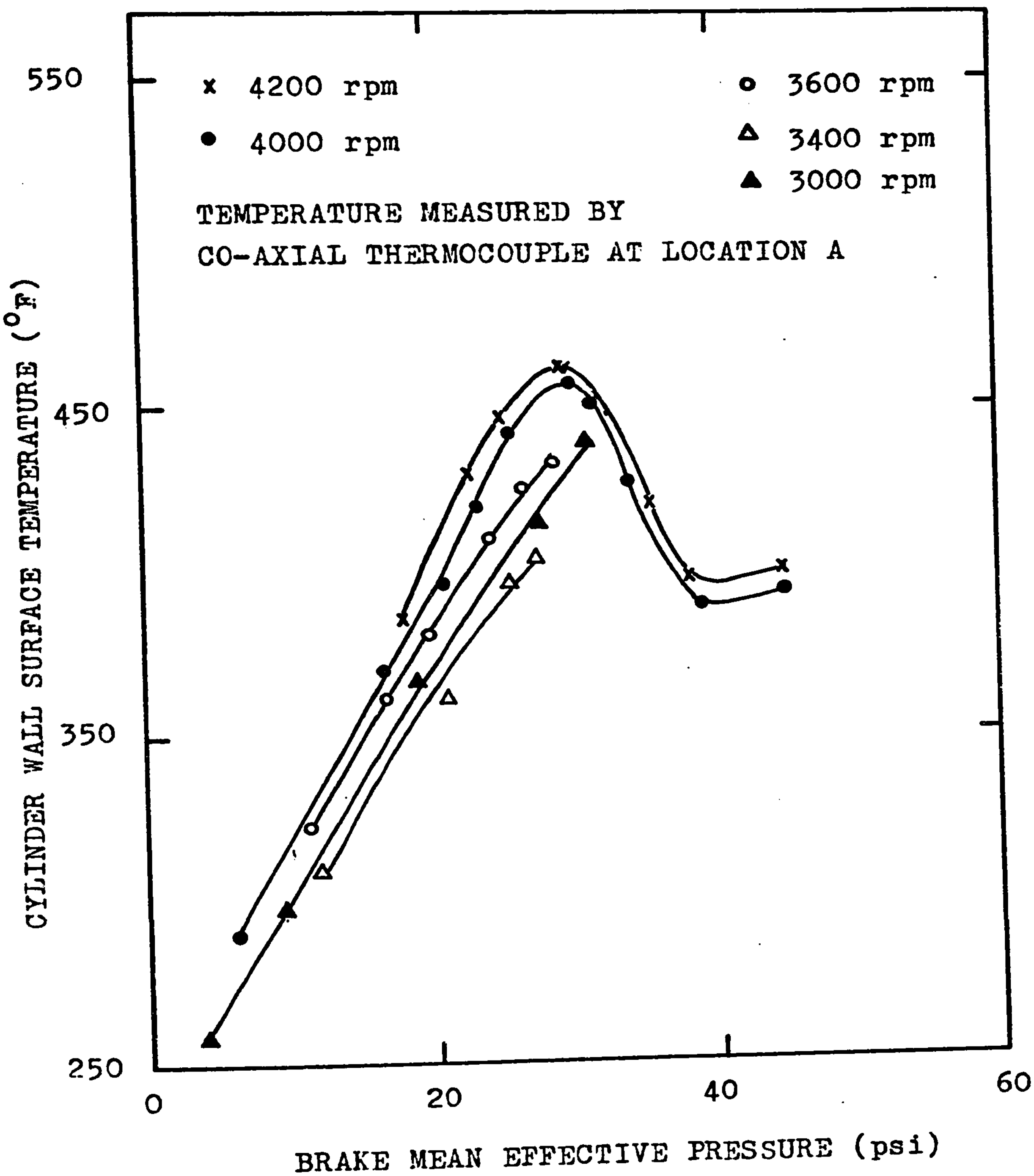

Fig. 4.3 CST as a Function of Bmep (F/O = 60)

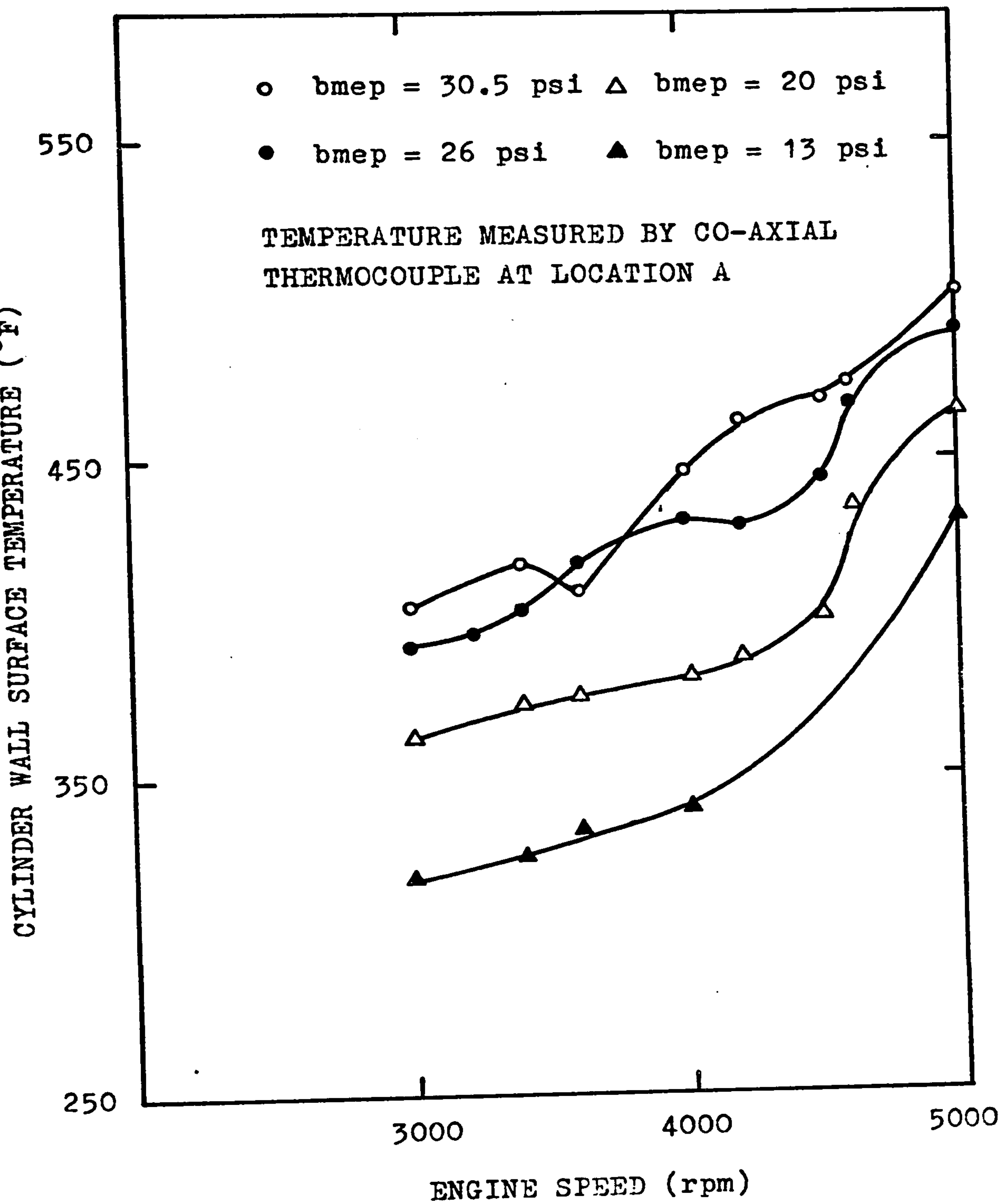

Fig. 4.4 CST as a Function of Speed (F/O = 20)

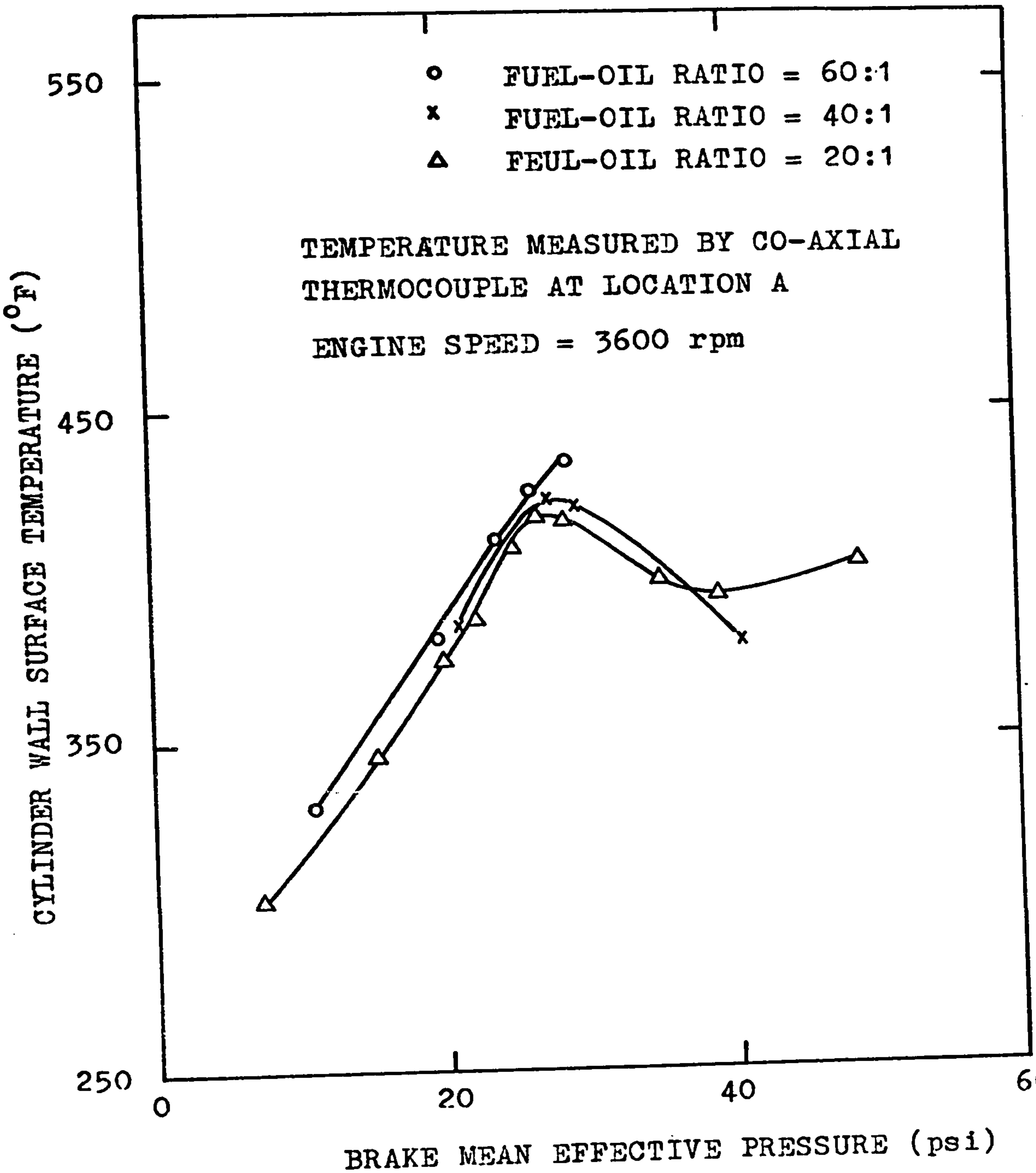

Fig. 4.5 Effects of Fuel-oil Ratio on CST

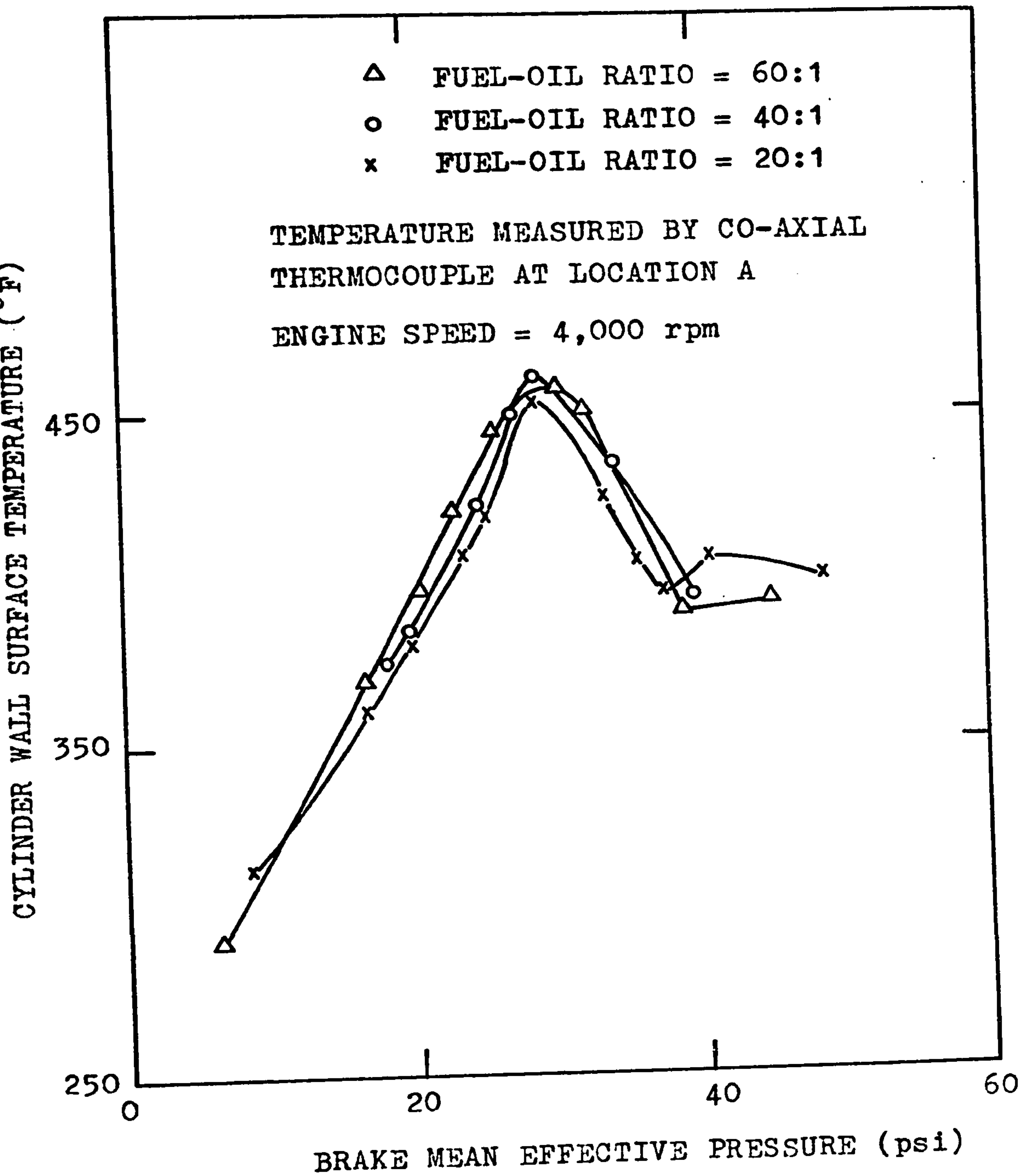

Fig. 4.6 Effects of Fuel-oil Ratio on CST

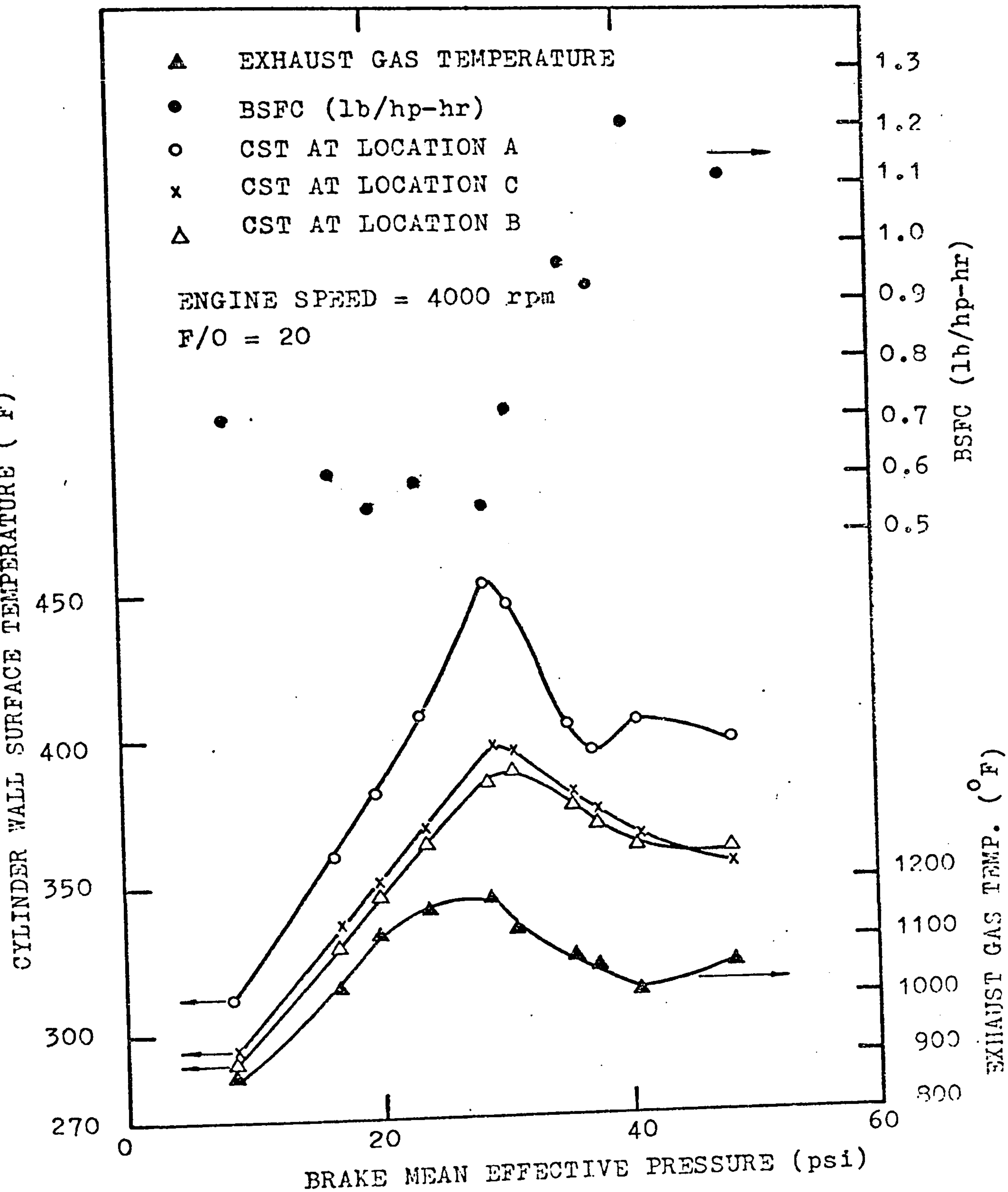

Fig. 4.7 Bsfc and Its Effect on CST

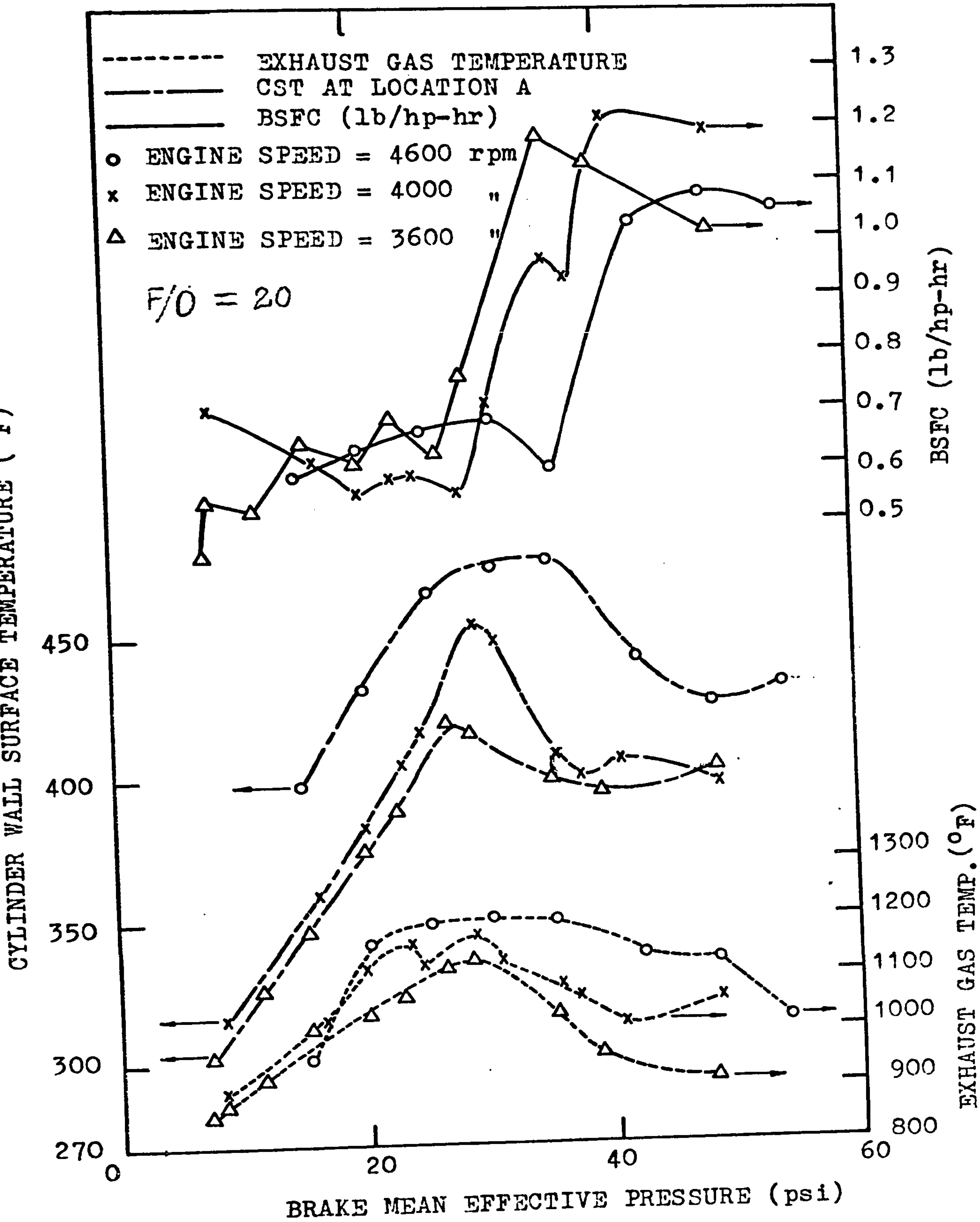

Fig. 4.8 Bsfc and Its Effect on CST

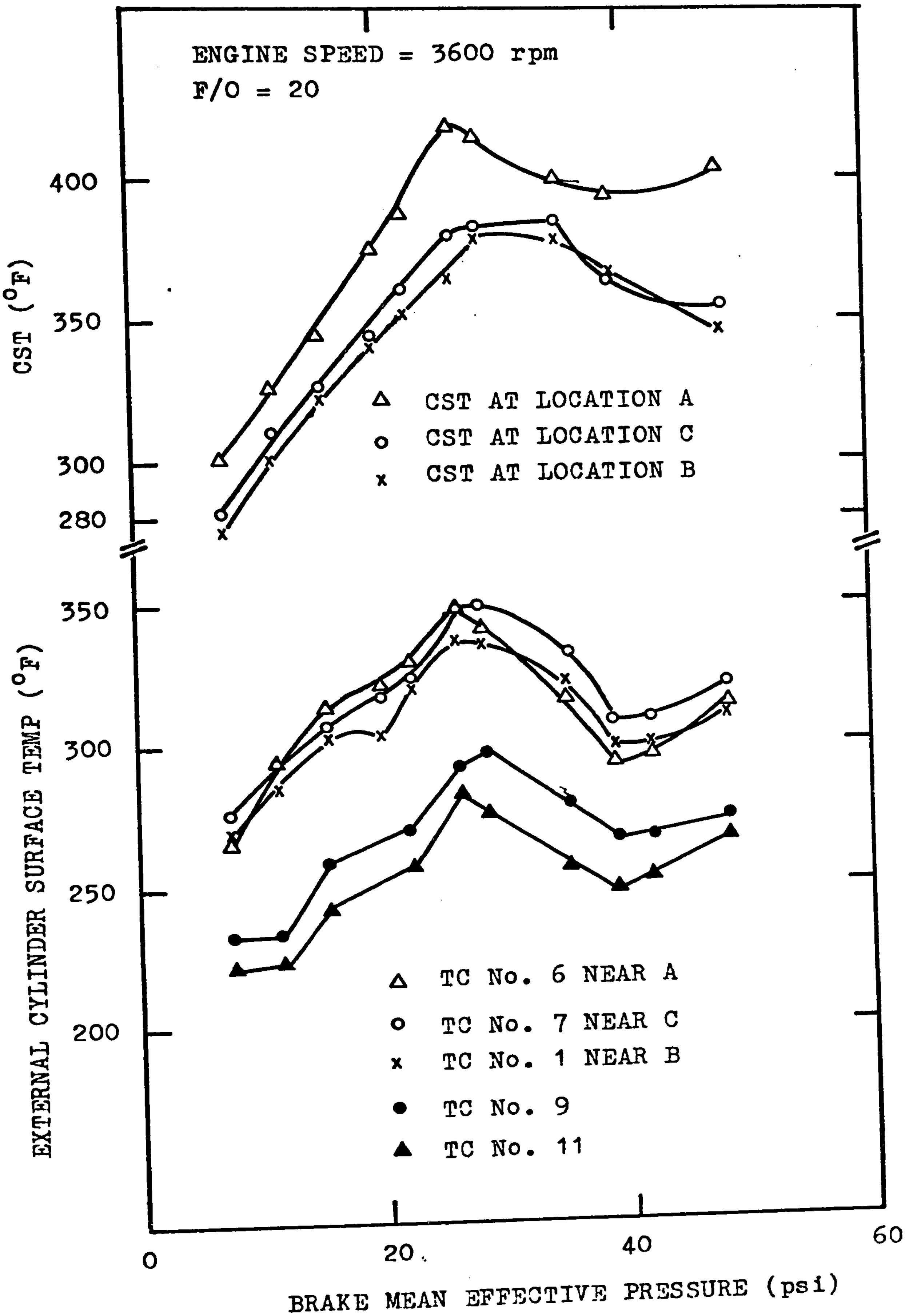

Fig. 4.9 External Cylinder Wall Temperature

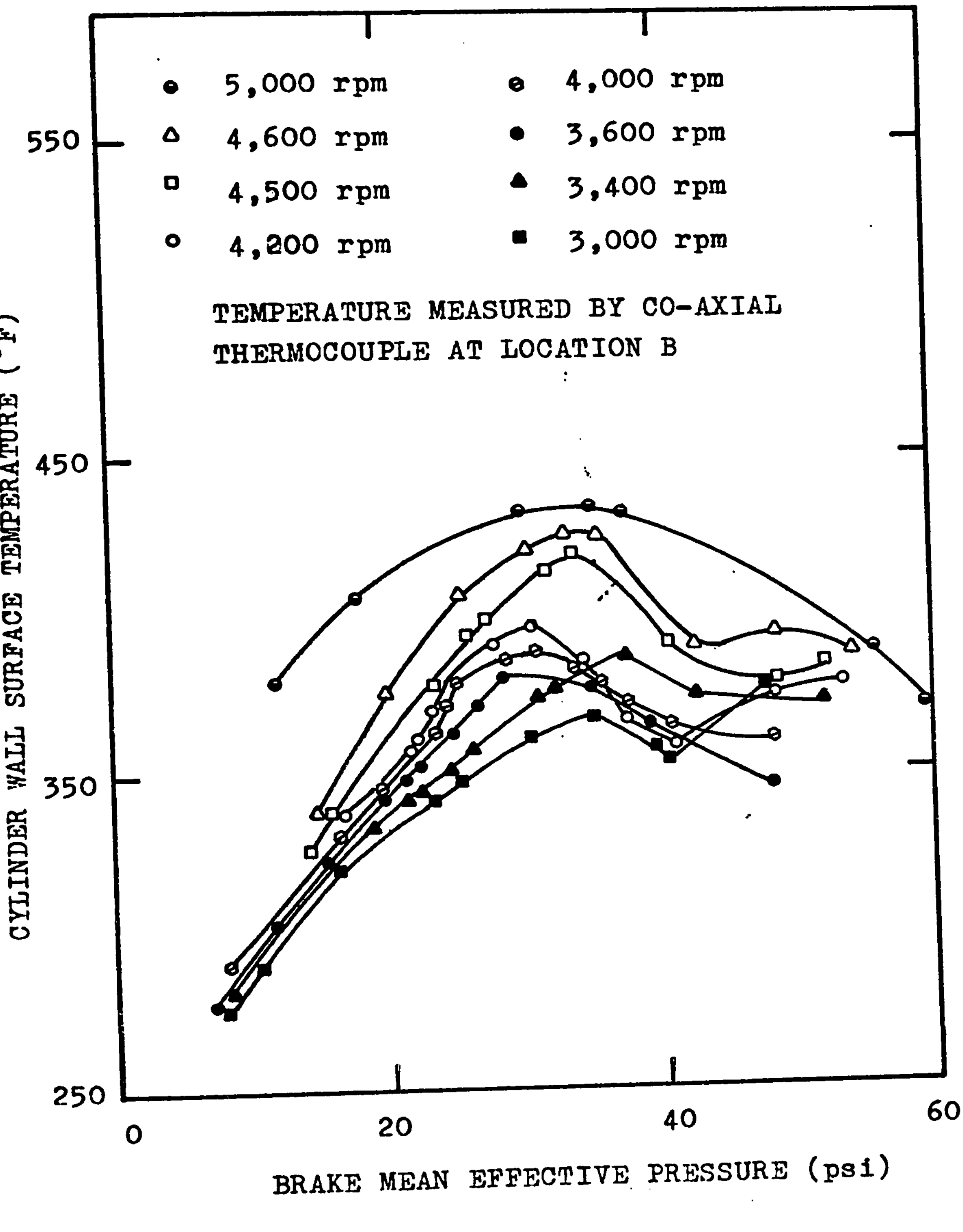

Fig. 4.10 CST as a Function of Bmep (F/O = 20)

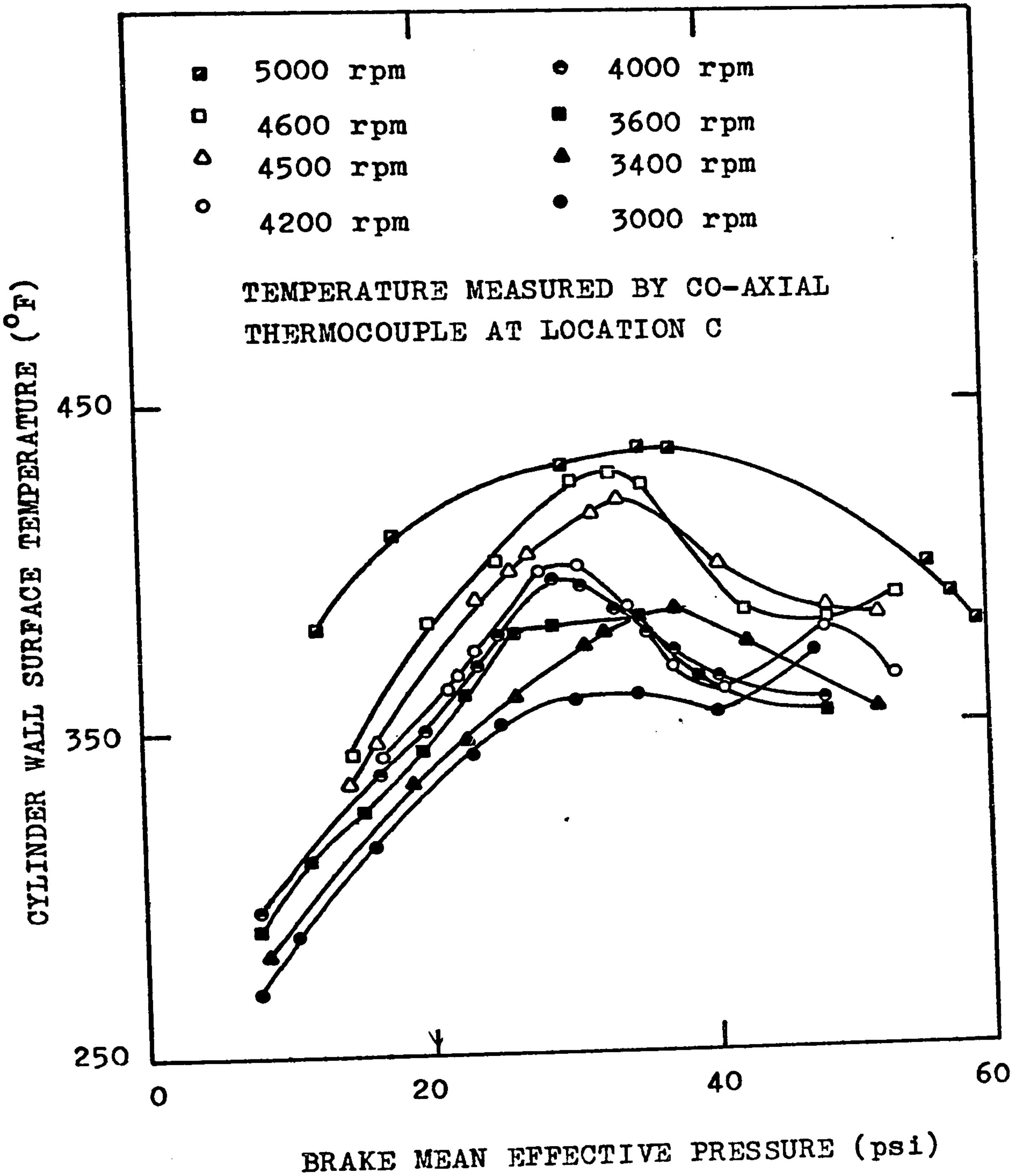

Fig. 4.11 CST as a Function of Bmep (F/O = 20)

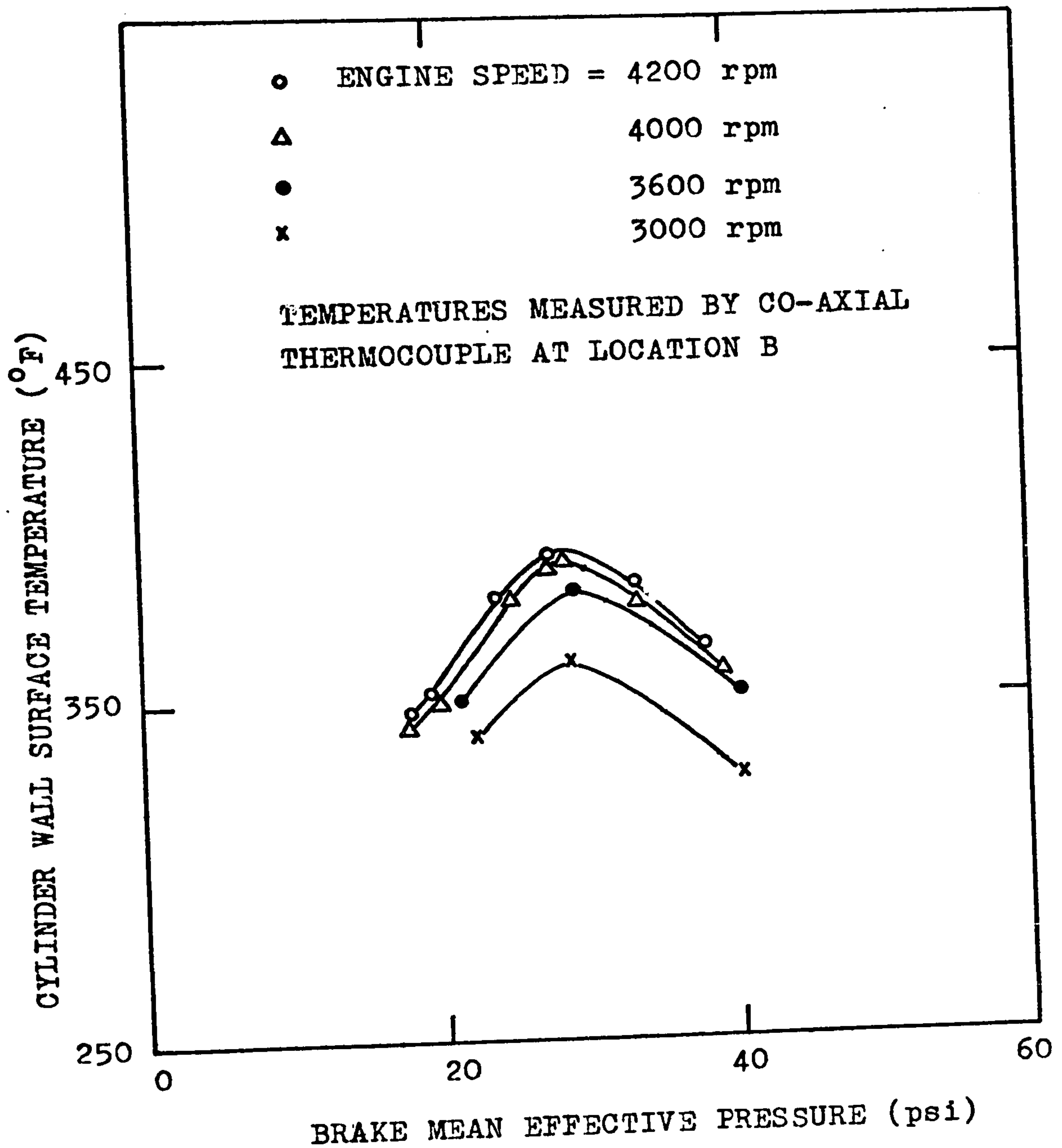

Fig. 4.12 CST as a Function of Bmep (F/O = 40)

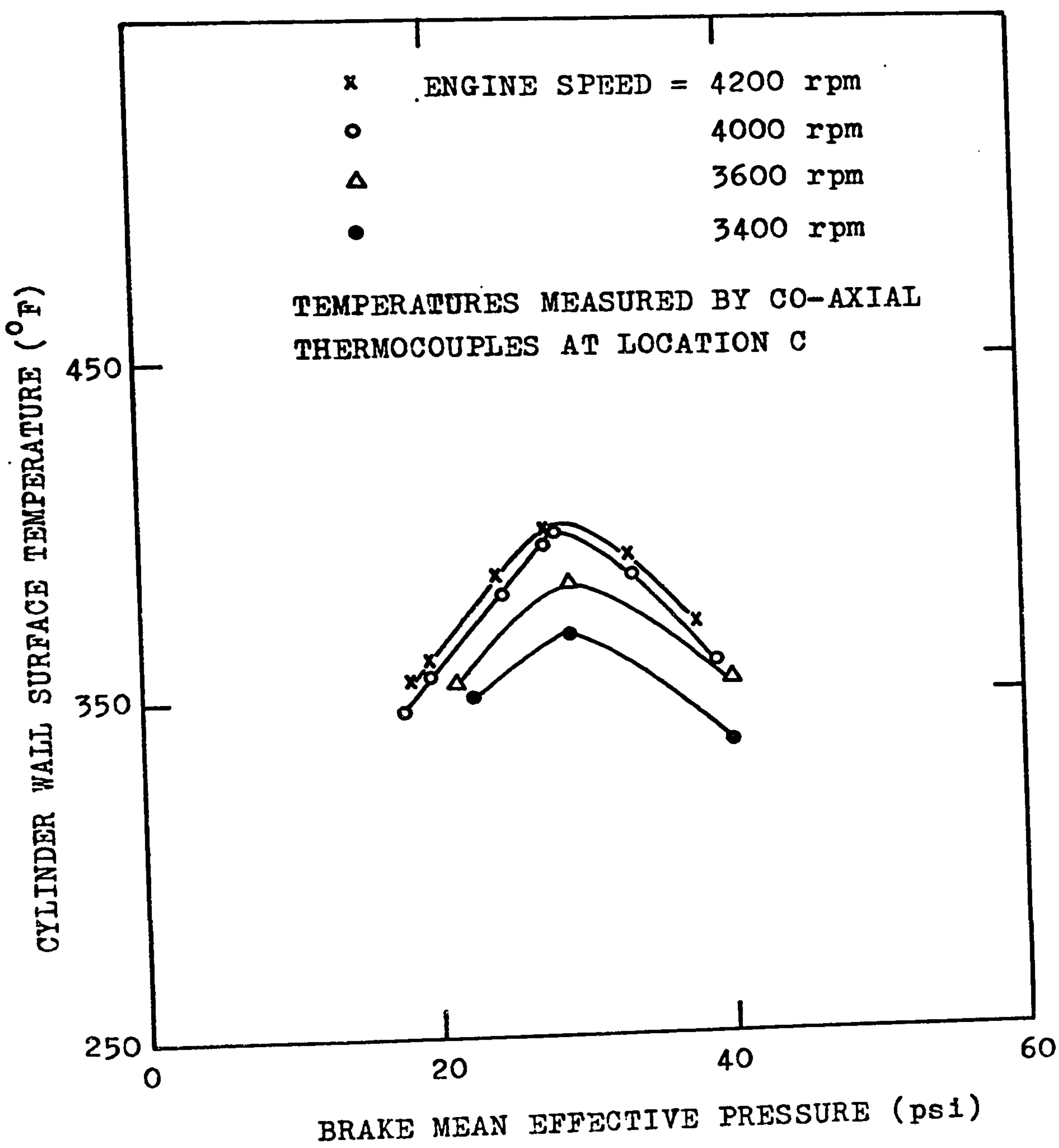

Fig. 4.13 CST as a Function of Bmep (F/O = 40)

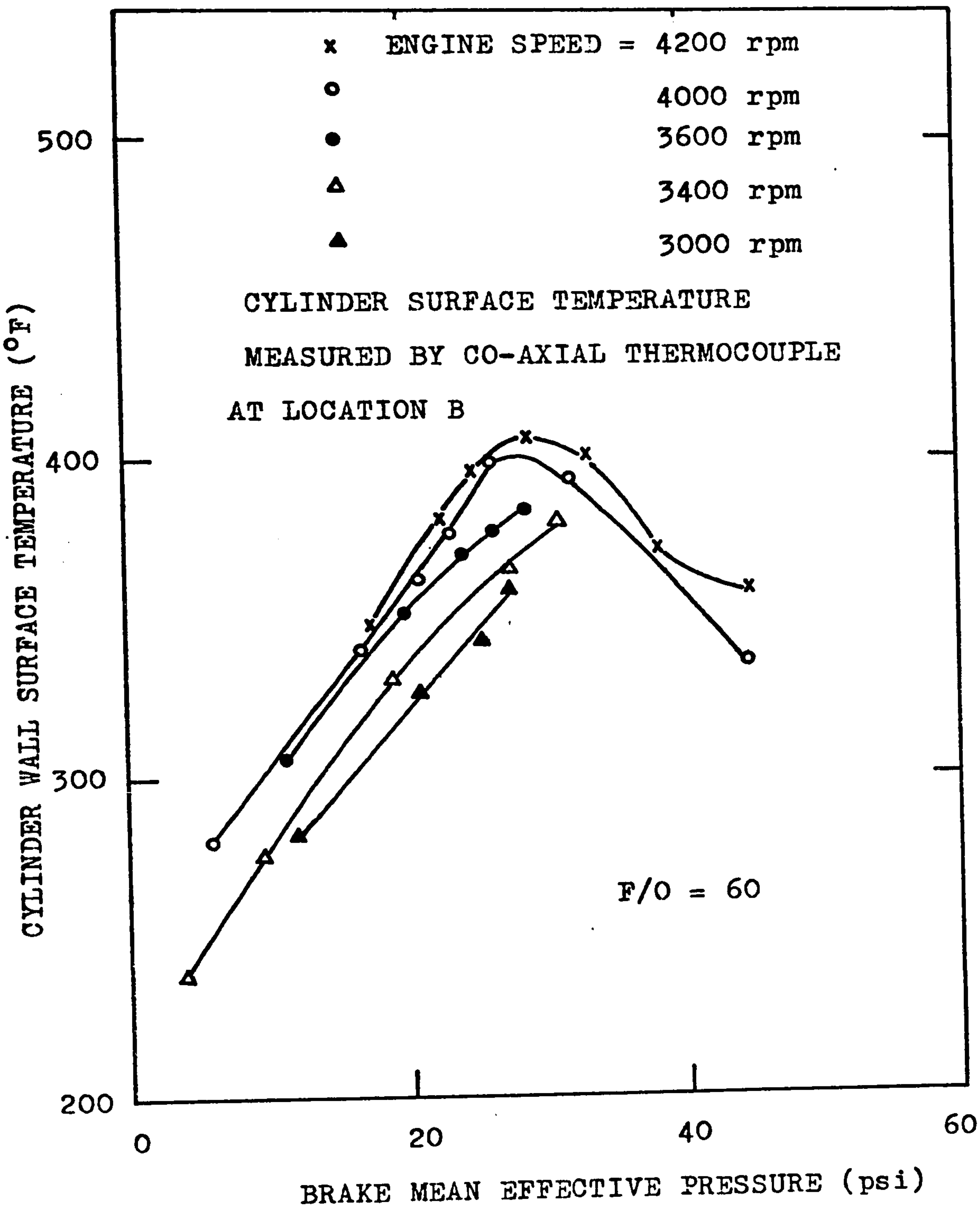

Fig. 4.14 CST as a Function of Bmep (F/O = 60)

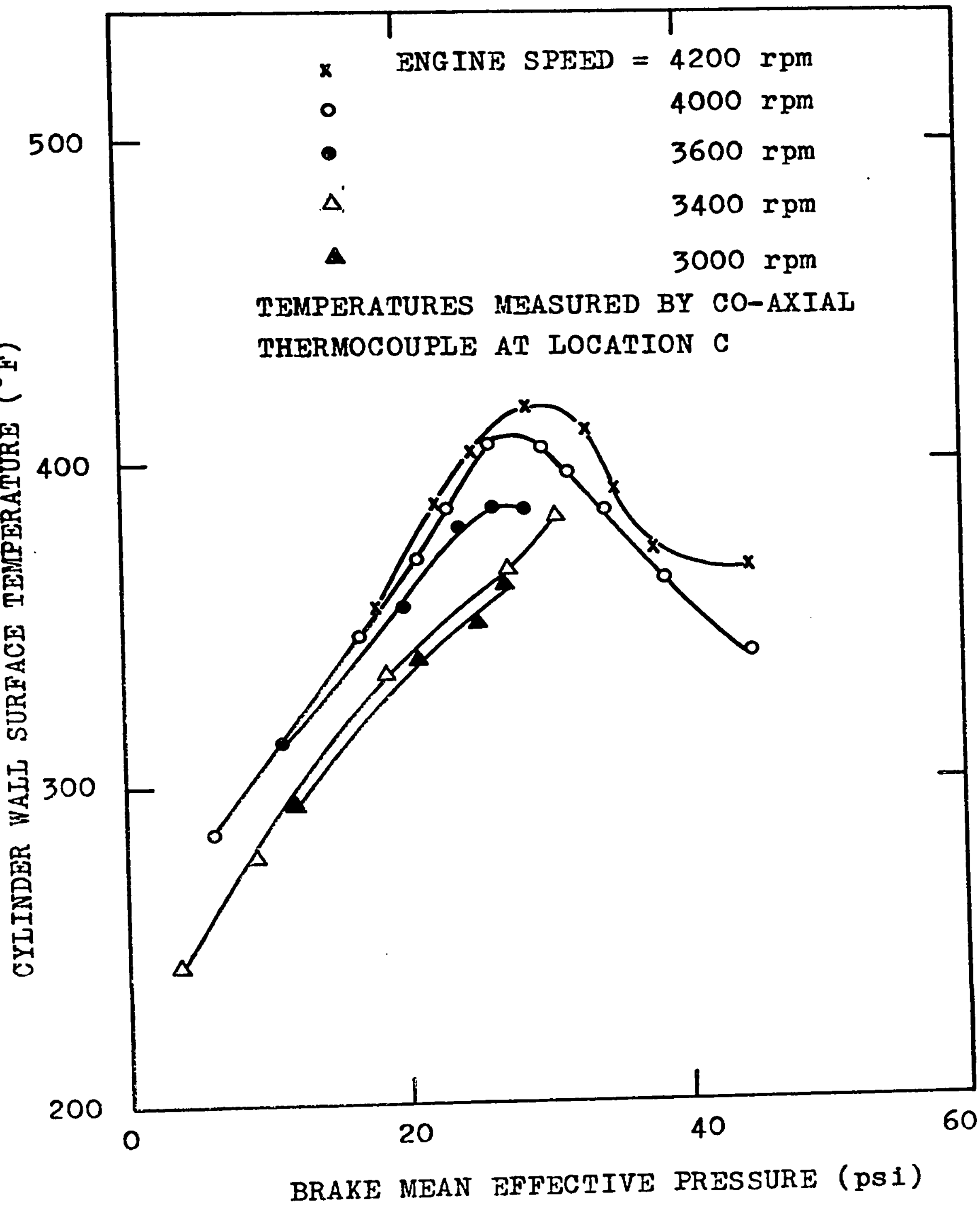

Fig. 4.15 CST as a Function of Bmep (F/O = 60)

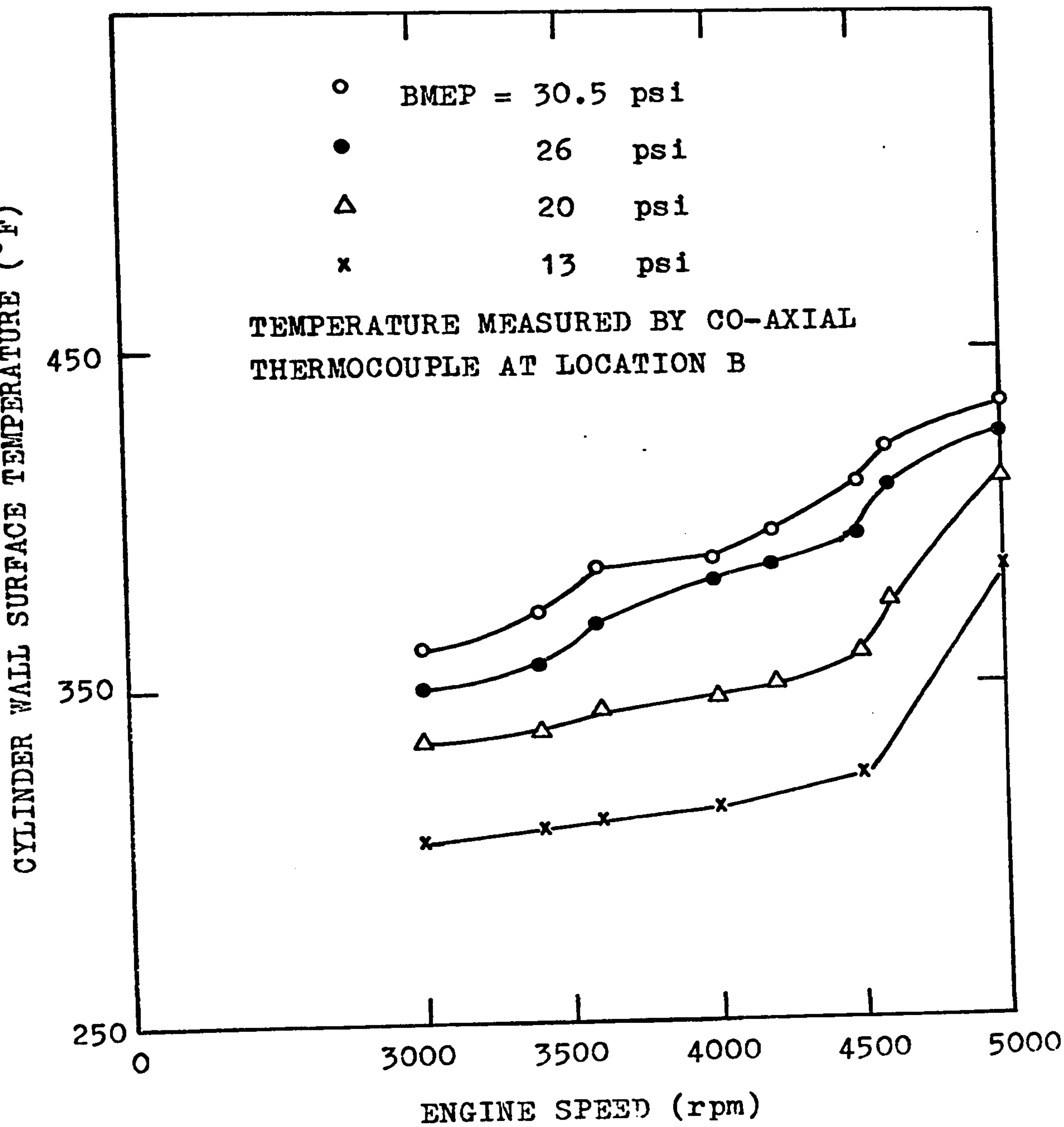

Fig. 4.16 CST as a Function of Speed (F/O = 20)

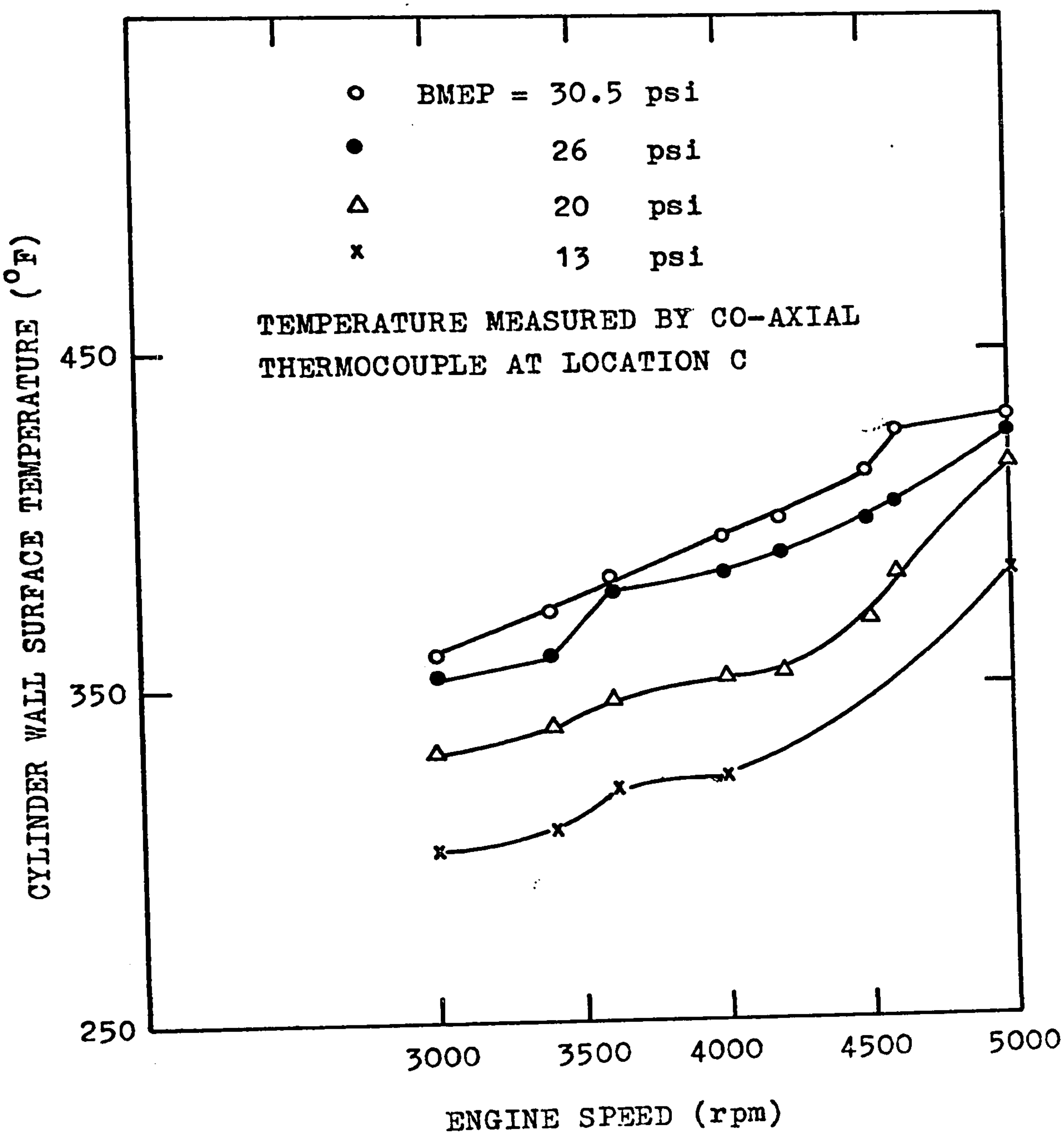

Fig. 4.17 CST as a Function of Speed (F/O = 20)

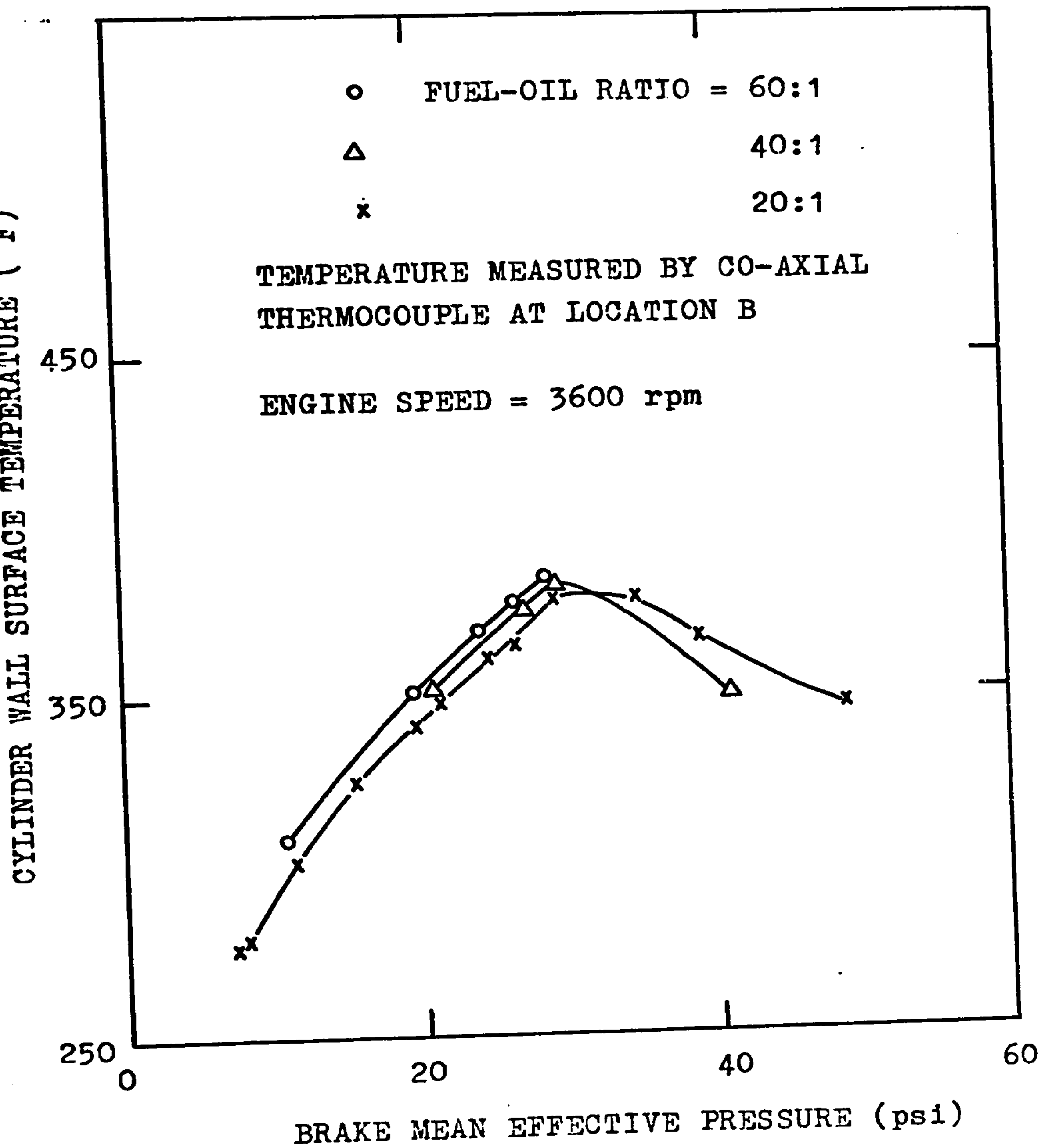

Fig. 4.18 Effects of Fuel-oil Ratio on CST

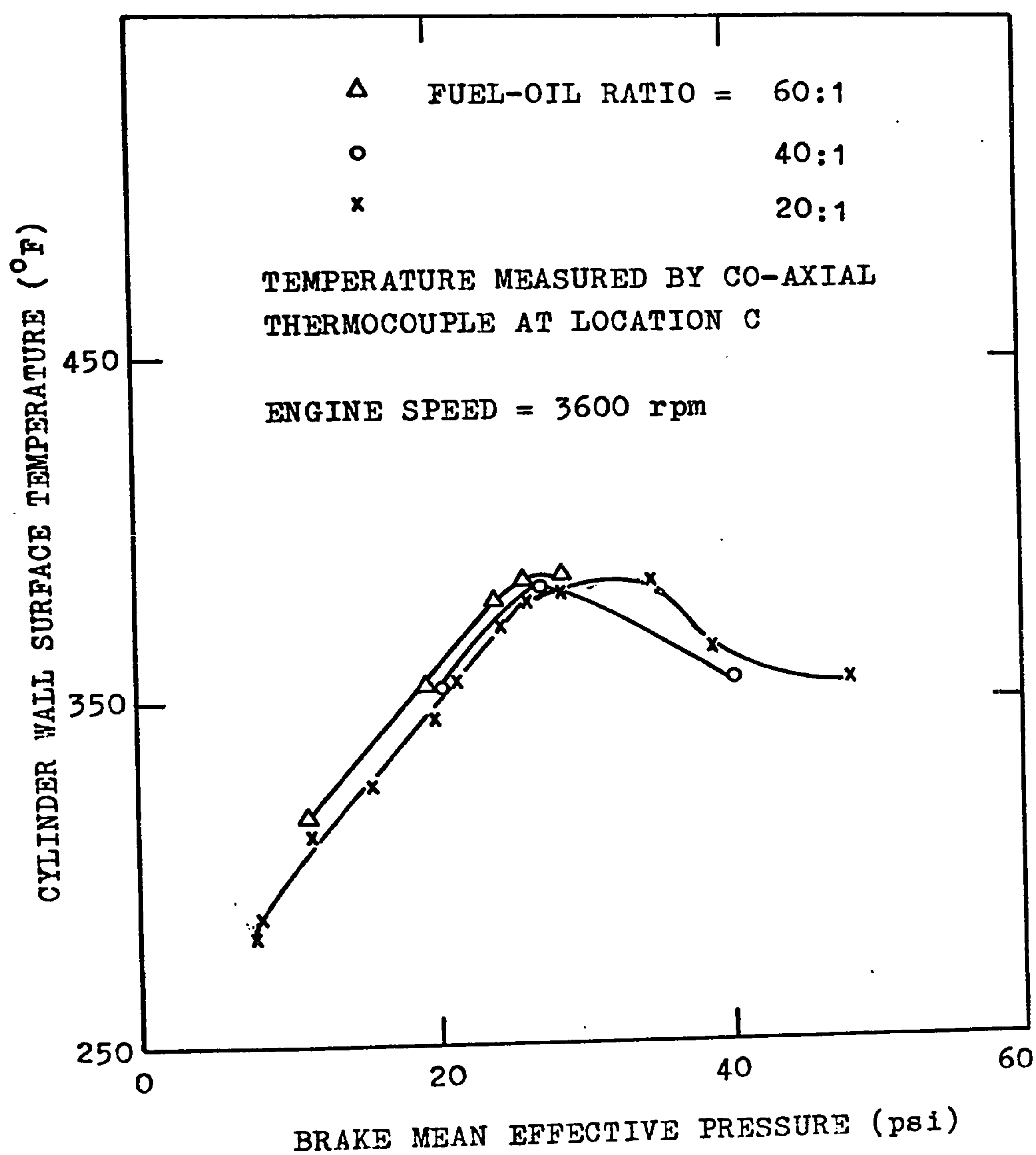

Fig. 4.19 Effects of Fuel-oil Ratio on CST

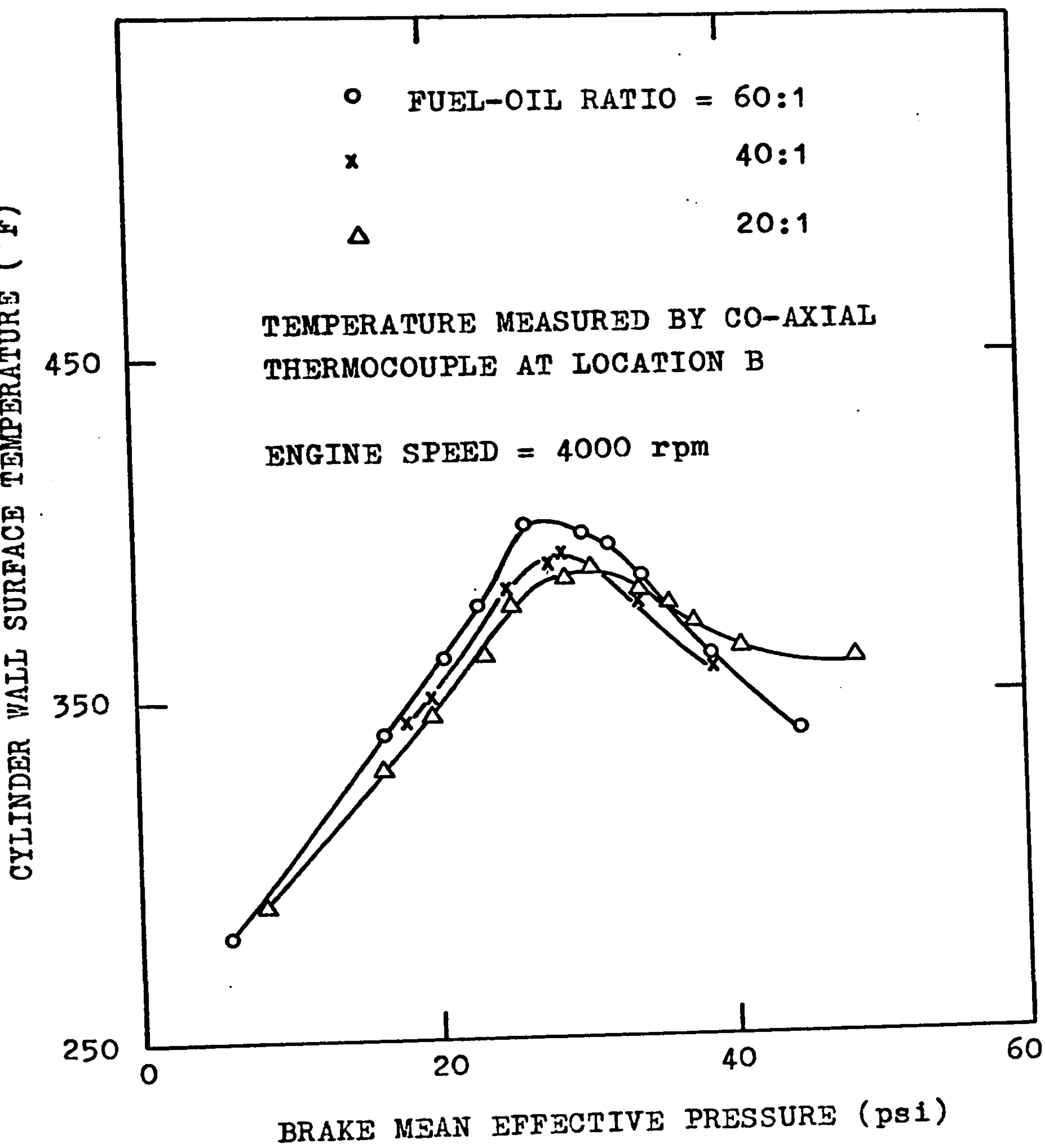

Fig. 4.20 Effects of Fuel-oil Ratio on CST

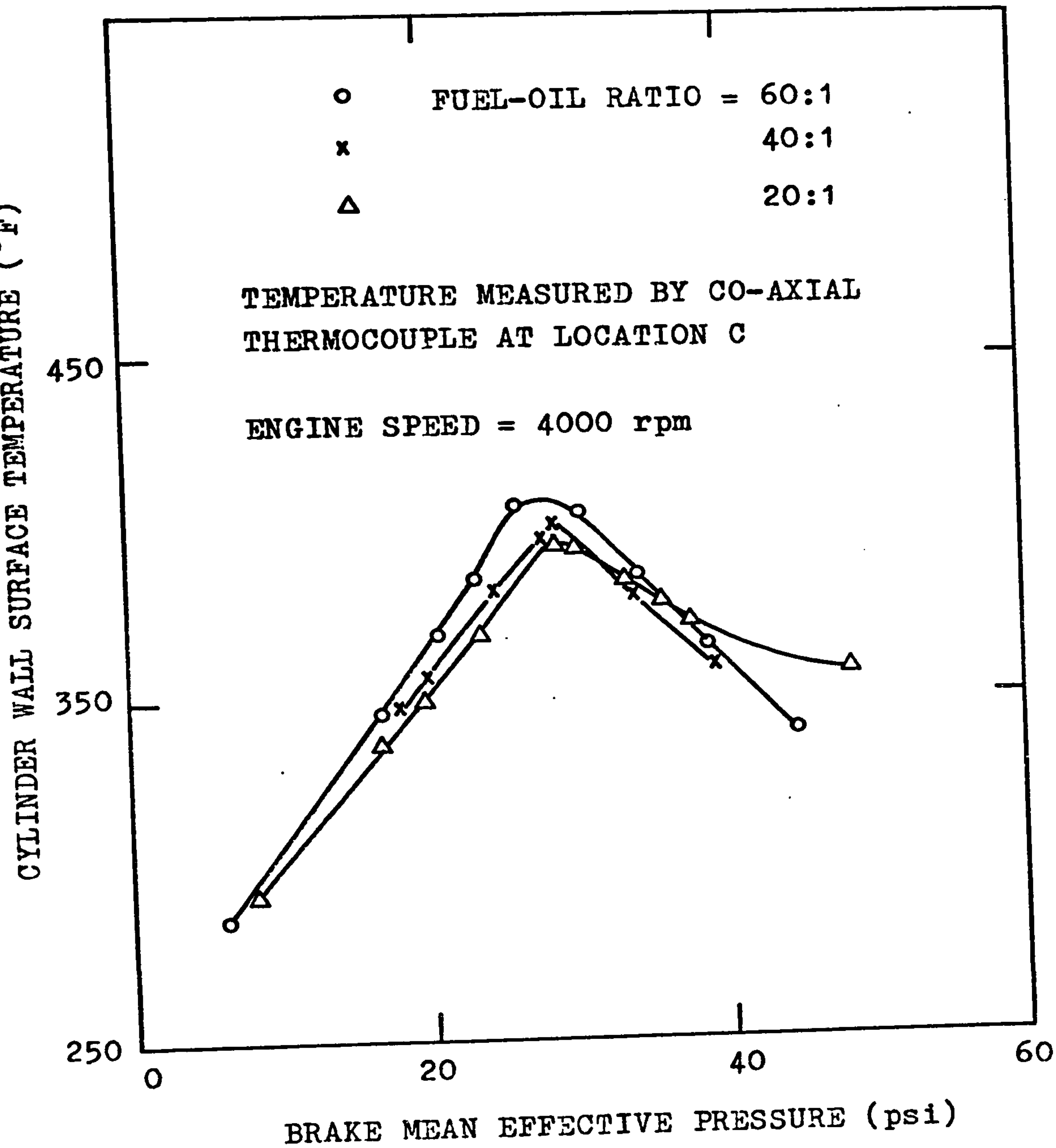

Fig. 4.21 Effects of Fuel-oil Ratio on CST

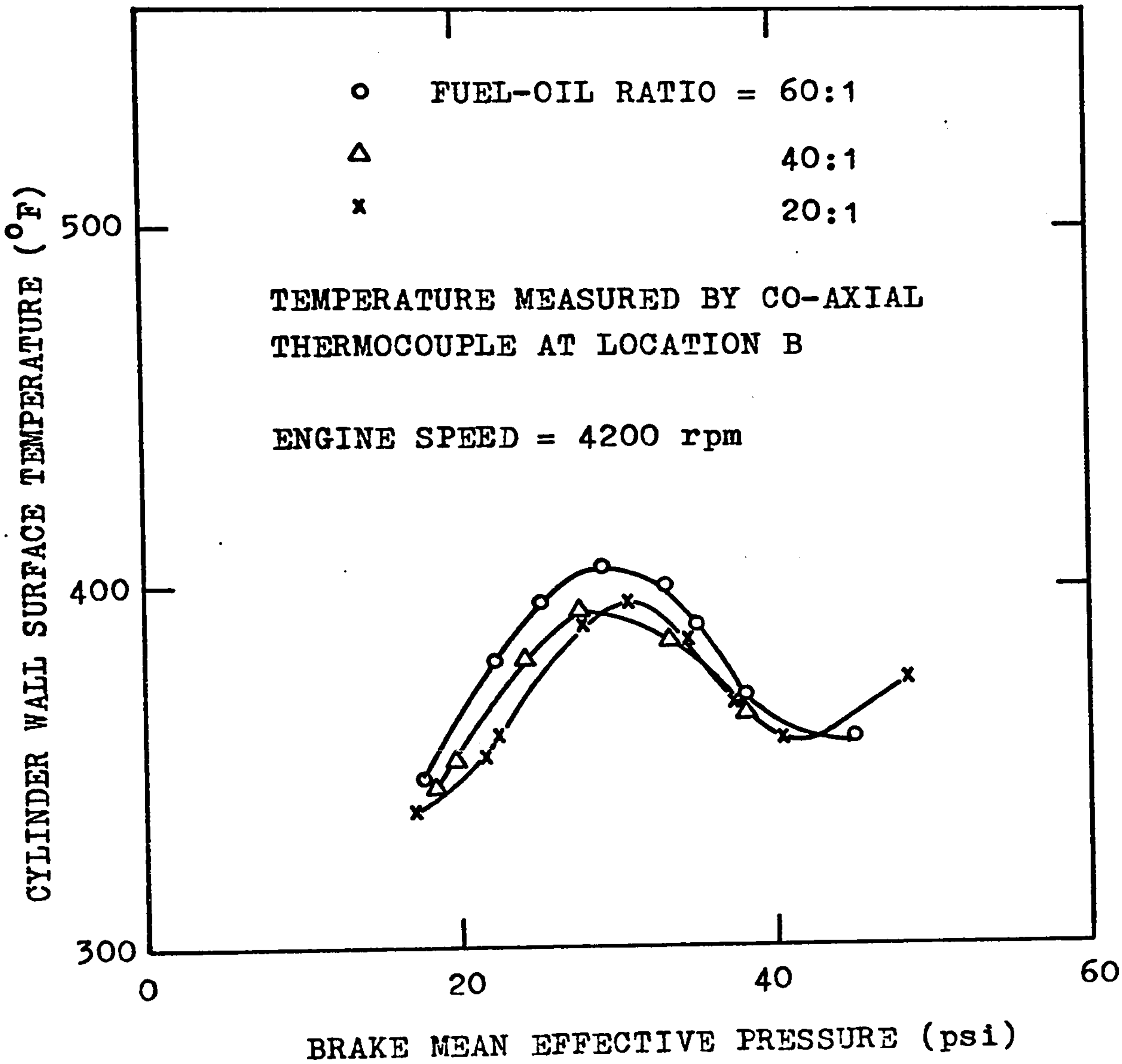

Fig. 4.22 Effects of Fuel-oil Ratio on CST

4200B

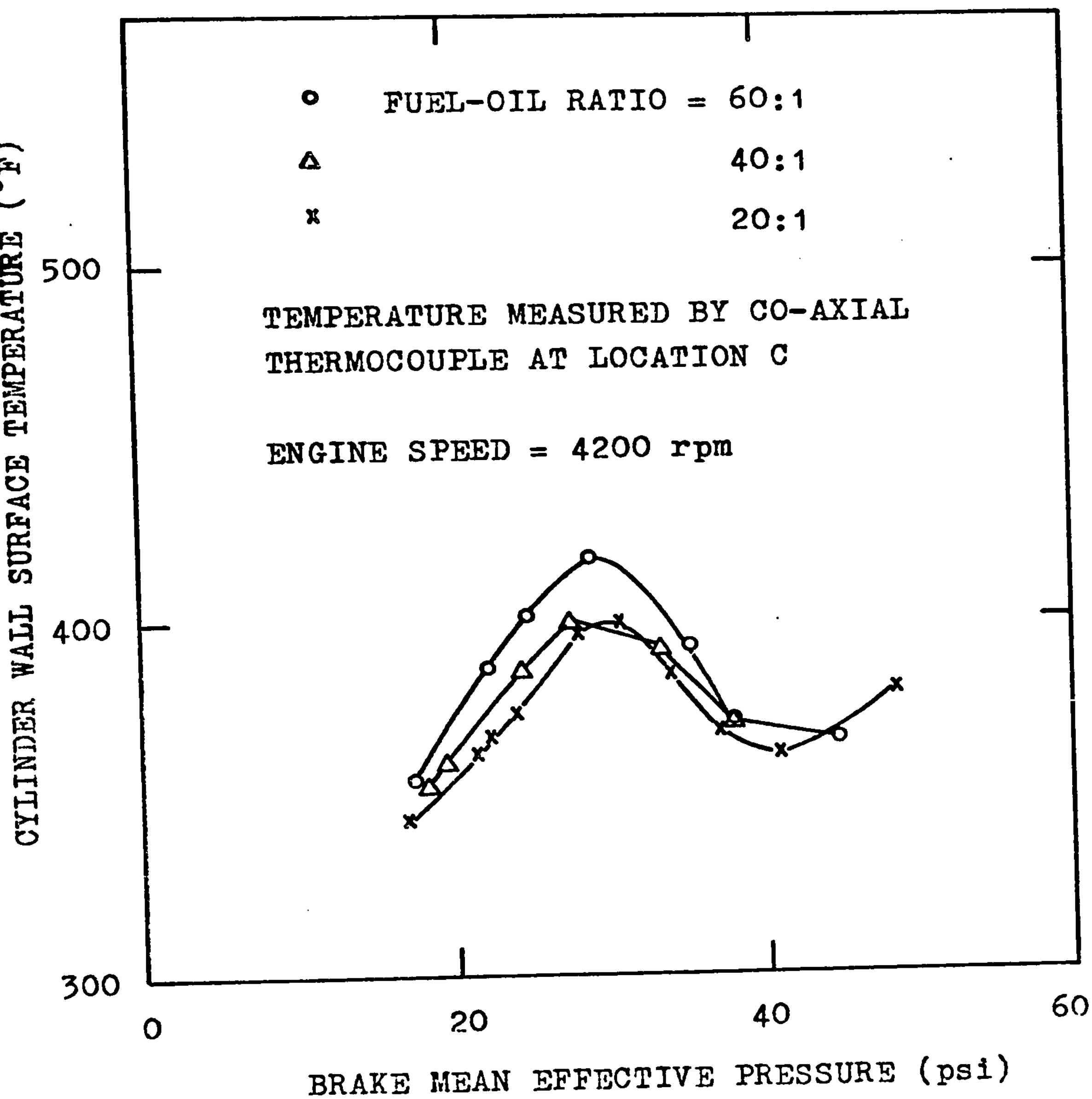

Fig. 4.23 Effects of Fuel-oil Ratio on CST

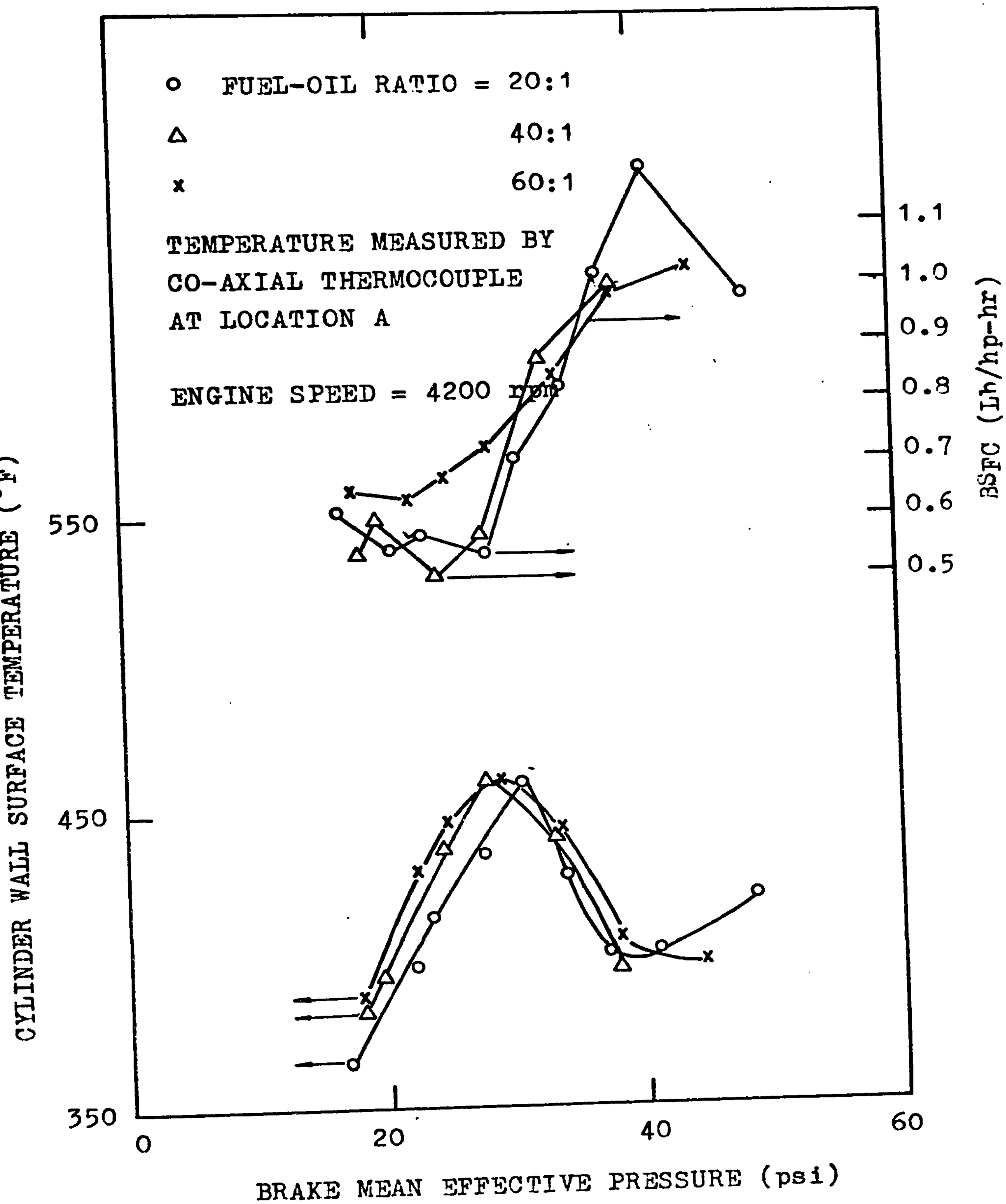

Fig. 4.24 Bsfc and Its Effect on CST at Various Fuel-oil Ratio

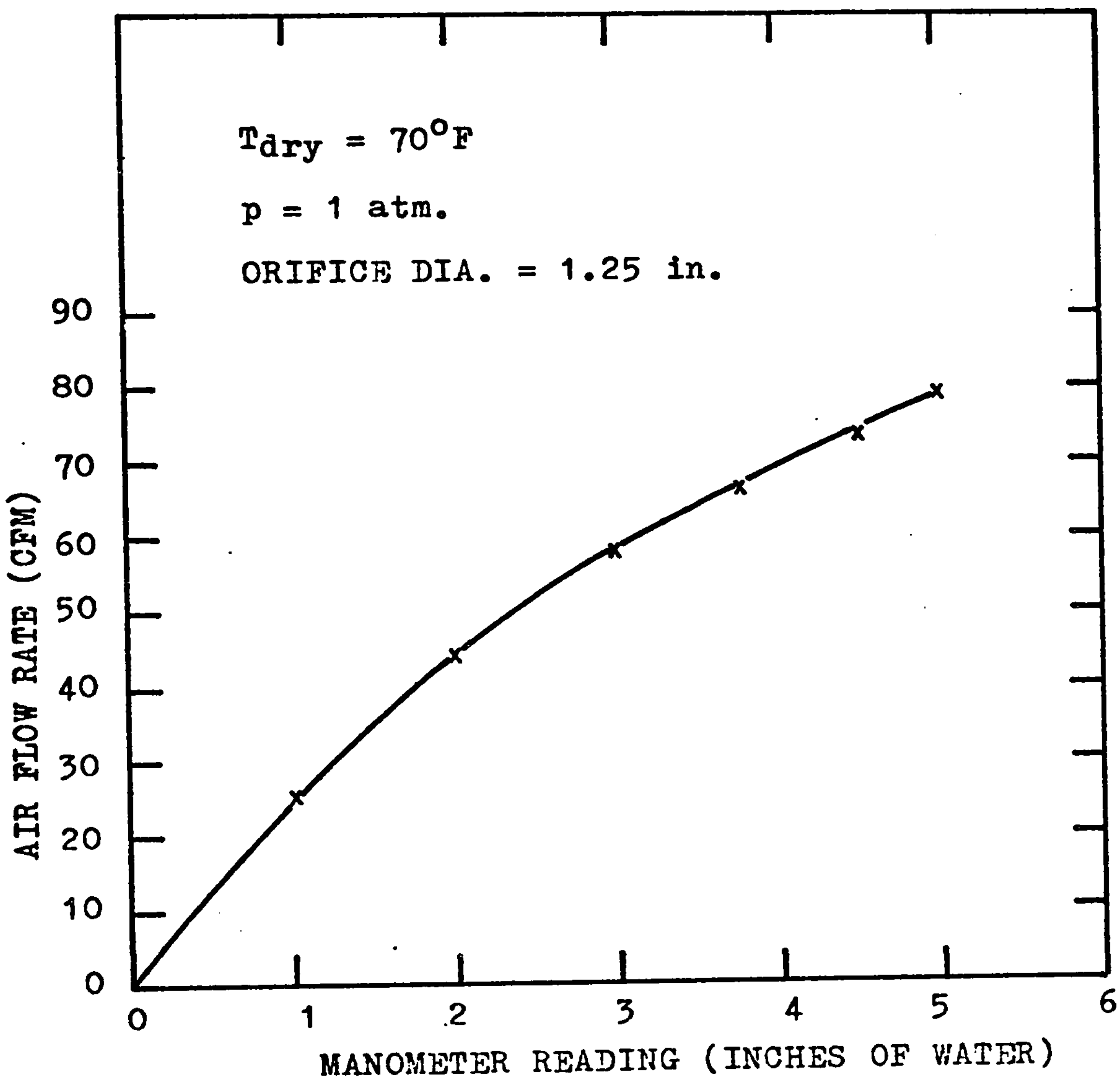

Fig. C.1 Calibration Curve of Air Flow Measurement

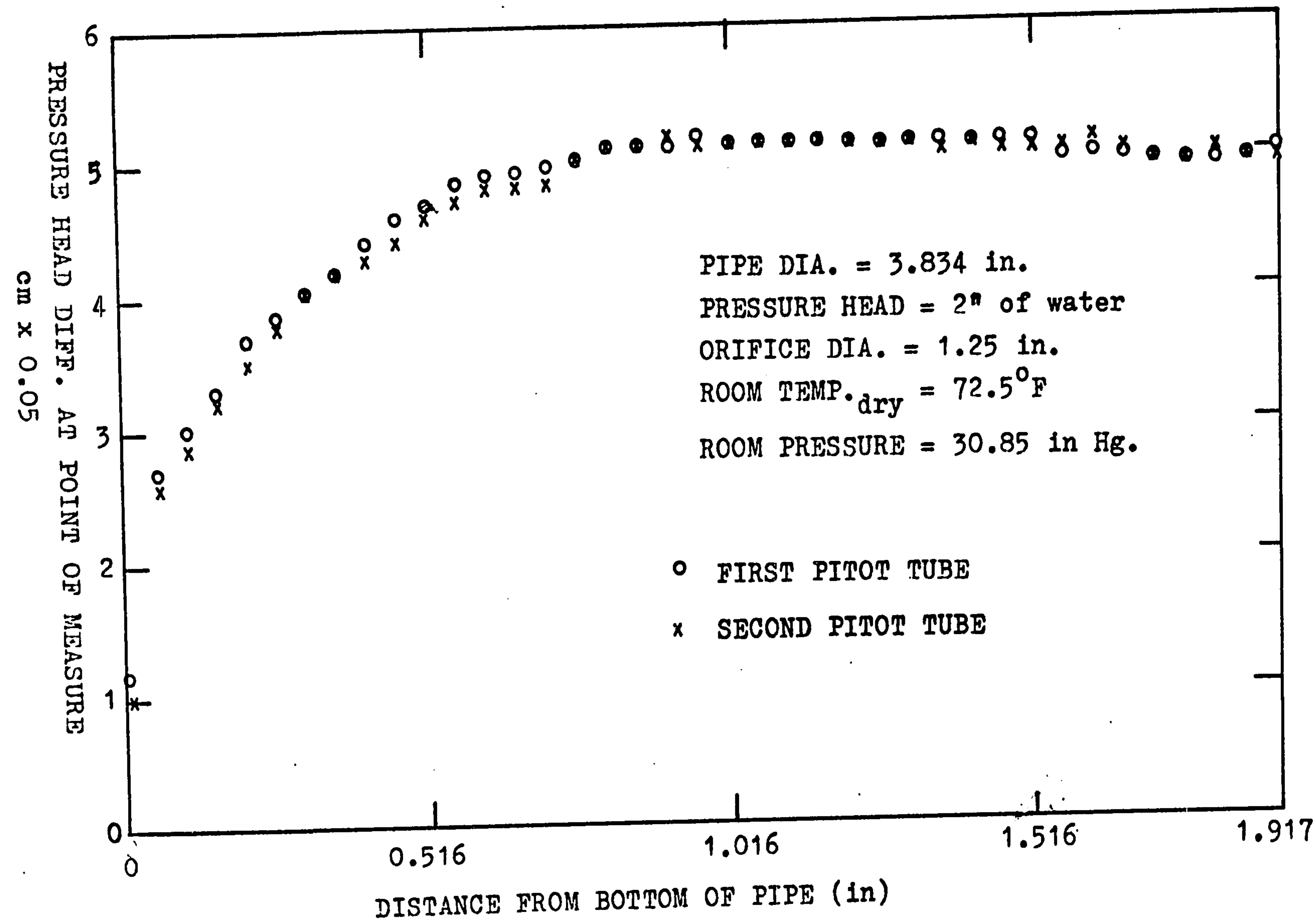

Fig. C.2 Velocity Profiles of Fully Developed Flow Under Measurement

Experimental Apparatus
from Inlet End.

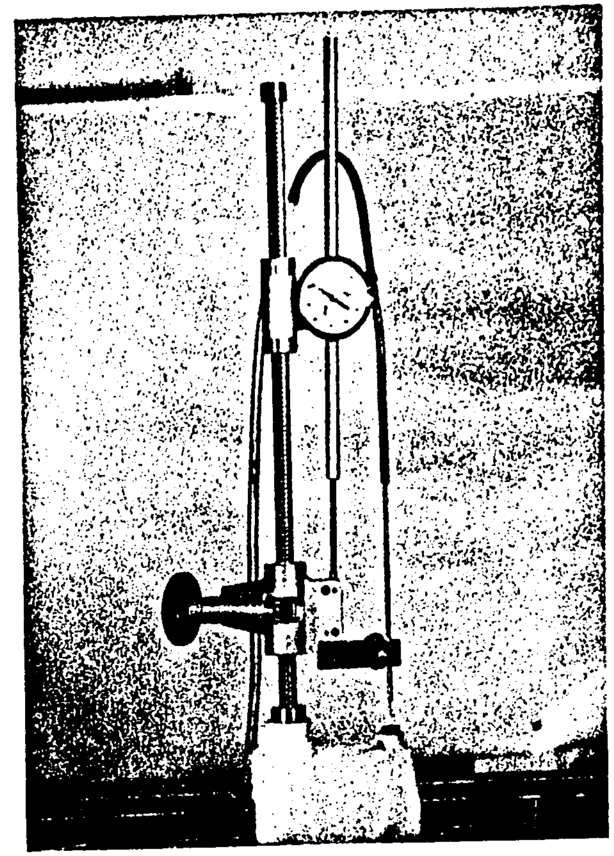

Traversing Machanism
with a Probe.

Fig. C.4 Apparatus for Air Flow Calibration
(From S.D. Park's Ph. D. Thesis (32), Univ. of Ottawa, 1972)

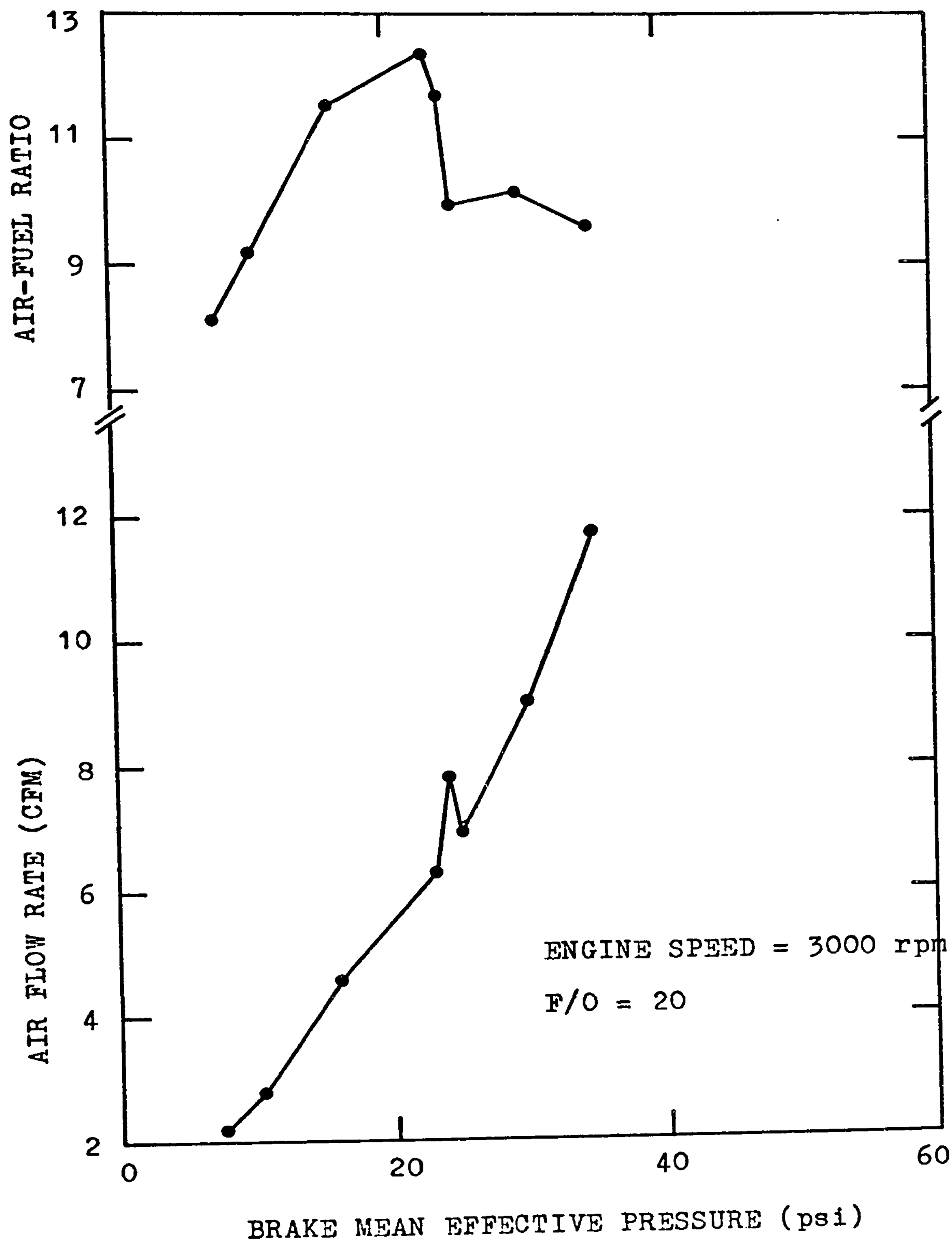

Fig. C.4 Air Flow Measurement

REFERENCES

1. D. Bendersky, "A Special Thermocouple For Measuring Transient Temperature", Mechanical Engineering Vol. 75, No. 2, 1953, pp 117-121.

2. O'Connor and Boyd, "Standard Handbook of Lubrication Engineering", McGraw-Hill 1968.

3. R. Poppinga, "Wear And Lubrication of Piston Rings And Cylinders", translated from German by Dr. E. Kurz published by ASLE through arrangement with the office of Alien Property, Department of Justice, Washington, D.C.

4. M.C. Shaw, T.J. Nussdorfer, "Camera Techniques Expose Oil Film Behavior", SAE Journal, Oct. 1946, pp 68-72.

5. J.S. Courtney-Pratt, G.K. Tudor, "Analysis Of Lubrication Between Rings And Cylinder Wall Of Running Engines", Proc. of Inst. Mech. Engrs. Vol. 155, pp 293-322, 1946.

6. D. Tabor, "Effect Of Temperature On Lubricant Films", Nature Vol. 145, No. 3669, pp 308, 1940.

7. H.V. Nutt, E.W. Landen and J.A. Edgar, "Effect Of Surface Temperature On Wear Of Diesel-Engine Cylinders And Piston Rings", SAE Transactions Vol. 63, 1955, pp 694-704.

8. W.J.D. Annand, "Heat Transfer In Cylinders Of Reciprocating Internal Combustion Engines", Proc. Inst. of Mech. Engrs. Vol. 177, No. 36, 1963.

9. G. Eichelberg, "Some New Investigations On Old Combustion Engine Problems", Engineering Lond. 1939, pp 148, 463, 547.

10. V.D. Overbye, "Unsteady Heat Transfer In Engines", Trans. Soc. Automot. Engrs. NY 1961, Vol. 69, 461, pp 973-989.

11. T. LeFeuvre, P.S. Myers and O.A. Uyehara, "Experimental Instantaneous Heat Fluxes In A Diesel Engine And Their Correlation", SAE paper 690464.

12. T. LeFeuvre, P.S. Myers, O.A. Uyehara and J.H. Shipinski, "A Tape Recording And Computer Processing System For Instantaneous Engine Data", SAE paper 680133,

13. E.T. Vincent and N.A. Henein, "Thermal Loading And Wall Temperature As Functions Of Performance Of Turbocharged Compression Ignition Engines", SAE Transactions Vol. 67, 1959, pp 478-494.

14. W.A. Daniel, "Engine Variable Effects On Exhaust Hydro-Carbon Composition", SAE Transactions Vol. 76, 1967, paper No. 670124.

15. E.W. Beckman, W.S. Fagley and J.V. Sarto, "Exhaust Emission Control By Chrysler - The Clean Air Package", SAE Transactions Vol. 75, 1967, paper 660107.

16. J.T. Wentworth, "Effect of Combustion Chamber Surface Temperature on Exhaust Hydrocarbon Concentration", SAE paper 710587.

17. S. Ohigashi and Y. Hamamoto, "Cylinder Gas Composition Of Small 2-Stroke Cycle Gasoline Engine", SAE paper 710143.

18. H.G. Freeston, "Test Bed Installations And Engine Test Equipment", I. Mech. Engrs. 1958, pp 245-260.

19. H.I. Hazzard, "The McCulloch BP-399-T Snowmobile Engine And Its Installation", SAE paper 720260.

20. T.G. Beckwith and N.L. Buck, "Mechanical Measurements", Addison-Wisley Publishing Company Inc., Reading, Mass., Palo Alto, London, 1961.

21. "Safety Standards For Small Craft", American Boat And Yacht Council Inc. New York, N.Y., 1972.

22. L.E. Haas, "Lubrication Of Air-Cooled And Water-Cooled Two-Stroke Cycle Engines", Nov. 1959. Lubricating Engineering, pp 436-449. Vol. 15, n. 11.

23. L.A. McReynolds and G.E. Holman, "Can One 2 Cycle Engine Oil Serve The Growing Outboard Market?", SAE paper No. 550B, Aug. 1962.

24. "Conversion Tables", Copyright 1967, 1969 by Honeywell Inc., Industrial Division, Fort Washington, Pa. 19034.

25. A.F. Underwood and A.A. Catlin, "An Instrument For Continuous Measurement Of Piston Temperatures", SAE Journal (Transactions) Vol. 48, No. 1, pp 20-27.

26. J.W. Savin, "Some Lubrication Problems In Air-Cooled Two-Cycle Engines", Feb. 1962, Lubrication Engineering, pp 78-82, Vol. 18, n. 2.

27. D.D. Fuller, "Theory And Practice Of Lubrication For Engineers", Wylie, Fourth Printing, Oct. 1966.

28. B. Pugh, "Some Notes On The Mechanical Factors Affecting Ring Gumming In Petrol Engines With Particular Reference To The Rating Of Lubricating Oils", Proc. of Inst. Mech. Engrs. Vol. 155, pp 303-306.

29. C.C. Colyer and W.L. Sicker, "Two Cycle Engines Require Special Oils", SAE paper 371A, 1961.

30. A.B. Weinberg, "Application Of BIA TC-W Reference Oil To Air-Cooled 2-Cycle Engines", SAE paper 710731, 1971.

31. W.E. Sytz and K. Izumi, "Lubrication of Japanese Two-Cycle Engines", SAE paper 680764, 1968.

32. S.D. Pak, "Developing Turbulent Flow and Heat Transfer In Concentric Annuli; an Analytical and Experimental Study", Ph. D. Desertation, U. of Ottawa, 1972.

33. Hilber Schenck, Jr., "Theories of Engineering Experimentation", 2nd ed., McGraw Hill 1968.

UNIVERSITE D'OTTAWA / UNIVERSITY OF OTTAWA
École des études supérieures/School of Graduate Studies

Title of thesis CYLINDER WALL TEMPERATURE MEASUREMENT IN AN AIR-COOLED TWO-STROKE CYCLE S.I. ENGINE

Name of candidate LEE, Man Fung

Degree M.A.Sc. Department MECHANICAL ENGINEERING

Date of defence July 5, 1973.

We, the undersigned, certify that we have approved this thesis and that the candidate has defended it successfully.

R.P. Henry R. P. Henry
(Signature of Examiners)

J.A. Newman

A.S. Krausz

T. LeFeuvre T. LeFeuvre
(Thesis Supervisor)

Paul Hagen
(Dean of Graduate Studies)

UNIVERSITÉ D'OTTAWA / UNIVERSITY OF OTTAWA
École des études supérieures/School of Graduate Studies

NAME OF AUTHOR LEE, Man Fung

TITLE OF THESIS CYLINDER WALL TEMPERATURE MEASUREMENT IN AN AIR-COOLED TWO-STROKE CYCLE S.I. ENGINE

DEGREE M.A.Sc. (Mechanical Engineering) YEAR GRANTED 1973

(Signed) (Author)

Date: July 5, 1973.

Permanent Address:
649 Rue St Luc
Gatineau P.Q.